

THESIS

A DERIVATIZATION PROTOCOL FOR MYCOLIC ACIDS DETECTION USING
LIQUID CHROMATOGRAPHY/MASS SPECTROMETRY

Submitted by

Paulina Zurita Urrea

Department of Microbiology, Immunology, and Pathology

In partial fulfillment of the requirements

For the Degree of Master of Science

Colorado State University

Fort Collins, Colorado

Fall 2012

Master's Committee:

Advisor: John T. Belisle

Robert Jones
Mo Salman

ABSTRACT

A DERIVATIZATION PROTOCOL FOR MYCOLIC ACIDS DETECTION USING LIQUID CHROMATOGRAPHY/MASS SPECTROMETRY

New tools for the diagnosis and control of Tuberculosis are major challenges. In this context the use of biomarkers can be applied for detecting characteristic signatures from the tuberculosis-infected host and the pathogen. Mycolic acids are considered as a hallmark of the *Mycobacterium* genus being abundant in the mycobacterial cell wall. In this study a derivatization protocol was tested to enhance the detection of mycolic acid after the attachment of a quaternary amine and analysis of the derivatized products in the positive ionization mode with liquid chromatography/mass spectrometry. Three groups were considered i) mycolic acid standard ii) human urine spiked with mycolic acid standard, and iii) human serum spiked with mycolic acid standard. Each group included the analysis of a set of non-derivatized mycolic acids in positive and negative ionization mode, and derivatized mycolic acids in positive mode. The derivatization process applied to the mycolic acid standard and to the urine samples spiked with mycolic did not improve the ion volume value compared to the respective non-derivatized samples. Serum samples, however, showed a significant enhancement in the ion volume of the different mycolic acids analyzed compared to the non-derivatized serum samples ($\alpha=0.05$). The method detection limit for the three groups was also achieved. Urine and serum samples spiked with mycolic acids showed higher detection limits compared to the mycolic acid standard; this was expected due the lipid extraction protocol and the complex nature of these fluids. The derivatization protocol did not improve the method detection limit compared to the non-derivatized samples. The overall results

make the derivatization protocol questionable to be applied routinely in biological samples. However, the results obtained after the derivatization of serum samples could point to the advantages of using a derivatization protocol to study possible interactions between mycolic acids and other molecules present in serum that could be impeding their detection.

ACKNOWLEDGMENTS

I would like to express my sincere gratitude to all the people that helped me to achieve the culmination of this study, by giving me support, advice, editing my manuscripts and offering me their friendship.

I am especially grateful to my advisor Dr. John T. Belisle for trust in me and sharing his knowledge. During this time I came to realize his exceptional human and professional qualities.

Thanks to my committee members Dr. Robert Jones and Dr. Mo Salman for giving me guidance during my research, and Dr. Salman for his time and patience helping me with the statistical analysis.

DEDICATION

To my parents Gabriela and Livio

TABLE OF CONTENTS

1. Introduction	1
1.1 Epidemiology of mycobacterial infections	1
1.1.1 The <i>Mycobacterium tuberculosis</i> complex	1
1.1.2 The nontuberculous mycobacteria and Leprosy.....	4
1.2 Anti-tuberculosis therapy and drug resistance.....	6
1.3 Pathogenesis of Tuberculosis.....	8
2. Mycobacterial cell wall and lipids compounds	11
2.1 Mycobacterial cell wall	11
2.2 The lipids compounds of the mycobacterial cell wall	15
2.2.1 Mycolic acids.....	15
2.2.2 Phosphatidylinositol based glycolipids	19
2.2.3 Glycolipids based on trehalose	20
2.2.3.1 Sulfolipids.....	21
2.2.3.2 Other acylated threhalose molecules	23
2.2.4 Phenol glycolipids	24
2.2.5 Mycobacterial waxes.....	24
3. Diagnosis of tuberculosis	26
3.1 Introduction.....	26
3.2 An overview of the use of biomarkers in TB diagnosis	27
3.2.1 DNA/RNA biomarkers in TB	28
3.2.2 Immunological biomarkers	30
3.2.3 Biomarkers identified by the use of proteomics.....	33
4. TB lipids as biomarkers in Mtb	35
4.1 Application of lipidomics for the study of Mycobacterium lipids as.....	35
4.2 Mycolic acids as biomarkers for Mtb detection	37
5. Project Rationale.....	40
6. Material and methods.....	43
6.1 Material and reagents.....	43
6.1.1 Material	43

6.1.2 Reagents	43
6.2 Extraction and purification of mycolic acids	43
6.2.1 Extraction of the mycolic acid-peptidoglycan-arabinogalactan (mAGP) complex	44
6.2.2 Base hydrolysis of mAGP.....	44
6.3 Synthesis of derivatizing reagents 2-Bromo-1-methylpyridinium Iodide (BMP) and 3-Carbinol-1-methylpyridinium Iodide (CMP).....	45
6.4 HPLC ESI/APCI-MS	46
6.5 Tandem mass spectrometry	46
6.6 Sample derivatization	47
6.7 Mycolic acid extraction from serum samples	48
6.8 Mycolic acid extraction from urine.....	48
6.9 Method validation.....	49
6.10 Data processing and analysis	49
6.10.1 Statistical analysis.....	49
7. Results	51
7.1. Mycolic acid standard derivatization.....	51
7.1.1 The derivatization reaction	51
7.1.2 Solvent testing solubility during the mycolic acids derivatization reaction	52
7.1.3 Tandem mass spectrometry of derivatized mycolic acids	54
7.1.4 Cleaning of the sample from derivatizing reagents	55
7.2 Comparison of derivatized and non-derivatized mycolic acid standard	59
7.2.1 Method detection limit of mycolic acids standard	76
7.3 Spiking of mycolic acids in serum and urine	80
7.3.1 Mycolic acids detection in urine by LC/MS	80
7.3.2 Mycolic acids detection in serum by LC/MS	91
8. Discussion and conclusions	103
9. Future directions.....	109

LIST OF TABLES

Table 1. Cleaning of the sample after derivatization	56
Table 2. Analysis of MAs standard by using Kruskal Wallis test	68
Table 3. MDL (ng) for non-derivatized and derivatized MAs	79
Table 4. Analysis of urine samples spiked with MAs by using Kruskal Wallis test ...	84
Table 5. MDL (ng) for non-derivatized and derivatized MAs spiked in urine.	91
Table 6. Analysis of serum samples spiked with MAs by using Kruskal Wallis test .	95
Table 7. MDL (ng) for non-derivatized and derivatized MAs spiked in serum	102

LIST OF FIGURES

Figure 1. Mycobacterial cell wall.	12
Figure 2. MA structure and mycolate classes in Mtb.....	16
Figure 3. Derivatization reaction of mycolic acids	51
Figure 4. Flow chart of the derivatization reaction comparing two solvent.	53
Figure 5. Comparison of solvents performance during MAs derivatization reaction.	54
Figure 6. ESI tandem mass spectra showing fragmentation of α -C78 (m/z 1243.2427) Collision energy was applied to α -C78 (m/z 1243.27).....	55
Figure 7. Cleaning process for derivatized samples. Samples were washed with acetonitrile.....	58
Figure 8. Extracted ion chromatogram for derivatized and non-derivatized MAs (Rt 17-22 min).....	62
Figure 9. Retention time and m/z of derivatized and non-derivatized MAs.....	64
Figure 10. Extracted ion chromatogram (1000-1500 m/z) for derivatized and non-derivatized MAs.....	65
Figure 11. MAs extracted ion chromatogram (1000-1500 m/z)	66
Figure 12. Ion volume comparison between derivatized and non-derivatized MAs at 100 ng/10 μ l (A), and 1 ng/10 μ l (B).	67
Figure 13. Significant differences in ion volume between groups based on the Nemenyi test	69
Figure 14. Significant differences in ion volume of individual MAs at 1 ng/10 μ l by using Nemenyi test.....	71
Figure 15. Ion profile comparison between derivatized and non-derivatized MAs in (+) mode.....	72

Figure 16. Identified and non-identified compounds in Rt range 20-24 min	73
Figure 17. Reproducibility of MAs standards	76
Figure 18. MAs standard curve	78
Figure 19. Extracted ion chromatogram (1000-1500 m/z) for derivatized and non-derivatized MAs in urine	81
Figure 20. Ion volume comparisons between derivatized and non-derivatized MAs spiked in urine at concentrations of 10 µg/10µl (A), and 100 ng/10µl (B)	82
Figure 21. Significant differences in ion volume between MAs spiked urine-groups based on the Nemenyi test.....	85
Figure 22. Significant differences in ion volume of the α-C82 MA isolated from urine at 10 µg/10µl by using Nemenyi test.	86
Figure 23. Reproducibility of results in urine samples spiked with MAs.	88
Figure 24. MAs spiked in urine standard curve.	90
Figure 25. Extracted ion chromatogram (m/z 1000-1500) of derivatized and non-derivatized MAs spiked in serum samples	92
Figure 26. Ion volume comparison between derivatized and non-derivatized MAs spiked in serum.	94
Figure 27. Significant differences in ion volume between MAs spiked in serum-groups based on the Nemenyi test.....	96
Figure 28. Significant differences in ion volume of individual MAs at 100 µg/10µl by using Nemenyi test.....	97
Figure 29. Reproducibility of results in serum samples spiked with MAs standard ..	99
Figure 30. Standard curve of MAs spiked in serum.....	101

1. Introduction

The genus *Mycobacterium* belongs to the order *Actinomycetales*, family *Mycobacteriaceae* and is comprised of the *Mycobacterium tuberculosis* complex (MTBC), *Mycobacterium leprae* and the nontuberculous mycobacteria (NTM). The MTBC includes *Mycobacterium tuberculosis* (Mtb), *Mycobacterium africanum*, *Mycobacterium canettii*, *Mycobacterium bovis*, *Mycobacterium pinnipedii*, *Mycobacterium caprae* and *Mycobacterium microti*. The NTM are represented by several species such as *Mycobacterium avium* complex (MAC) comprised of *M. intracellulare* and *M. avium* and the four subspecies included into *M. avium*: *avium*, *hominissuis*, *silvaticum*, *paratuberculosis* and *intracellulare*. Other NTM with clinical significance are *Mycobacterium fortuitum*, *Mycobacterium kansasii*, *Mycobacterium marinum*, *Mycobacterium ulcerans* and *Mycobacterium scrofulaceum* (Olsen et al., 2010).

1.1 Epidemiology of mycobacterial infections

1.1.1 The *Mycobacterium tuberculosis* complex

The mycobacteria belonging to the MTBC have a 99.9% similarity at the nucleotide level. However, they differ in their host tropism and pathogenicity. Mtb, *M. africanum* and *M. canettii* affect almost exclusively humans, while *M. microti* is a rodent pathogen (Brosch et al., 2002), and *M. bovis* has a broad host spectrum. Two new species with a zoonotic character have been included in the MTBC, *M. pinnipedii* has been reported in fur seals and sea lions (Thoen et al., 2009) and *M. caprae* is primarily isolated from goats, but is also a common source of bovine tuberculosis (TB) in central Europe (Prodinger et al., 2005).

The MTBC has been proposed to derive from a pool of ancestral tubercle bacilli, collectively called “*Mycobacterium prototuberculosis*”. Genetic studies link the migration of population from east Africa, 40,000 years ago, with the propagation of the most common ancestor, *M. canettii*, followed by the radiation of two major lineages, one of which was disseminated from humans to animals (Wirth et al., 2008).

M. bovis was hypothesized to be the origin of human TB, based on its broader host range. However, several genome deletions in *M. bovis* relative to Mtb have been shown, indicating a smaller genome, pointing to Mtb as the ancestor of *M. bovis*. The DNA loss in *M. bovis* could explain the clonal expansion of the bacteria linked to the success of this pathogen in new hosts (Brosch et al., 2002).

M. bovis causes a zoonotic disease identified in humans in several countries, and affecting in a higher proportion people related to farms and slaughterhouses. Bovine TB eradication programs have reduced the disease and death by *M. bovis* in human population (OIE, 2009). Despite the fact that cattle are considered the true hosts of *M. bovis*, the disease has been reported in several domesticated and non-domesticated animals. Examples of TB in wildlife include ungulates such as the African buffalo (*Syncerus caffer*) and the North American bison (*Bison bison*) as major reservoirs of the pathogen. European badgers (*Meles meles*) in the United Kingdom, brushtail possums (*Trichosurus vulpecula*) in New Zealand and several cervids species are also recognized reservoirs of *M. bovis* (Thoen et al., 2009).

Mtb, isolated for the first time in 1882 by Robert Koch, is the most common *mycobacterium* spp. That causes disease (Wagner et al, 2004) and is the second cause of death from an infectious disease worldwide. According to the World Health Organization (WHO), one third of the world population is currently infected,

estimating 9.4 million TB incident cases for 2010 (estimated from predict values from 2006–2009) and localized principally in South-East Asia, Africa and Western Pacific regions (WHO, 2010).

Primary infection with Mtb produces an active disease in a small proportion of the population; only 5 to 10% of recently exposed individuals develop clinically active TB during the first 2 years after exposure (Demissie et al., 2006). However, a higher percentage of exposed individuals can contain the infection and develop latent TB. This latency state, characterized as symptom-free and non-infectious can persist during all the lifetime of the individual or can reactivate because of different causes; such as human immunodeficiency virus (HIV) infection, malnutrition, advanced age, immunosuppressive medication, or other situations that overall affect the immune response of the individual (Tufariello et al., 2003).

One of the central strategies of WHO is to combat TB through a directly observed treatment short course (DOTS). A pivotal component of the DOTS program is the diagnosis of active TB by sputum smear microscopy (WHO, 2010). Despite the availability of treatment and the high rate of cure, a major difficulty in fighting this disease is the case detection rate (CDR). In 2009 the CDR was 63% (range 60-67%), with the highest rates in the European region (WHO, 2010) and the lowest level in the African region with a rate of 50% (WHO, 2010). The consequences of the CDR are reflected in a delayed start of treatment, affecting the prognosis of the patients, perpetuating the contact rate case, and fomenting the propagation of the disease (McNerney et al., 2011).

Immunosuppressed individuals and children often have a different clinical pattern compared to immunocompetent adults, resulting in poor sensitivity for the smear microscopy test (McNerney et al., 2011). Fewer acid-fast bacilli (AFB) in the

sputum of HIV-infected persons makes the smear microscopy less reliable (Samb et al., 1999). The diagnosis of childhood TB represents a major challenge in terms of having an appropriate diagnostic sample and test. Children usually do not produce sputum, and gastric aspirates can be collected for smear microscopy. However, detection is less than 20% when sputum or gastric aspirates are used (Shingadia et al., 2003). The culture of Mtb is also limited for clinical samples from children because of the paucibacillary characteristics of the disease in this population group (Marais et al., 2006). Infection in children has been categorized as a sentinel event or proof of the ongoing transmission of the disease in a population. Unrecognized cases without therapy become an important and long-term reservoir of TB in the population (Smith, 2001).

1.1.2 The nontuberculous mycobacteria and Leprosy

Approximately 50 NTM species are considered to be etiological agents of human disease, naturally inhabiting environmental sources such as soil and drinking water. Animals can also serve as reservoirs of NTM (Wagner et al., 2004). The traditional Runyon system groups the NTM according to their growth rates as slow growers (groups I to III) and rapid growers (group IV). Slow growers are also subdivided based on their pigment production in group I photochromogens (pigment producers in the presence of light), group II scoto-chromogens (pigment producers in the absence of light), and group III non-chromogens (Jarzembowski et al., 2008). For the diagnosis of NTM different tools are available. High performance liquid chromatography allows rapid identification by the analysis of mycolic acids (Butler et al., 2001). Commercial DNA probes (AccuProbe; Gen-Probe Inc.) contain a chemiluminescent label and hybridize with the complementary ribosomal RNA of the

target organism. They are available for the identification of *M. avium*, *M. intracellulare*, MAC, *M. kansasii* and *M. goodii*. Samples that cannot be identified with the mentioned methods can be analyzed using 16 rRNA gene sequencing. The advantages of using this gene are that it is present in all bacterial species and contains variable and conserved regions. By sequencing two of the hypervariable regions, the majority of the mycobacterial species can be identified (Soini et al 2001).

As a result of the HIV epidemic, NTM infections increased, showing a disseminated clinical process. However, after the introduction of the highly active antiretroviral therapy (HAART) for HIV there was a notorious rate decline of all opportunistic infections, including NTM. Currently, NTM affect non-treated or treatment failure HIV patients and also can appear during the early period of HAART, before the immune recovery. Other conditions that can predispose individuals to NTM infections are chronic obstructive pulmonary disease and cystic fibrosis (Gopinath et al., 2010). NTM infections can present as pulmonary disease, lymphadenitis, skin and soft tissue disease, skeletal infection, and disseminated infection (Wagner and Young, 2004). *M. avium* and *M. intracellulare*, members of the MAC, are the most common cause of NTM in AIDS patients (Jones et al., 2002). *M. ulcerans*, included in the NTM group, is the third major mycobacterial disease of humans (Wagner et al, 2004). It produces the toxin mycolactone that leads to the destruction of the subcutaneous adipose tissue and subsequent formation of a characteristic ulcer (Demangel et al., 2009).

NTM can be underestimated in endemic TB countries, mainly because of the lack of a reporter system and proper infrastructure for their identification (Gopinath et al., 2010). Treatment of NTM pulmonary infection includes long-term therapy. For *M. avium* and *M. intracellulare* at least three drugs are recommended to avoid the

emergence of resistance. Macrolides are always included because of their effectiveness (Jarzembowski et al., 2008).

M. leprae is the second most prevalent mycobacterial species in humans (Wagner et al., 2004). *M. leprae* is the cause of leprosy, a chronic disease found in several developing countries, reaching an estimated global prevalence of 213,000 cases (WHO, 2010). Traditionally humans were thought to be the only natural host for *M. leprae*; however, in 1975 nine-banded armadillo (*Dasypus novemcinctus*) were reported to harbor the disease (Walsh et al., 1975). *M. leprae* from human and armadillo cases in the Southern United States were subjected to comparative genomic analysis showing that the genome sequences of the predominant armadillo in that area and human strains shared a same unique genotype, suggesting a zoonotic character for the disease (Truman et al., 2010).

In humans, leprosy elicits a range of cellular immune responses, clinically manifested as a demarcated lesion or multiple nodular lesions in the skin. It can also affect eyes and cause nerve damage (Britton et al., 2004). *M. leprae* is not cultivable *in vitro*, and the “gold standard” diagnosis corresponds to a skin biopsy sample. Serological tests are challenging because of limited sensitivity and specificity. Results of PCR analysis can vary depending if the disease has a paucibacillary or multibacillary form, but together the histopathological analysis offer the best diagnosis approach (Scollard et al., 2006).

1.2 Anti-tuberculosis therapy and drug resistance

Following the WHO guidelines for TB therapy, newly detected cases of pulmonary TB should receive a regimen combining isoniazid (INH), rifampicin (RIF), pyrazinamide (PZA) and ethambutol (EMB) during the first two months, followed by a

4-month treatment with INH and RIF (WHO, 2010). TB chemotherapy is affected by the slow-growing characteristics and the metabolic intracellular state of the bacilli (Blanchard et al., 1996). The mechanism of action varies between the drugs having different mycobacterial targets. INH is a prodrug that requires activation by the mycobacterial catalase peroxidase enzyme (KatG). INH is active in the growing state of the bacilli, inhibiting the synthesis of mycolic acids (Tripathi et al., 2005). RIF interferes with bacterial transcription by binding to the β -subunit of the RNA polymerase (Johnson et al., 2006) and can be active in bacilli with reduced metabolism or actively growing (Mitchison et al., 2000). EMB is a synthetic amino alcohol having as a site of action the biosynthesis of arabinan present in arabinogalactan and lipoarabinomannan (Tripathi et al., 2005). Finally, PZA is a structural analog of nicotinamide and is more effective in non-replicating tubercle bacilli compared to metabolically active bacilli (Zhang et al., 2002). The mechanism of action of PZA has been proposed to be through acidification of the bacterial cytoplasm and de-energization of the membrane (Zhang et al., 2005). However, a recent study also demonstrated that PZA inhibited translation by targeting ribosomal proteins (Shi et al., 2011).

In 1994, WHO initiated the global project on anti-TB drug-resistance surveillance. Currently, there is an estimated of 650,000 cases of multidrug-resistance (MDR)-TB among the worldwide TB prevalent cases (WHO, 2011). As part of the DOTS strategy, patients have a supervised treatment and monthly sputum samples are collected until having two consecutive negative results for the smear examination (Johnson et al., 2006). TB drug resistance dates back to the 1950s and 1960s. At that time, treatment was characterized by the use of a monotherapy either with streptomycin, INH or PZA. This drug regimen was followed

by a rapid development of bacterial resistance, leading to the use of a combination therapy (Hall et al., 2009).

Combination therapy and the introduction of RIF by the end of the 1960s produced a decrease in drug resistance in developed monitored countries. However, during the 1980s, the establishment of HIV-acquired immune deficiency syndrome (AIDS) impacted the increase of TB transmission and outbreaks of MDR-TB resistant to INH and RIF (Johnson et al., 2006). Moreover, the situation was worsened by the emergence of extensively drug-resistant (XDR)-TB, defined as TB with resistance to at least INH, RIF, any fluoroquinolone (FQ) and one of three second-line injectable drugs (amikacin, kanamycin or capreomycin) (Banerjee et al., 2008).

Drug susceptibility of Mtb can be determined at the molecular level, detecting mutations in the genes involved in the drug mechanism or by inhibition of the bacteria growing in a medium with the antituberculous drug (Kim, 2005).

1.3 Pathogenesis of Tuberculosis

Mtb enters the respiratory route contained in aerosol droplets and reaches the alveoli. The bacilli are then disseminated by the lymphatic circulation to regional lymph nodes in the lung, forming the primary or Ghon complex (Smith, 2003). Macrophages and dendritic cells play a pivotal role during the immune response. The bacteria contact tissue dendritic cells that are activated and migrate to the draining lymph node, stimulating naïve T cells (Saunders et al., 2000). CD4+ and CD8+ T cells that participate in the activation of Mtb infected macrophages through cytokines such as gamma interferon (IFN- γ) and lysis via apoptosis and cytotoxic T cell action (Flynn et al., 2001).

The bacteria also contact resident macrophages of the respiratory tract through mannose and/or complement receptors, leading to the phagocytosis process and the formation of an endocytic vacuole called the phagosome. The normal phagosomal maturation implies phagosome-lysosome fusion, providing a hostile environment for the bacteria, including acid pH, reactive oxygen intermediates, lysosomal enzymes, and toxic peptides. However, pathogenic mycobacteria can subvert this, by inhibiting the phagosome-lysosome fusion (Smith, 2003). Lipids contained in the cell wall of mycobacteria, such as lipoarabinomannan and its precursor phosphatidylinositol mannoside, have been shown to be involved in the arrest of phagosome trafficking (Vergne et al., 2004).

The formation of the granuloma is a characteristic histo-pathological feature of TB triggered by chemokines produced by infected macrophages at the infectious site, leading to the accumulation of macrophages, lymphocytes and dendritic cells (Peyron et al., 2008). Tumour necrosis factor (TNF)- α is the dominant cytokine responsible for chemokine production and subsequent cell recruitment. The downregulation of this proinflammatory response is linked to a cellular immune response mediated by IFN- γ (Russell, 2007).

With the development of the cellular immunity, macrophages carrying the bacilli are killed, and result in a caseous center in the granuloma surrounded by a cellular zone of fibroblasts, lymphocytes and blood-derived monocytes. Despite the low pH, low oxygen and toxic fatty acids that characterize the caseous center, some bacilli remain dormant (Smith, 2003). In vitro studies showed that Mtb activates metabolic pathways for using fatty acids as the sole carbon source under anaerobic conditions (Flynn et al., 2001). Also oxygenated mycolic acids are one of the major compounds of the TB cell wall and are proposed to be crucial for the formation of

macrophages filled with lipid-containing bodies, called foamy macrophages (FM) where the bacilli can hide and persist inside the granuloma (Peyron et al., 2008). Bacteria have been also found associated with macrophages present in the peripheral leukocytic area of the granuloma, being positive for the expression of isocitrate lyase. This enzyme is important for the use of fatty acids as a carbon source and has been shown upregulated by Mtb in those inflammatory macrophages where there is a hostile environment and restricted access to nutrients (McKinney et al., 2000).

The cellular immune response defines the future of the infection, leading to an arrest or progression of the disease., also referred as latent or active disease, respectively (Tufariello et al., 2003). The progress of the disease is characterized by a liquefactive necrosis and loss of the fibrous granuloma capsule integrity. Caseous material will be discharged into proximal blood vessels and airways, causing a systemic dissemination of the bacilli (Dheda et al., 2005). This state of the disease is highly infectious because of the large number of bacilli in aerosolized droplets and in sputum. Consequently, sputum is the primary clinical sample used for TB diagnosis (Wallis et al., 2001).

Lymph nodes are the most common site for extrapulmonary TB, but eventually the disease can be disseminated to several locations in the organism (Sharma et al., 2004). The clinical manifestations of disseminated TB, also called military TB, are non-specific and can include fever, anorexia, weight loss and cough (Sharma et al., 2005).

2. Mycobacterial cell wall and lipids compounds

2.1 Mycobacterial cell wall

Because of their cell wall structure, mycobacteria have long been considered Gram- positive; despite this, they also possess some features common to the Gram-negative cell wall (Rastogi, 1991), including an outer membrane like structure (Zuber, 2008). Using the standard reference of bacterial phylogeny based on 16S ribosomal RNA sequence comparison, Mtb belongs to the high G+C Gram-positive bacteria. However, measuring the distance between ancestral units in the genome tree, Fu et al. (2002) showed that the evolutionary distance from Mtb to the nearest ancestor of Gram-positive bacteria is 16.0% and to the nearest ancestor of Gram-negative bacteria is 5.4%. The acid-fastness of the cell wall has been attributed to several cell wall compounds, including outer lipids, mycolic acids bound to the arabinogalactan fraction and free hydroxyl and carboxylate groups of cell wall lipids. This hydrophobic barrier allows phenol-based stains to penetrate and make it resistant to decolorization by acid-alcohol (Bhatt et al., 2007).

The mycobacterial cell wall has an indisputable role in the success achieved by these pathogens. The high content of lipid in the cell envelope is responsible for the notable hydrophobicity and the consequent resistance to chemical injury and lytic enzyme attack from the host (Ratledge, 1982). They exhibit resistance to most common antibiotics and general chemotherapeutic agents; atypical mycobacteria are especially resistant (Brennan and Nikaido, 1995). Differences in permeability can exist between species, *Mycobacterium chelonae*, has a very low permeability compared with Mtb, possibly because the former is a soil inhabitant (Jarlier and Nikaido, 1994).

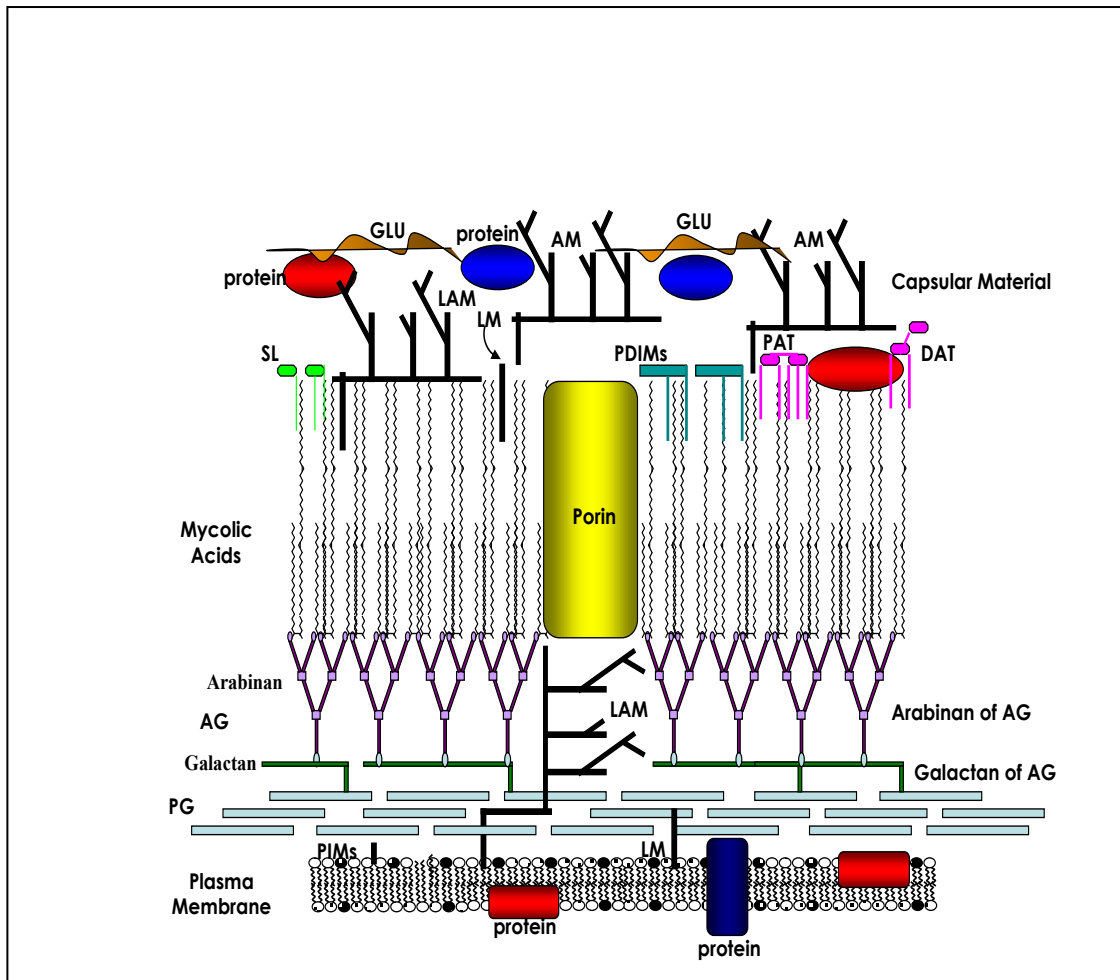


Figure 1. Mycobacterial cell wall. The scheme shows some of the most relevant compounds in the plasma membrane, outer membrane and capsule. Arabinogalactan (AG), Arabinomannan (AM), diacyl trehalose (DAT), glucan (GLU), lipoarabinomannan (LAM) lipomannan (LM), pentaacyl trehalose (PAT), dimycocerosates of the phthiocerol family (PDIMs), peptidoglycan (PG), phosphatidyl inositol mannoside (PIMs), sulfolipid (SL). (Adapted from Chatterjee et al., 1998 and Minnikin et al., 2002; copyright permission obtained).

The general architecture of the Mtb cellular envelope (Figure 1) is a plasma membrane surrounded by a covalently linked mycolic acid, arabinogalactan and peptidoglycan complex (mAGP). The mycolic acids of mAGP form a membrane like

structure with lipids that are present on the surface of the cell envelope. A polysaccharide-rich capsule like material has also been described (Daffé, 1999; Crick et al., 2001).

The plasma membrane of the mycobacterial cell has a basic conformation that does not differ from other plasma biological membranes. It is structured of polar lipids with hydrophilic head groups and fatty acid chains, combining a mixture of straight chain, unsaturated and mono methyl branched fatty acid residues with less than 20 carbons. The main fatty acids isolated from the plasma membrane are palmitic (C 16:0), octadecenoic (C 18:1) and 10-methyl octadecanoic (or tuberculoestearic) (Daffé, 2008). The common amphipatic polar phospholipids of mycobacteria are diphosphatidylglycerol, phosphatidylethanolamine (PE), and phosphatidylinositol (PI). Menaquinones and carotenoids are also present, having a role in the respiratory system of membranes and as protective agents against photodynamic damage, respectively (Minnikin, 1982).

The peptidoglycan of the cell wall core of Mtb consists of N-acetylglucosamine (GlcNAc) and modified muramic acid residues. Muramic acid is modified to N-acetyl muramic acid as in the peptidoglycan of other bacteria, but it is also oxidized to N-glycolyl and substituted with tetrapeptide (L-alanyl-D-isoglutaminy-meso-diaminopimelyl-D-alanine) chains. Finally, cross-linking can occur between two meso-diaminopimelic acid (DAP) residues or between DAP and D-alanine residues (Crick et al., 2001).

The arabinogalactan (AG) that is covalently attached to the 6 carbon of the N-acetyl or N-glycoly-muramic acid of peptidoglycan and has a branched structure consisting mainly of 1 → 5 linked D-arabinofuranose units and 1 → 4 linked D-

galactopyranose units, in an approximate ratio of 5 to 2. Some of the arabinose units also form non-reducing terminal ends (Lederer et al., 1975). AG is esterified with mycolic acids and it has been proposed that the non-mycolated motifs work as epitopes for interaction with the immune system, which could explain the antigenicity of the arabinan component (Mc Neil et al., 1991).

Minnikin (1982, 1991) originally proposed a double layer model for the outer membrane (OM), in which the mycolic acids are, in part, covalently linked to the cell wall arabinogalactan and form the inner leaflet of the asymmetrical bilayer. The outermost leaflet is proposed to be composed of various glycolipids, and of species-specific lipids such as glycopeptidolipids, phthiocerol dimycocerosate, and sulfolipids (Minnikin 1982., Rastogi, 1984).

Mycolic acids (MAs) in mycobacteria exist in the cell in two basic forms. The major portion is covalently bound to the cell wall, esterified to the 5-hydroxy groups of arabinofuranosyl residues to form the terminal [5-mycoloyl- β -Araf- (1 \rightarrow 2)-5-mycoloyl- α - Araf-(1 \rightarrow)] units of AG. MAs are also found loosely associated with the cell wall, esterifying a variety of carbohydrate containing molecules like glucose, trehalose or polyprenylphosphomannose (Mc Neil et al., 1991)). Mtb can also release the MAs as free fatty acids (Ojha et al., 2008)

The capsule structure is the most external component of the mycobacterial cell, and its true existence and structure has been controversial. The putative capsule is not covalently attached to the cell wall (Daffé et al., 1999). Polysaccharides and proteins are the main components and it only contains 1 to 6 % of lipids. A 120 kDa glycogen-type glucan, a 13 kDa arabinomannan and a 4 kDa mannan have been identified as the major capsular polysaccharides (Ortalo-Magné et al., 1995). Phospholipids such as phosphatidylinositol mannosides and

phosphatidylethanolamine (PE), commonly found in the plasma membrane, were also observed as part of the capsular material (Ortalo-Magné et al., 1996). The α -glucanes found in the capsular region have been proposed to play a role in the host immune response. Gagliardi et al., (2007), showed that α -glucane is capable to interfering with class I CD1 molecule expression, a family of major histocompatibility complex (MHC)-class-I-like glycoproteins that present unique lipids found in Mtb to activate diverse T cells (Barral et al., 2007). They are also associated with interference of monocyte differentiation to dendritic cells (Gagliardi et al., 2007). The capsule composition and thickness differ between different species of mycobacteria and influence the interaction with macrophages. Saprophytic and opportunistic pathogenic mycobacteria are more readily ingested than are members of the Mtb family which exhibit a thicker capsule (Stokes, 2004).

2.2 The lipids compounds of the mycobacterial cell wall

2.2.1 Mycolic acids

MAAs are very abundant in the mycobacterial cell wall. They comprised about 34% of the weight in *M. microti* and they are considered as a hallmark of the *Mycobacterium* genus (Davidson, 1982). MAAs have been extensively used for taxonomic purposes and can be distinguished from other MAAs containing genera, including *Corynebacterium* (C₂₀ to C₃₈), *Rhodococcus* (C₃₄ to C₅₂) and *Nocardia* (C₄₀ to C₆₀) according to the longer length of their carbon chain (Butler et al, 2001).

The basic structure of MAAs (Figure 2) is comprised of a β -hydroxy-alkyl branched unit. The meromycolate moiety is up to C₅₆ in length and the saturated α -branch has a length of C₂₀ to C₂₄. In the meromycolate chain there are positions that can be occupied by double bonds, cyclopropane rings or polar modifications that

contain oxygen functions and that tend to be at the distal position (Barry et al., 1998). Regarding this, the least polar MAs without oxygen functional groups are termed α -mycolates and the more polar MAs possess an oxygen function that can be a keto-, a methoxy- or a hydroxyl-group in slow growing species and an epoxy ring in rapid-growing species. In some mycobacterial species the keto-mycolic acids can be oxidized yielding a wax ester (Rafidinaviro et al., 2009)

Non-polar modifications occur at the distal and the proximal positions and include *cis* or *trans* double bonds and *cis* or *trans* cyclopropanes (Barry et al., 1998). In *Mtb*, α -MAs have two cyclopropane rings, mostly present in the *cis* configuration and the keto- and methoxy-MAs have one cyclopropane that can be in *cis* or *trans* configuration (Watanabe et al., 2001).

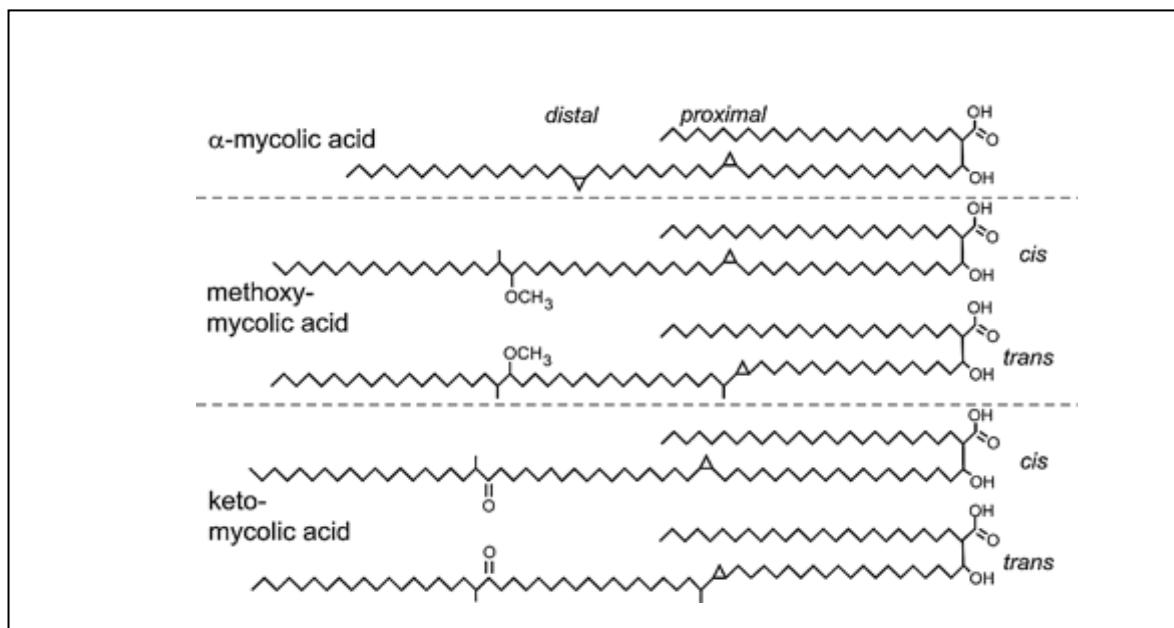


Figure 2. MA structure and mycolate classes in *Mtb*. (Takayama et al., 2005; copyright permission obtained).

The saturated structure of the α -branch (typically 24 carbon) and the length of the meromycolic chain (almost 60 carbon) may be influencing the regular parallel packing of their hydrocarbon chain, as well as the oxygen functions with *cis* double bonds and *cis* cyclopropane structures by producing kinks in the chains (Brennan and Nikkaido, 1995).

Cis-cyclopropanation of the α -MAs was found to be critical for the activation of the innate immune responses during early infection (Rao et al., 2005). In contrast, *trans*-cyclopropanation in Mtb has shown to limit the virulence by suppressing inflammatory response during infection, implying a mechanism for bacterial persistence (Rao et al., 2006). Cyclopropanation of the meromycolate chain is also related to other potential virulence determinants. *Mycobacterium smegmatis* does not modify its mycolates with cyclopropanation. However, when *M. smegmatis* was genetically modified such that it converted its distal *cis* double bond to a *cis* cyclopropane ring there was enhanced protection of the cell to oxidative stress (Yuan et al., 1995).

α -mycolates (C₇₄₋₈₂) are the most widespread and have been found in every mycobacterial species examined, followed by ketomycolates. The ω -1 methoxy-mycolates are the most restricted, occurring in some fast growing strains (Kremer and Besra, 2005). α' -mycolates have a shorter carbon chain (C₆₀₋₆₈) than α -mycolates and have been observed in various rapid growers such as *M. smegmatis*, *M. chelonae*, and *M. parafortuitum* (Kaneda et al., 1986). Methoxy-mycolates, with few exceptions, appear to be only present in pathogenic mycobacteria and slow growers (Barry et al., 1998). Evidence suggests the ability of slow-growing pathogenic mycobacteria, to modify their mycolate profile depending on the environmental conditions. Ketomycolate production from the Mtb H37Rv strain

appears to be increased during exponential growth and bacteria growing within macrophages (Yuan et al., 1998).

The role of the different mycolate classes was addressed by Vander Beken et al. (2011). Synthetic MAs of the major classes, α -, keto- and methoxy-mycolate that varied in *cis* versus *trans* cyclopropane configuration were studied for their ability to elicit a pulmonary inflammatory response. Whereas the non-oxygenated α -MAs did not exert a response, the oxygenated keto- and methoxy MAs with a *cis*-cyclopropane configuration showed an inflammatory response that was stronger in the methoxy-MA class. This situation was different in the *trans* orientation where the keto-MAs showed an anti-inflammatory activity and methoxy-MAs diminished their inflammatory role. The origin and biological function of free MAs have been studied by Ojha et al. (2008, 2010). Free MAs were shown to be present in biofilms formed in *Mtb* cultures and further studies in *M. smegmatis* linked the presence of free MAs with the trehalose dimycolate (TDM) hydrolysis produced by a serine carboxyesterase.

MAs can be presented to T cells by the CD1 family of MHC-like molecules (Beckman et al., 1994). Montamat-sicotte et al. (2011) showed MAs as one of the major targets during active TB, showing a T cell response similar to that obtained with immunoprotein antigens such as ESAT-6 and CFP10. The IFN- γ response triggered by MAs inserted into liposomes as a tracheal treatment, prevented the airway inflammation of sensitized mice used as an asthma model, supporting the role of MAs in the development of a protective Th1 response (Korf et al., 2006).

2.2.2 Phosphatidylinositol based glycolipids

Another molecule that has a major presence in the mycobacterial cell envelope is the lipoglycan lipoarabinomannan (LAM). LAM and the LAM precursor lipomannan (LM) are anchored to the plasma membrane by a phosphatidylinositol mannoside (PIM), commonly PIM₂. The mannan core is based on an α 1→6 linked backbone branched by single mannopyranosyl residues, followed by a D-arabinan domain in the case of LAM. The predominant fatty acyl chains are palmitate (C16:0) and 10-methyloctadecanoate (tuberculostearate, C19) (Chatterjee, 1998).

The non-reducing terminus of the arabinan of LAM can be uncapped (AraLAM) or either capped with mannose (ManLAM) or inositol phosphate (PILAM). The differences between the AraLAM and ManLAM motifs were proposed as an indicator between virulent and avirulent strains, respectively (Chatterjee et al, 1992). However, the avirulent *Mycobacterium bovis* Bacille Calmette Guerin (BCG) strain and the virulent Mtb H37Rv strain were found to belong to the ManLAM class (Venisse et al., 1993). PILAMs has been isolated from rapidly growing mycobacteria such as *M. smegmatis* (Khoo et al., 1995) and are characterized as proinflammatory molecules, stimulating the production of TNF- α and IL-12, while ManLAMs play an anti-inflammatory role, inhibiting the human macrophages/dendritic function for their production (Vercellone et al., 1998). These facts are in agreement with the capacity of Mtb and *M. bovis* BCG to survive and multiply inside macrophages (Nigou et al., 2002). Evidence has been provided about the role of LAM during the immune response. LAM induces a physical association between the signaling domains of Toll-like receptor (TLR) 1 and TLR2. TLR1 and TLR2 are pivotal components of the mammalian innate immune response and would mediate the mechanism for LAM-induced cellular activation (Tapping et al., 2003), and cytokine production. The

induction by LAM of TNF- α release could explain some of the characteristics of TB, such as fever, weight loss, and necrosis (Moreno et al., 1989). ManLAM triggers a preferential induction of interleukin (IL)-10 that is going to negatively regulate the caspase and prevents the Mtb-induced calcium influx. These events are responsible for the inhibition of apoptosis in Mtb-infected macrophages (Nigou et al., 2002).

As mentioned, PIMs play a role as the common anchor for LM and LAM, but they can also exist as free glycolipids in the plasma membrane or in the cell wall. They are synthesized by all species of mycobacteria and the predominant forms are mono- and diacylated PIM2 and PIM6. PIMs activate human and murine natural killer (NK) T cells via CD1d, triggering antigen-specific IFN- γ production and cell-mediated cytotoxicity in a CD1d-restricted way (Fischer et al., 2004). PIM6 and PIM2 activate primary macrophages to secrete TNF- α via TLR-2 activation, contributing to the innate immunity necessary to contain latent infection (Gilleron et al., 2003).

2.2.3 Glycolipids based on trehalose

Another important group of lipids in the Mtb cell wall structure are the acylated trehaloses. The cord factor, trehalose 6, 6'- dimycolate (TDM), consists of one trehalose attached to two MAs moieties (Noll et al., 1956). Hunter et al. (2006) discovered that depending on its conformation, TDM has two sets of biological activities. In aqueous suspension it has a micellar conformation, where the surface consists in trehalose moieties with no exposed fatty acids. This form is non-toxic and protects organisms from killing by macrophages, preventing phagosome/lysosome fusion and acidification. Conversely, in a monolayer conformation becomes highly toxic and immunogenic.

The molecular structure of TDM, exhibits differences according the mycobacterial species and subspecies (Fujita et al., 2005). TDM can induce granuloma formation associated with neovascularization through cytokine-dependent mechanisms (Saita et al., 2000). This lipid also modulates critical immunological mediators like cytokines and nitric oxide (Lima et al., 2001) and provides striking resistance to desiccation of membranes (Harland et al., 2008). TDM affects the integrity of the mitochondrial membrane system, inhibiting the oxidative phosphorylation process (Kato, 1970). Despite all these properties, TDM has also been found in non-pathogenic mycobacterial species (Mompon et al., 1978). It has been proposed that the cyclopropane modification of TDM is necessary for the cording morphology, associated with virulence. The avirulence of saprophytic mycobacteria would be explained by the absence of TDM with cyclopropanation of MAs (Glickman et al., 2000).

Other members of the trehalose containing glycolipids group are made of an α - α' -D-trehalose esterified with up to five multiple methyl-branched long-chain fatty acids and are characteristic of the envelope of pathogenic mycobacteria. The trehalose esters are comprised of sulpholipids (SL), diacyltrehaloses (DAT), triacyltrehaloses (TAT) and polyacyltrehaloses (PAT) (Rousseau et al., 2003). Their role in serodiagnostic studies has been evaluated by comparing the antigenicity between SL, DAT, TAT and TDM. SL-I showed the best sensitivity and specificity for IgG and IgA responses (Julián, et al., 2002).

2.2.3.1 Sulfolipids

Sulfolipids (SL) are trehalose derivatives acylated with two to four fatty acids. The sulphate ester is at position 2 of trehalose, a straight-chain fatty acid (palmitic or

stearic acid) is found at position 2' and one to three hepta- or octa-methyl-branched phthioceranic and hydroxy-phthioceranic (C_{31-C46}) acids are found in the 3', 6 and 6' positions (Neyrolles et al., 2011). Sulfatides have been only isolated from Mtb and *M. canetti*, but not from other members of the MTBC (Neyrolles et al., 2011). Studies performed by Goren et al. (1976) using chromatographic separation and mass spectrometry, described SL-I as the principal sulfatide in Mtb. However, in a recently study of Mtb H37Rv, employing high-resolution multiple-stage linear ion-trap mass spectrometry with electrospray ionization, SL-II was described as the major class (Rhoades et al., 2011).

Between the biological activities of purified SL, the most controversial is their ability to prevent phagosome lysosome fusion in murine macrophages (Goren et al., 1976). Other biological activities associated with SL-I are strong inhibition of the respiration and phosphorylation in the mitochondria, and disruption of the mitochondrial membranes (Kato et al., 1974). The generation of mycobacterial mutants has contributed to deciphering the role of these compounds. *Pks2* gene mutants are incapable of producing major acyl constituents of SL such as hydroxyphthioceranic acids and hepta and octamethyl phthioceranic acids (Sirakova et al., 2001). The SL deficiency of a *pks2* mutant of Mtb H37Rv did not contribute significantly to the virulence of the Mtb strain (Rousseau et al., 2003). Other *in vivo* studies showed no toxic effects with the use of high doses of SL-I in mice; however, a synergistic activity with the toxicity of cord factor was achieved when the two lipids were injected simultaneously into mice (Kato et al., 1974).

2.2.3.2 Other acylated trehalose molecules

The fatty acyl substituents of trehalose can be of three types: i) trehaloses acylated with mycolipenic acids (C₁₆-C₁₉), ii) acylated with mycolipanoic acid (C₂₄-C₂₈), and iii) acylated with mycosanoic acids (C₂₁-C₂₅) (Besra et al., 1992).

Mycolipenic acids (phthienoic acids) are the major acyl substituents found in the trehalose containing glycolipids PAT, TAT and some forms of DAT, and they are easily detected using simple gas-liquid chromatography. They have been isolated only from the TB complex, specifically Mtb, *M. bovis* and *M. africanum* but not detected in the avirulent Mtb H37Ra or in the attenuated vaccine strain *M. bovis* BCG (Daffé et al., 1988). These fatty acids are noted as potent inhibitors of leucocyte migration *in vitro* (Husseini and Elberg, 1952).

Dubey et al. (2002) achieved the inhibition of mycolipanoic and mycolipenic (phthienoic) acids synthesis by disrupting the mycocerosic acid synthase like gene (*msl3*). As a consequence of this mutation, the growth pattern and morphology changed, and the cells appeared to stick to each other. This situation could be explained by the absence of the acylated trehaloses producing an exposure of hydrophobic surfaces of components like dimycocerosyl phthiocerol. The wild type H37Rv strain and the *msl3* mutants were compared by the study of mouse bone marrow macrophages. The mutant strains showed a higher entry rate into host cells as compared to the wild type strain, but not significant differences in the persistence and replication. It was concluded that deficiencies in DAT and PAT produced by *msl3* mutants, modified the surface properties of the bacteria, however other amphiphilic molecules, such as SL, can ensure the attachment of the capsule to the host cell (Rousseau et al., 2003).

2.2.4 Phenol glycolipids

Phenol glycolipids (PGLs), also called mycosides, are present in some mycobacterial strains and possess mycocerosic acids (C₂₇-C₃₄), esterified to a phenolphthiocerol glycosylated with an oligosaccharide (Minnikin, 1982). PGLs are known to be produced by *M. leprae* (PGL-1), *M. kansasii* (mycoside A), *M. bovis* (mycoside B), a few strains of Mtb (PGL-tb) and a few of other slow-growing mycobacteria such as *M. marinum*, *M. gastri*, *M. ulcerans*, *M. microti* and *M. haemophilum* (Guilhot et al., 2008).

In the case of *M. leprae*, PGL-1 has been vinculated to the binding of Schwann cells, affecting the function of the peripheral nervous system (Ng et al., 2000). Generally, clinical isolates of Mtb lack PGL production due a mutation in a polyketide synthase gene (pks1-15) (Constant et al., 2002). The exception is the W-Beijing family of Mtb that possesses an intact pks1-15 (Reed et al., 2007). Beijing strains stimulate weaker production of TNF- α and IL-12 when infecting human monocytes. Despite this, PGL-tb is not considered a dominant suppressor factor for the cytokine response, but is proposed to be part of an orchestrated response for the particular strain (Sinsimer et al., 2008).

2.2.5 Mycobacterial waxes

The mycobacterial waxes present in the cell wall are complex lipids with a high molecular weight. The phthiocerol dimycocerosates (PDIMs) are composed of a long β -diol chain diesterified with methyl-branched long chain mycocerosic acids (Minnikin et al., 1985). PDIMs have been found in Mtb, *M. bovis*, *M. gastri*, *M. haemophilum*, *M. kansasii*, *M. leprae*, *M. marinum* and *M. ulcerans* (Minnikin et al., 2002), and were found to be a virulence factor in mice (Cox et al., 1999). These

lipids interact with the host during the phagocytosis of Mtb, by inducing changes in the lipid ordering of the plasma membrane and the prevention of phagosomal acidification (Astarie-Dequeker et al., 2009). In Mtb, insertional mutants unable to synthesize or translocate PDIMs exhibit higher cell wall permeability and are more sensitive to detergent action (Camacho et al., 2001).

3. Diagnosis of tuberculosis

3.1 Introduction

An early diagnosis of the individuals with active TB, leads to an effective therapy, reducing the transmission rate (Menzies et al., 2011). A definitive case of TB can be diagnosed from a clinical specimen by culture or by non-conventional techniques such as a molecular line probe assay (Goto et al., 1991). Several biomarkers are used for TB diagnosis, in the area of clinical trials, a biomarker is defined as a characteristic feature that is objectively measured and evaluated as an indicator of a normal or a pathological process, or the response to an intervention (Biomarkers Definitions Working Group, 2001).

In countries that lack enough resources and laboratory capacity, the smear examination is fundamental, and diagnosis of TB can be done through one or more sputum smear examinations positive for acid-fast bacilli (AFB) (WHO, 2010). Conventional light microscopy is routinely used, but it is noted for low sensitivity, because of the need for more than 10^4 bacilli per ml of sputum. Thus, half or more of the cases of active pulmonary TB are misclassified as smear-negative (Chan et al., 2000). To strengthen the technique, fluorescence smear microscopy has been introduced, using an acid-fast fluorochrome dye (eg, auramine O or auramine-rhodamine) and a halogen or high-pressure mercury vapour lamp as a light source. The technique has shown to be more sensitive than conventional microscopy, and has similar specificity. It also has the advantage of using a lower power objective lens compared to a light microscopy, allowing the microscopist to cover the same area of the slide in less time (Steingart et al., 2006).

Culture remains as the gold standard for diagnosis of TB and is about 100 times more sensitive than the smear microscopy applied to sputum samples (Aryan

et al., 2010). The main limitation to culture is the long period of incubation (4 to 8 weeks), also called turn around time (TAT) (WHO, 2007). An improvement was achieved with the use of semi-automated commercial liquid systems that can reduce the TAT to 10 days. BACTEC 460 and BACTEC MGIT 960 (Becton Dickinson) are examples of these liquid systems. The BACTEC 460 uses ^{14}C -labelled fatty acid as a substrate to measure Mtb growth based on the amount of $^{14}\text{CO}_2$ released. The MGIT system does not require a radioactive substance and is a fully automated system that detects the amount of oxygen consumption of growing microorganisms by the use of a fluorescence quenching-based oxygen sensor (Pheiffer et al., 2008).

Another diagnostic tool that reflects the presence of viable Mtb is the use of mycobacteriophages. FASTplaqueTB assay (BIOTEC laboratories) utilizes a mycobacteriophage to target the mycobacterial cells. The use of a virucidal agent eliminates the bacteriophages that have not infected a target and only the bacteriophage progeny is amplified in sensor cellsTM (a rapidly growing mycobacterial strain, susceptible to the phage). The presence of plaques in the Petri dish is evidence of viable TB in the original sample (Marei et al., 2003).

Despite these improvements, culture tests are technically demanding and time-consuming. Chest radiography is also used, but it lacks of specificity especially in those immunocompromised individuals, because of the atypical x-ray patterns (McNerney et al., 2011). Therefore, there is a need of other methods to subvert the weakness of the conventional tools applied in TB diagnosis (Aryan et al., 2010).

3.2 An overview of the use of biomarkers in TB diagnosis

The use of biomarkers in TB includes their application for immunologic responses detection, transcriptomics and proteomics of differentially expressed

genes and proteins, and metabolomics. Any combination of these has been proposed or studied as a tool to distinguish latent TB from active disease, predict risk of disease progression or portray the status of the infection (Parida, 2010). The use of biomarkers is also promoted as an alternative prognostic tool for the establishment of an adequate prophylactic chemotherapy, given the high percentage of worldwide TB infected population and the subsequent risk to progress to an active disease after an immune system weakness (Kaufmann et al., 2008).

Moreover, biomarkers can be used as surrogate endpoints in vaccine development. In this case biomarkers intend to substitute a clinical endpoint, predicting clinical outcome in terms of benefit, or harm, or lack of benefit or harm (Biomarkers Definitions Working Group, 2001). In this scenario, biomarkers could help to accelerate the development process at different stages of clinical trials (Kaufmann et al., 2008). Because of the biological complexity of most infections, the use of a set of biomarkers increases the possibility of an accurate diagnostic. In the case of TB, the detection of circulating biomarkers that are secreted by the pathogen has the advantage of being detected in samples such as blood, urine or sputum, avoiding invasive procedures such as cerebrospinal fluid, lymph node aspirate or other biopsies and can be especially useful in patients with advanced humoral immunosuppression (Mc Nerney et al., 2011).

3.2.1 DNA/RNA biomarkers in TB

Nucleic acid amplification (NAA) tests are used to amplify targeted nucleic acid regions of the Mtb complex and they can be applied directly to clinical specimens, such as sputum. Thus they are also called “direct amplification tests” and are present as commercial kits or in-house assays (Nahid et al., 2006). The main

advantage of NAA is reducing the TAT to one day. The Gen-Probe Amplified *Mycobacterium tuberculosis* Direct (MTD) test (Gen-Probe Incorporated, San Diego, CA) employs a single-stranded labeled DNA probe, complementary to the rRNA of the pathogen (Teo et al., 2011). Xpert MTB/RIF (Cepheid, Sunnyvale, CA) is a recommended test by the WHO that can be used directly on sputum samples and is an automated molecular test for Mtb and RIF resistance detection. A hemi-nested real-time polymerase-chain-reaction (PCR) assay is used to amplify a Mtb-specific sequence of the *rpoB* gene (involved in the coding of the β subunit of the RNA polymerase) that is probed with molecular beacons for mutations within the RIF-resistance region (Boehme et al., 2011). Another NAA test is the loop-mediated isothermal amplification (LAMP) where high amounts of insoluble salt of magnesium pyrophosphate are produced in the amplification reaction, allowing a visual naked-eye detection of positive reactions by changes in turbidity. LAMP has been used to target the insertion sequence (IS) 6110 and the genes *rrs* and *gyrB* of Mtb. This diagnostic tool has been used for the detection of Mtb in sputum samples. The advantages of this technique include its lower cost and rapidity when compared to the IS6110 targeted by classical PCR, and it also does not require a thermal cycler because reactions are performed at a fixed temperature (60–65°C) (Aryan et al., 2010).

Other biomarkers from host origin include the DNA fragments of Mtb, termed transrenal DNA (tr-DNA). Tr-DNA have been detected in the urine of patients infected with pulmonary TB, suggesting the possibility that Mtb DNA could be cleared through the kidneys after an apoptotic process of the infected cells (Cannas et al., 2008). The use of PCR followed by amplicon characterization using electrospray ionization mass spectroscopy has been used for Mtb genotyping, and

NTM and MDR characterization (Massire et al., 2010). By the use of softwares the organism can be identified by the measure of the mass-to-charge ratio of the amplicon and also the base composition (Wolk et al., 2009).

3.2.2 Immunological biomarkers

Biomarkers involved in the immunological response have been used for the study of TB in active and non-active individuals, and also in the evaluation of antituberculosis therapy. The MycoDot™ assay is based on the detection of LAM antibodies using an immuno-dot-blot technique. Because this technique is developed on solid membranes supports, it has the advantages of being fast and does not require special equipment. Thus, it was suggested as a platform to use in rural or undeveloped areas with limited resources (Antunes et al., 2002). LAM has been explored in a number of studies using serum, urine, sputum and cerebrospinal fluid (CSF). Studies in unprocessed urine, provides a tool for the diagnosis of pulmonary, as well as extrapulmonary mycobacterial infection, using a direct antigen enzyme-linked immunosorbent assay (ELISA) for LAM detection. LAM has been proposed to be released from metabolically active or degrading bacterial cells. Once in the bloodstream, LAM can be filtered by the kidneys, and detected (Boehme et al., 2005). Clearview-TB® is a LAM antigen-detection ELISA, standardized for urine samples. Using this test, Dheda et al. (2010) determined the diagnostic accuracy of LAM in urine and sputum samples from HIV-infected patients belonging to different CD4 T cell categories. Results showed a promising use of this diagnostic tool, but limited to the group of HIV infected patients with smear negative and a CD4 count less than 200 cells/mm³. Sputum-LAM showed good sensitivity (86%) but poor specificity (15%) probably due to cross-reactivity with LAM-like microbial

carbohydrate surface molecules in the cell walls of mouth-residing organisms such as *Candida*, and many species of *Actinobacteria*. Clearview-TB ® was also used as a diagnostic for tuberculous meningitis (TBM) using CSF samples. The results also suggested this assay as useful for TBM in HIV-infected individuals with advanced immunosuppression (Patel et al., 2010).

Antigen 5 (38 kDa antigen), A60 antigen (a thermostable component of PPD), 30kDa antigen and cord factor are examples of other antigens used (Cole et al., 1996., Lu et al., 1996., Mc Donough et al., 1992). The groups that would benefit from these serological diagnosis correspond to young children, the elderly, HIV-positive individuals, and patients with extrapulmonary TB. This is because the difficulty in obtaining sputum samples from these individuals and the lower incidence of AFB in respiratory samples. The serological assays have the issue of a low sensitivity in the negative smear/positive culture group. This is a main limitation since this group would receive significant benefit using these diagnostic techniques (Chan et al., 2000).

Monocytes/macrophages have been proposed to be the main source in humans of neopterin, classified as a biochemical marker of cell-mediated immunity, released into body fluids (Berdowska et al., 2001). Serum neopterin is shown to be higher in patients with active TB than in healthy control groups and has also been used as a biomarker to evaluate the response of antituberculosis therapy showing a steadily decrease from the baseline point to the end of antituberculous therapy (Turgut et al., 2006).

The importance of identifying those latent tuberculosis infection (LTBI) cases lies in providing an adequate therapy that prevents development of active disease (Ziv et al., 2001). The available tests to identify LTBI include the *in vivo* tuberculin

skin test (TST) and the *ex vivo* IFN- γ release assays (IGRAs), which can identify an adaptive immune response (Mack et al., 2009). The TST is one of the few tests that has been continuously in use for about 100 years in clinical medicine and consists in the use of a purified protein derivative (PPD) which measures a delayed-type hypersensitivity (DTH) response in the skin (Mack et al., 2009). Tuberculin PPD is a crude mixture of antigens shared by different mycobacteria, thus affecting the sensitivity of the test (Jasmer et al., 2002). When individuals sensitized by *Mtb* are exposed to mycobacterial antigens, T-cells release IFN- γ in a response to those antigens and this cytokine can be detected using IGRAs as *ex vivo* enzyme-linked immunospot (ELISPOT) assay or by the whole blood ELISA (Mack et al., 2009). ESAT-6 (Andersen et al., 1995) and CPF-10 (Berthet et al., 1998) are two proteins coded by the genes contained in the region of deletion 1 (RD1) present in *Mtb* and *M. bovis*, but excluded from the avirulent BCG strain. The deletion of RD1 in BCG has been suggested as an original attenuating mutation of this strain (Mahairas et al., 1996). The IFN- γ based T cell response assay to ESAT-6 and CPF-10 has been shown to detect active and latent TB (Lalvani et al., 2001). The commercially available assay T SPOT-TB (Oxford Immunotec, Oxford, UK) was used by Meier et al. (2005) to compare the results between T SPOT-TB and TST in 45 patients with confirmed TB, indicating a sensitivity of 100% versus 89% respectively ($p=0.056$). As Mack et al. (2009) proposed in his review, individuals diagnosed as positive by TST or IGRAs have a higher risk to progress to active TB. However, a proportion of them will not develop the disease because their immune system is able to control the infection or simply because they are no longer infected with living bacteria. Thus positive individual would best indicate “lasting TB immune responses” but not necessarily true “latent TB infection”.

Differences between contacts of TB patients, who later develop TB disease (progressors), versus contacts who remain healthy (non-progressors), were analyzed using different immunologic biomarkers. The major difference in the adaptive immune response was a significantly lower proportion of CD4+ T cells in progressors compared to non-progressors. This was related with the concomitant decrease of the of the antiapoptotic gene Bcl2 leading to T cells apoptosis, a detrimental situation in the control of disease progression. Higher levels of IL-18, a precursor of IFN- γ production, were also founded in progressors pointing to have a role in the early stages of Mtb infections (Sutherland et al., 2011).

3.2.3 Biomarkers identified by the use of proteomics

Serum proteomic profiles from patients with active TB and controls were analyzed by surface-enhanced laser desorption ionization time of flight mass spectrometry. Amyloid A and transthyretin were identified as biomarkers associated with the inflammatory state of TB and the transport of retinoic acid, which stimulates monocyte differentiation respectively (Agranoff et al., 2006). Proteomics has also been explored in the biomarker field in the study of *M. bovis* and *M. paratuberculosis* in cattle. Sera protein profiles of experimentally infected animal either with *M. bovis* or *M. paratuberculosis* were compared, identifying common and distinct biomarkers for both diseases. A common biomarker was vitamin D binding protein precursor (DBP), known to be involved in macrophage activation and vitamin D transportation (Kisker et al., 2003). In the particular case of *M. paratuberculosis*, cathelicidins (a group of antimicrobial peptides) were identified at greater levels when 10 month post infection groups were compared to control groups (Seth et al., 2009).

3.2.4 Metabolites as biomarkers for TB

Metabolomics allow the study of all detectable metabolites of bacterium or host origin in a small number of experiments. TB can be detected by the analysis of very small metabolites including volatile compounds (VOCs). Surprisingly Hippocrates, an ancient Greek physician, recorded as one of the first test for TB the placing of sputum samples on hot coals, assessing the foul odour that was given off (Mc Nerney et al., 2011). In the same context, African giant pouched rats (*Cricetomys gambianus*) were trained for the diagnosis of TB in human sputum. Within the advantages of this method, the authors mentioned the resistance of the sniffers rats to TB infection and the larger amount of samples able to be screened. In this study the average daily ranging for sensitivities was from 72% to 100%, and the false-positives ranging was from 0.7% to 8.1% (Weetjens, 2009).

Species-specific volatile metabolites from *Mtb* and *M. bovis* cultures grown *in vitro* were identified using gas chromatography/mass spectrometry. Four compounds corresponded to methyl phenylacetate, methyl p-anisate, methyl nicotinate and o-phenylanisole, were detectable before the visual appearance of colonies. From the characterized compounds, methyl nicotinate was selected for validation *in vivo*. Nicotinic acid has an important role in oxidation-reduction reactions in mycobacterial metabolism. Higher levels of methyl nicotinate were shown in the smear positive samples from TB patients, compared with the control group (Syhre et al., 2009).

In another study, VOCs in the breath of suspected TB patients and control individuals were analyzed by gas chromatography/mass spectroscopy and compared to VOCs produced by *Mtb in vitro*. A similar profile of VOCs was observed in breath and culture VOCs, and included naphthalene, 1-methyl- and cyclohexane, 1,4-dimethyl- (Phillips et al., 2007).

4. TB lipids as biomarkers in Mtb

4.1 Application of lipidomics for the study of Mycobacterium lipids as biomarkers

Because of the unique features of the TB cell wall, different cell wall compounds have been studied for their use as biomarkers. Through the use of lipidomics, lipid molecular species and their interacting moieties are characterized. Analytical methods, and in particular mass spectrometry (MS) and liquid chromatography (LC) have been used broadly in this research field (Wenk, 2005).

Other techniques include in lipid research are thin layer chromatography (TLC), gas chromatography (GC) and high-performance liquid chromatography (HPLC). GC typically requires derivatization of the sample to make the analytes more volatile. Normal phase LC leads to separation of lipids on the basis of their class and reversed-phase chromatographic methods lead to retention time differences according to fatty-acyl composition. Initial separation of lipids by LC resolves compounds prior to enter into a mass spectrometer, resulting in less ion suppression, high ionization and enhancement of the sensitivity for minor molecular species (Wenk, 2005).

A mass spectrometer measures the mass-to-charge ratio (m/z) of gas-phase ions. For electrospray (ES)-MS the sample is typically delivered to the mass spectrometer through a chromatographic device (e.g. column), afterwards it is ionized and vaporized in the ion source, and the resultant ions are sorted according to their m/z in the mass analyzer, providing a mass spectrum that displays the abundance and the m/z of the different ions (Griffiths et al., 2009). In addition to electron impact (EI) ionization and the soft ionization techniques electrospray ionization (ESI), matrix assisted laser desorption/ionization (MALDI) is also applied in

lipidomic studies. The choice of the ionization technique is going to depend of the chemical properties of the analyte. ESI is very efficient for the ionization of polar compounds and has the advantage of coupling the HPLC system to MS (Siuzdak, 1994). For the analysis of less polar compounds atmospheric pressure chemical ionization (APCI) is more suitable. The main difference between these two techniques is that ions are generated in the liquid phase by using ESI and in the gas phase by using APCI (Schmitz and Benter, 2007).

The mechanism of ion formation can vary. Analytes suitable for ESI analysis already possess charged groups such as quaternary amines, or can be charged by the gain or loss of protons. In the case of the positive ion mode, lipids tend to form positive ion adducts. Sodium adducts are the most common in crude lipids extracts from biological samples. Ammonium adducts can also be present when ammonium salt are used in the system. Fatty acids are typically observed deprotonated species detected in the negative ion mode (Cole, 2010).

Mass spectral databases and software protocols for automated ion detection and identification; facilitate the differentiation of the mycobacterial lipid classes. “Mycomass”, “Mycomap” (Layre et al., 2011) and “Mtb LipidDB” are examples. “Mtb LipidDB” uses accurate mass measurements for lipid identification, providing 2,512 lipid entities identified in negative or positive ionization mode, depending on their chemical structure (Sartain et al., 2011).

Lipidomics have been applied for mycocerosic acids and tuberculoestearic acid (TSA) detection in sputum and CSF samples respectively. However, TSA detection has been questioned in specificity, because it is also present in other microorganisms of the *Actinomycetales* order (Alugupalli et al., 1998, Larsson et al., 1987). Minnikin et al. (1993) tested the detection of TSA and mycocerosic acids by

GC and MAs by LC in sputum samples from TB patients. The integrated method showed characteristic profiles for each lipid category, supporting the idea that the use of a set of lipid biomarkers can help to subvert the lack of specificity. Mycocerosic acids have been also used as biomarkers for diagnosis of ancient TB. Rib bone samples from individuals who died between 1910 and 1936 (48% being associated with TB as a cause of death after clinical examination) were processed and analyzed by normal phase HPLC. 33% of the 49 samples were negative for the analysis. For the positive samples, C32, C29 and C30 mycocerosates, were the major components detected. In this study the detection of C27 mycolipenates (a multimethyl-branched group of fatty acids present in the TB cell wall) was also achieved (Redman et al., 2009). A characteristic feature of *M. ulcerans* is the production of the lipidic-nature toxin mycolactone. Skin samples from *M. ulcerans*-infected patients were analyzed by using TLC and MS. Mycolactone was detected from early to ulcerative lesions and also from lesions from patients under antibiotic therapy (Sarfo et al., 2010).

4.2 Mycolic acids as biomarkers for Mtb detection

Given the MAs role in immunogenicity and pathogenicity, they have been used as antigens for the serodiagnosis of TB. However, the sensitivity of the assays has been postulated to be affected by the interaction of MAs with cholesterol. A similar structural conformation and attraction between free carboxylic group of individual MAs was also proposed as a reason the poor sensitivity of the ELISA tests (Benadie et al., 2008). Another approach for the antibody detection is the use of MAs liposomes immobilized on a biosensor cuvette that allow to monitor and quantify the interaction of analytes in real time (Thanyani et al., 2008).

The different classes of MAs can be separate using normal TLC, however, the profile is not a diagnostic criteria for the Mtb complex because it is shared with other mycobacterial species. The use of reverse HPLC allows the separation by length and polarity, producing characteristic peaks to identify *Mycobacterium* species by the different profiles obtained (Buttler et al., 2001). Moreover, HPLC coupled to MS can produce an improvement in MA detection by providing accurate molecular weights (Shui et al., 2007; Minnikin et al., 2010). The presence of MAs in biological fluids has been studied in sputum samples from TB patients. MAs converted to anthrylmethyl esters were detected using fluorescence HPLC obtaining characteristic profiles for these lipids (Minnikin et al., 1993). The use of ESI/MS has also been applied for the direct measurement of MAs in sputum samples (Shui et al., 2011). To evaluate the use of MAs as biomarkers for diagnosis and drug therapy monitoring, Shui et al. (2011) analyzed sputum based in a retrospective, multi-center, case control study using MS. Non-oxygenated MAs with C₂₆ α-chains were the best MAs biomarkers to classify active versus non-active (cured) patients originating from South Africa, Vietnam and Uganda. For monitoring drug efficacy, lung tissue of mice infected with Mtb was analyzed for MAs presence and compared with mice infected with Mtb, treated with RIF until obtaining negative culture for Mtb. Results showed a decrease of MAs in the last mentioned group. However, when the Korean patients study was performed, no differences were observed in MAs profiles between infected individuals who received anti-TB chemotherapy and those who did not.

Analysis of archeological samples can provide important information about ancient microorganisms and the tracking of their evolution using molecular techniques. The study of TB in archeological samples can be performed by the analysis of morphological changes in skeletal material, like spinal destruction.

However, the specificity of the diagnosis using these parameters can be affected by other diseases that cause similar physiological changes (Redman et al., 2009). Skeletal remains dating from 9250-8160 years ago of a woman and a child with characteristic lesions of TB were analyzed by HPLC and PCR to explore the use of MAs as biomarkers. The results showed the characteristic profile for α , keto and methoxy mycolates using normal and reverse phase HPLC. Mtb complex DNA was detected giving positive results for the multi-copy IS6110 and IS1081 (HersHKovitz et al., 2008). These data not only help to validate MAs as robust markers of TB, but also demonstrate the long term stability of these products.

5. Project Rationale

Development of new tools for the diagnosis and control of TB is a major challenge. In this context the use of biomarkers can be applied for detecting characteristic signatures from the pathogen. The unique and rich lipid profile of the mycobacterial cell wall make it an interesting target for lipidomics studies and the analysis of biomarkers that can be used in diagnosis or prognosis of drug efficacy in TB infected patients. If a specific biomarker or set of biomarkers are identified to have a good correlation with the clearance of the disease, they can be measured after the establishment of the treatment to evaluate the progress of the treatment and identify if the drug is being effective or not.

MAAs represent an important percentage of the Mtb cell wall and are characteristic of this pathogen. These lipids have been detected in clinical samples such as sputum, by using LC-MS. However, analyses in other biological fluids such as serum or urine from TB patients are still unavailable.

Biological fluids can be challenging for the detection of MAAs using LC-MS, mainly because of many compounds compete in the ionization process and those in less abundance can be in a detrimental situation with respect to the more abundant compounds. In this scenario, the derivatization of chemical structures can be used as a tool to improve the sensitivity of the LC-MS technique. Fatty acids are comprised in their structure of carboxylic acids, this fact make them negatively charged through deprotonation of the acidic group and as a result they can be analyzed in the negative-ion mode by MS (Cech et al., 2002). However, the detection sensitivity and specificity can be affected because of the high background noise (Santa et al., 2007). Ionization efficiency is related to quantification in LC/MS. Matrix suppression of ionization can greatly reduce sensitivity and complicate

quantification. Ionization efficiency of analytes can be variable, depending on the concentration of other analytes in the mixture that could suppress their ionization. Increasing the ionization is one way to subvert these problems; this can be achieved by using derivatization methods to improve the ionization (Yang et al., 2007). Chemical derivatization involves a reaction between the analyte molecule and the derivatization reagent. For LC/MS it is common to incorporate cationic groups for positive-ion mode and strongly acidic groups for negative-ion mode, or other groups that improve ionization (Eggink et al., 2010). As a consequence of the derivatization process, the physical and chemical properties of the analyte change, allow an increase in the ionization efficiency. Another advantage of the derivatization process is the change in the chromatographic retention of the analyte, reducing the suppression of ionization due to the presence of molecules that co-elute with the target analyte (Gao et al., 2005).

There are different ways to derivatize compounds that are comprised of carboxylic acids in their structure (Santa et al., 2010). In the case of MAs, phenacyl esters have been used to improve their detection by HPLC utilizing UV detection (Butler et al., 2010). Also methyl esters of MAs have been used for TLC and MS analysis. By the methyl esterification of the carboxylic acid, the MAs can separate properly by TLC avoiding interactions with the silica that make separation incomplete (Laval et al., 2001). As it was mentioned, enhancement of ionization efficiency is one of the final purposes when derivatization protocols are used. Yang et al., (2007) studied a derivatization protocol for fatty acids from C₁₀ to C₂₄ by adding a positive charge through the introduction of a quaternary amine. The detection of the fatty acids using the positive ionization mode, allowed a 2,500 fold enhancement of the

fatty acid detection, comparing the derivatized fatty acid in positive mode versus the non-derivatized in negative mode.

We hypothesize that enhanced detection of MAs will be achieved in the positive ion mode by applying the chemical derivatization method described by Yang et al., (2007). By using this method, a quaternary amine is expected to be attached to the carboxylic group of the MA structure, giving a positive charge to the compound, and allowing an improvement in the MA ionization that will be reflected in a better detection by using LC/MS in the positive mode.

6. Material and methods

6.1 Material and reagents

6.1.1 Material

The MA standard used during this study was extracted from Mtb strain H37Rv as is explained in section 6.2. To test the derivatization protocol the MA standard was considered as a sample to be derivatized. MA standard was also used to spike human urine and human serum previous the derivatization process. Serum was purchased from Sigma-Aldrich (St. Louis, MO) and urine from Gemini-Bio products (West Sacramento, CA).

6.1.2 Reagents

2-bromopyridine, 3-carbinolpyridine, triethylamine (TEA), iodo- methane, ammonium acetate, potassium hydroxide, hydrochloric acid, and sodium dodecyl sulfate were purchased from Sigma-Aldrich (St. Louis, MO). Acetonitrile, water, acetone, chloroform, methanol, hexane, and n-propyl alcohol were purchased from Honeywell Burdick and Jackson (Muskegon, MI) and diethyl ether from Alfa Aesar (Ward Hill, MA). All the chemicals were analytical or LC-MS grade.

6.2 Extraction and purification of mycolic acids

Mtb strain H37Rv is the reference strain used worldwide to study the pathogenesis and virulence of Mtb. It was originally isolated from a chronic case of pulmonary TB in 1905. Since then, the strain has been maintained and currently is part of the American Type Culture Collection (ATCC) (Zheng et al., 2008).

MA's were extracted from an ATTC reference strain to perform the different experiments during this study.

6.2.1 Extraction of the mycolic acid-peptidoglycan-arabinogalactan (mAGP) complex

For the MAs extraction, 13.325 g (dry weight) of Mtb cells (H37Rv) that had been delipidated with chloroform: methanol (2:1 v/v) were split into two Oakridges tubes and suspended in 30 ml of HPLC water. The main goal of the initial process is to remove proteins and free lipids from the mAGP. For this, 30 ml of 2% sodium dodecyl sulfate (SDS) were added to each tube, stirring them at room temperature for 30 minutes followed by centrifugation at 27,000 xg at 25°C for 10 minutes. The supernatants were decanted and the SDS wash was repeated. After this, 20 ml of 2% SDS plus 1 ml (5 mg) of proteinase K (Promega, Madison, WI) were added. The samples stirred at room temperature for 10 minutes. The samples were centrifuged at 27,000 xg for 10 minutes and the supernatants were decanted and 20 ml of 2% SDS were added to the pellets. Samples were stirred at 90°C for one hour and centrifuged at 27,000 xg, at 25°C for 10 minutes. The SDS wash at 90°C was repeated twice. The SDS extracted pellets were washed with 30 ml of HPLC water (8 times). To remove residual SDS the water washed pellets were extracted with 30 ml 80% acetone (x2) and 30 ml of 100% acetone (x1). The fully extracted mAGP was placed in a chemical fume hood and allowed to dry. The purified mAGP was transfer to a new pre-weighted 16 x 100 mm glass tube (Daffe et al, 1990).

6.2.2 Base hydrolysis of mAGP

Aliquots of mAGP (50 to 100 mg) were placed into 16 x 100 mm glass tubes. 1M potassium hydroxide (2ml) in methanol was added per tube and allowed to react for 2 h at 80°C. HPLC water (2.5 ml) was added, the pH was adjusted to approximately 3.0 with 6 N HCl, and the saponified material was extracted twice with

4.5 ml of diethyl ether. The upper layer of diethyl ether for each extraction was collected after centrifugation at 2,800 xg at 20°C for 5 min. The ether fractions were pooled and back extracted with HPLC water. The final organic phases were transferred to a pre-weighed 16 x 100 mm glass tube and dried under nitrogen. 89.6 mg of MAs were obtained and dissolved in 1 ml of chloroform/methanol (2:1 v/v). Subsequently, 100 µl of MAs were applied to C-18 Sep-Pak® Vac RC 100mg cartridges (Waters Corp., Milford, MA) equilibrated with 5 ml of 100% methanol. The elution process was comprised of three steps: (i) 5ml of methanol, (ii) 5 ml of methanol: n-propanol: hexane (20:4:1 v/v), and (iii) 5 ml of n-propanol: hexane (80:20 v/v). The third fraction contained the MAs and was dried under nitrogen to use as a standard. A total of 77.4 mg of MAs were recovered and the purity was checked by LC/MS as described in section 10.4 (Bhamidi et al, 2011).

6.3 Synthesis of derivatizing reagents 2-Bromo-1-methylpyridinium Iodide (BMP) and 3-Carbinol-1-methylpyridinium Iodide (CMP)

To generate BMP and CMP the protocol of Yang et al (2007) was followed. Briefly, five-fold excess of iodomethane was added to 2-bromopyridine (10 mmol, 0.97 ml) or 3-carbinolpyridine (10 mmol, 0.96 ml). The solution was stirred at room temperature for 1 h. Afterwards the crystals were washed with cold acetone, and dried. The crystals of BMP and CMP were suspended in acetonitrile to a final concentration of 50 µmol/ mL and 200 µmol/ mL, respectively. The reagent solutions were freshly prepared before derivatization and were not used longer than a week to ensure the stability of the compounds.

6.4 HPLC ESI/APCI-MS

An Agilent 1200 HPLC (Agilent Technologies, Palo Alto, CA) equipped with a Waters XBridge C18 column (2.1 x 150 mm, 3.5 μ m) was used for chromatographic separation of MAs using a gradient of 100% of solvent A (99% methanol, 1% 5 mM ammonium acetate) to 100% solvent B (79% n-propyl alcohol, 20% hexane, 1% 5 mM ammonium acetate) at a temperature of 45 °C. The flow rate was of 0.32 ml/min for a total run time of 45 min. The ESI/APCI-MS was performed on an Agilent 6220 TOF mass spectrometer. Samples for analysis (10 μ l) were applied to the C18 column and the multimode source (ESI/APCI) was operated in the positive and negative ion mode. The drying gas temperature was 300°C, and the vaporizer temperature was set at 200°C. The fragmentor voltage was set to 120 V and the mass spectrum was acquired from m/z 250 to 3200 Da with a frequency of 1 scan/s. An Agilent tune mix (Lot LB91098) was used for mass calibration and the data was collected with the Agilent MassHunter WorkStation Data Acquisition software version B.02.00 (Sartain et al, 2011).

6.5 Tandem mass spectrometry

An Agilent 6520 qTOF was used for MS/MS analysis of derivatized MA standard. Positive ion mass spectra were acquired in auto MS/MS form. The instrument was set up by using same parameters described on 6.4, except for the following: drying gas temperature was 310°C and the OCT RF was set at 750 V. Collision energies with slope of 6.5 V/100 Da and offset 2.0 V were used for fragmentation (Sartain et al, 2011).

6.6 Sample derivatization

Testing of the solvents to be used during the MAs derivatization process was performed by comparing chloroform: methanol (2:1 v/v) and chloroform: acetonitrile (2:1 v/v). One of the samples included 2.5 nmol of MAs and derivatizing reagents BMP and CMP suspended in chloroform: methanol (2:1 v/v). The other sample included 2.5 nmol of MAs and derivatizing reagents BMP and CMP suspended in chloroform: acetonitrile (2:1 v/v). The ion volume of the MAs comprised in α -, keto- and methoxy-class was recorded to compare the two different methods. Samples were analyzed in duplicate.

For the derivatization reaction all the samples were analyzed in triplicate. The samples included MAs standard (6 dilutions from 1 pg/10 μ l to 100 ng/10 μ l), urine samples spiked with the MAs standard (6 dilutions from 100 pg/10 μ l to 10 μ g/10 μ l) and serum samples spiked with MAs standard (6 dilutions from 1 ng/10 μ l to 100 μ g/10 μ l).

Samples (10 μ l) were derivatized with 20 μ l of BMP, 20 μ l of CMP and 1 μ l of triethylamine (TEA). Samples were incubated in a water bath at 50°C for 30 minutes (Yang et al, 2007). After the derivatization an additional cleaning step was performed to remove excess derivatizing reagents. Samples were dried under nitrogen and suspended in 100 μ l of acetonitrile, after homogenization the solvent was removed and the cleaning process was repeated followed by drying of the samples under nitrogen. Finally samples were suspended in 51 μ l of chloroform: acetonitrile (2:1 v/v) and analyzed by LC/MS in (+) or (-) ion modes.

6.7 Mycolic acid extraction from serum samples

C-18 Sep-Pak® Vac RC 100 mg cartridges were used to enrich the sample and the MAs spiked into human serum (Aldrich) samples. Different concentrations of MAs prepared in a final volume of 10 µl of chloroform: methanol: water (10:10:3 v/v) and spiked into 90 µl of human serum. The samples were loaded onto the C-18 cartridges equilibrated with 5 ml of methanol. Three fractions were obtained by elution with (i) 5ml of methanol, (ii) 5 ml of methanol: n-propanol: hexane (20:4:1 v/v), and (iii) 5 ml of n-propanol: hexane (80:20 v/v). The third fraction containing the MAs was dried under nitrogen and suspended in 51 µl of chloroform: acetonitrile (2:1 v/v) for LC/MS analysis in (+) and (-) ionization mode (Bhamidi et al, 2011; Sartain et al, 2011).

6.8 Mycolic acid extraction from urine

MAs were prepared at different concentrations and suspended in a final volume of 10 µl chloroform:acetonitrile (2:1 v/v) to be spiked into 990 µl ml of human urine (Gemini-Bio Products). The lipid extraction was performed by adding 3 ml of chloroform: methanol (2:1 v/v). Afterwards they were vortexed and incubated for one hour at room temperature. HPLC grade water (0.5 ml) was added and samples were centrifuged at 1,800 xg at 20°C for 10 min and the upper layer was removed. Following this, 0.5 ml of upper Folch's solution (chloroform: methanol: water in a ratio of 3:47:48 v/v) was added, and samples were vortexed and centrifuged at 1,800 xg at 20°C for 10 min (Khan et al, 2002). The chloroform fraction was recovered and samples were dried under nitrogen. Finally, samples were suspended in 51 µl of chloroform: acetonitrile (2:1 v/v) and analyzed by LC/MS in (+) and (-) ionization mode.

6.9 Method validation

Estimation of method detection limit (MDL) was made according to the 1996 analytical detection limit guidance (Wisconsin Department of Natural Resources Laboratory Certification Program) and included seven replicates for the blank and seven replicates for the sample in study. The standard deviation (SD) and the Student's *t* value for the appropriate degree of freedom were used to calculate the MDL with a 99% confidence limit.

6.10 Data processing and analysis

For the analysis of the data files, the MassHunter Qualitative Analysis Software version B.02.00 (Agilent Technologies, Santa Clara, CA) was used. Molecular features (MFs) were extracted using the Molecular Feature Extraction (MFE) algorithm, and the Mtb LipidDB was used for the MAs identification (Sartain et al, 2011). The identification of the MAs by using the database is based in the exact mass of the compound. Mtb LipidDB was extended by adding the protonated mass for MAs in (+) mode. Another database was created with Microsoft Excel 2007 Pro (Microsoft, Redmond, WA) to detect derivatized MAs by adding the AMMP mass and the different possibilities for adduct formation in the (+) ionization mode. The MFE features used for the data analysis included the ion volume value for the different MAs compounds and the retention time.

6.10.1 Statistical analysis

The non-parametrical test Kruskal-Wallis was used to compare the median ion volume value of MAs between the following groups: i) MAs non-derivatized in (-) mode, ii) MAs non-derivatized in (+) mode, and iii) MAs derivatized (+) mode. The

null hypothesis stated that the ion volume for the MAs was the same for the three groups analyzed. Where between-group differences were detected (null hypothesis for Kruskal-Wallis rejected) the Nemenyi test was used to identify which of the analyzed groups were significantly different. Kruskal-Wallis and Nemenyi test were also used to analyzed MAs individually, by comparing the ion volume value of triplicates between the three groups described above ($\alpha=0.05$) (Zar, 1999).

7. Results

7.1. Mycolic acid standard derivatization

7.1.1 The derivatization reaction

The protocol of Yang et al. (2007) was followed for the derivatization process. As shown in Figure 3, the reaction of the carboxylic group of MAs with the derivatizing reagents produces the final product of 3-acyl-oxymethyl-1-methylpyridinium iodide (AMMP) that should provide a (+) charge to the MA structure.

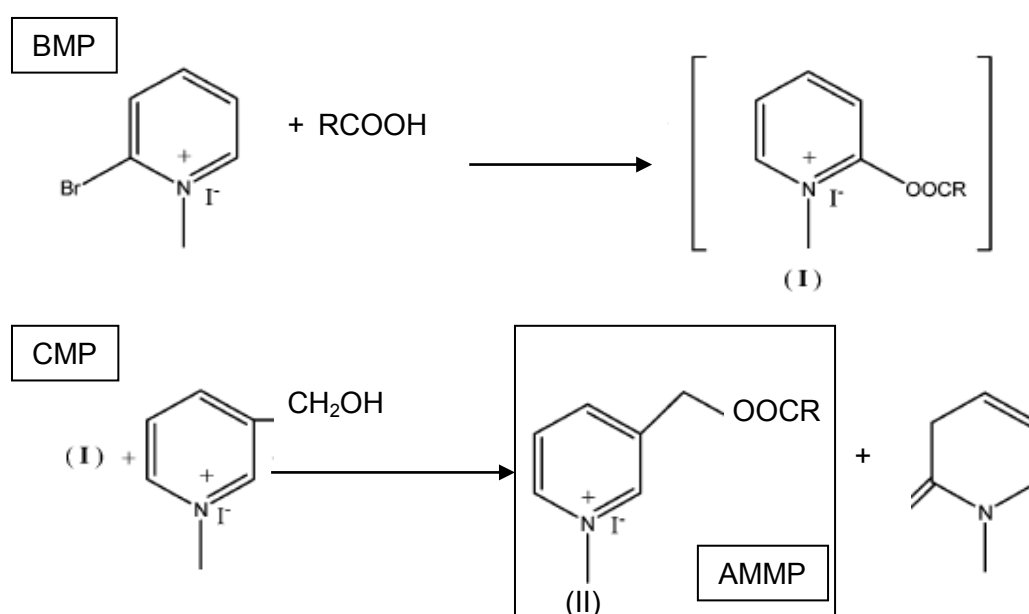


Figure 3. Derivatization reaction of mycolic acids. 2-Bromo-1-methylpyridinium iodide (BMP), 3-Carbinol-1-methylpyridinium iodide (CMP), triethylamine (TEA), R=MA, 3-acyl-oxymethyl-1-methylpyridinium iodide (AMMP). The carboxylic group of R reacts with TEA, removing a proton from the carboxylic group. Subsequently there is a formation of an ester linkage between BMP and R, forming the intermediate compound (I). TEA removes a proton from CMP, because of the electronegative nature of CMP, it is going to attract the intermediate compound I,

producing the final product AMMP (II). Adapted with permission from Yang et al, 2007. Copyright 2012 American Chemical Society.

7.1.2 Solvent testing solubility during the mycolic acids derivatization reaction

Yang et al. (2007) applied the derivatization AMMP protocol to fatty acids ranging from C₁₀ to C₂₄ and used acetone as a main solvent to solubilize the fatty acids. A modification of the protocol was considered, mainly because of the fact that MAs have a much longer carbon chain (C₆₀ to C₉₀), and less polar solvents are needed to solubilize them properly, this fact was confirmed by the poor solubilization of MAs in acetone (data not shown). A first approach was to test the solubility of the different compounds involved in the reaction by using different solvents. For this, two facts were considered (1) a mixture of chloroform: methanol (2:1 v/v) is usually used to solubilize the less polar MAs (Bhamidi et al, 2011) and (2) the more polar derivatizing reagents BMP and CMP are soluble in acetonitrile (Yang et al, 2007). Therefore the solvent mixtures to be tested were comprised of a more polar and a less polar solvent to achieve the solubilization of all the compounds during the derivatization reaction.

Two solvent mixtures were tested in duplicate: (1) chloroform: methanol (2:1 v/v) and (2) chloroform: acetonitrile (2:1 v/v). The derivatizing reagents BMP and CMP and MAs (2.5 nmol) were prepared using acetonitrile and chloroform: methanol (2:1 v/v) respectively. After this they were dried under nitrogen and the two different solvent mixtures were tested during the derivatization process and analyzed by LC/MS in (+) ionization mode (Figure 4).

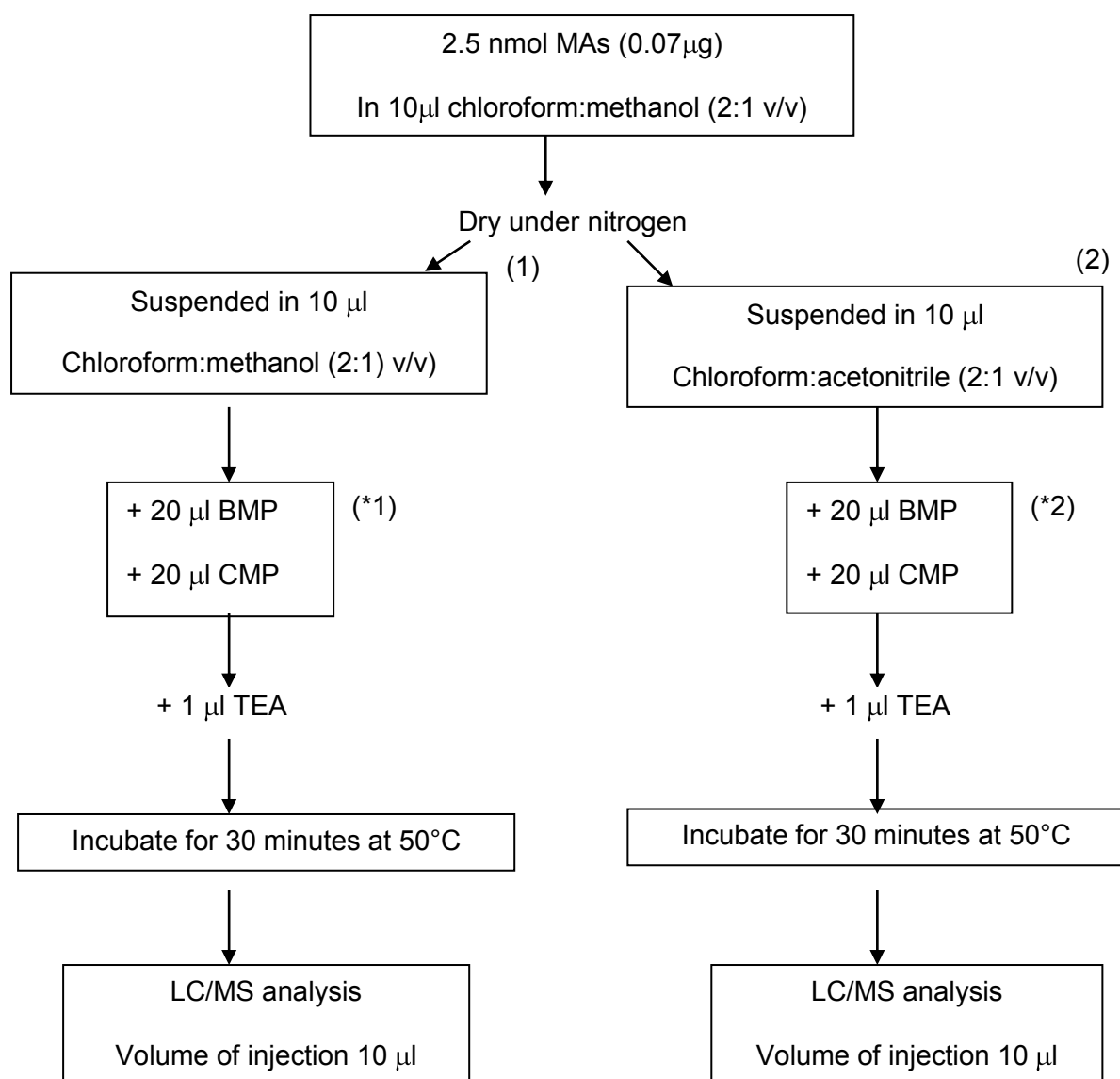


Figure 4. Flow chart of the derivatization reaction comparing two solvents.

Two solvents were compared (1, left side of flow chart) chloroform: acetonitrile (2:1 v/v) and (2, right side of flow chart) chloroform:methanol (2:1 v/v). (*) derivatizing reagents were originally suspended in acetonitrile and then dried under nitrogen and suspended in solvent 1 (*1) or 2 (*2).

The ion volume value, referred to as the total ion volume of all the peaks associated with the respective compounds ($m/z \times \text{retention time} \times \text{abundance}$) was

determined for the different mycolate classes by using the MFE of the Mass Hunter Agilent software. The use of chloroform:acetonitrile (2:1 v/v) improved the total ion volume value for the α -, keto- and methoxy- mycolate classes compared to the use of chloroform: methanol (2:1 v/v). Thus chloroform:acetonitrile (2:1 v/v) was chosen for the derivatization reaction and subsequent experiments (Figure 5).

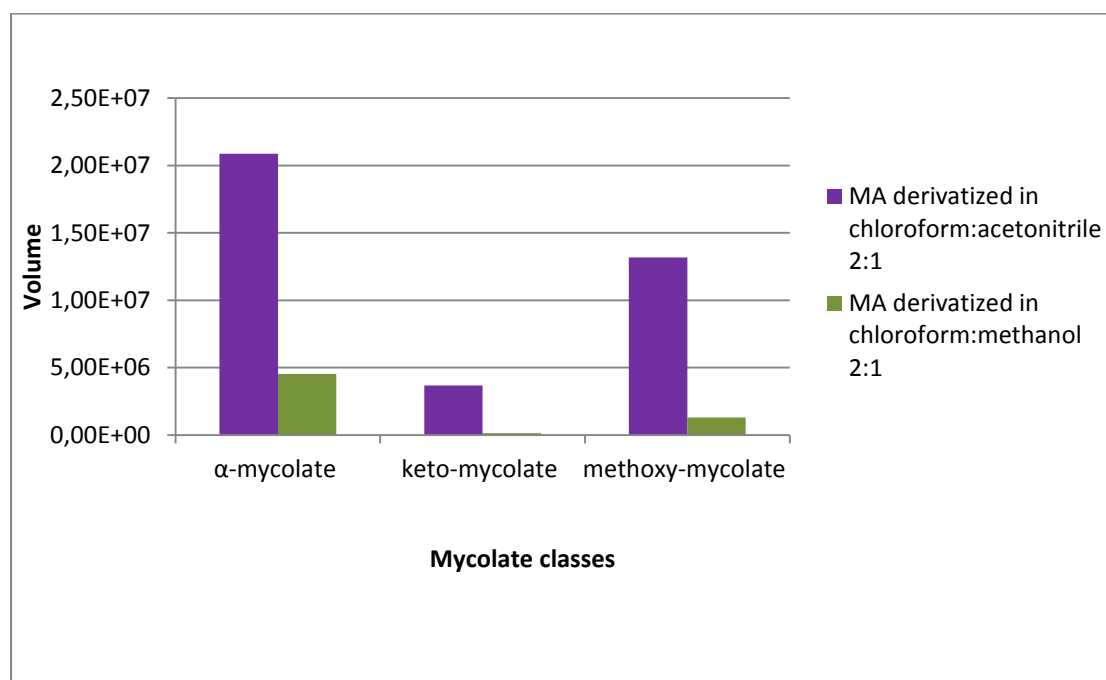


Figure 5. Comparison of solvents performance during MAs derivatization reaction. The ion volume of the different mycolate classes are shown, comparing the use of chloroform: methanol (2:1 v/v), and chloroform: acetonitrile (2:1 v/v). Results correspond to the average ion volume of duplicate samples.

7.1.3 Tandem mass spectrometry of derivatized mycolic acids

Because of the chemical structure of the MA, the attachment of the quaternary amine during the derivatization protocol was expected to occur in the α -

chain. To confirm this, 10 $\mu\text{g}/10 \mu\text{l}$ of the MAs standard were derivatized and analyzed by tandem mass spectrometry (Figure 6). Collision-induced fragment ion spectra for different derivatized MAs showed common ions at m/z 107 and 502. The m/z 107 ion derived from the *N*-pyridylcarbinol moiety and the m/z 502 represented the mass corresponding to the α -chain of the MA (24 carbon) plus the mass of the quaternary amine.

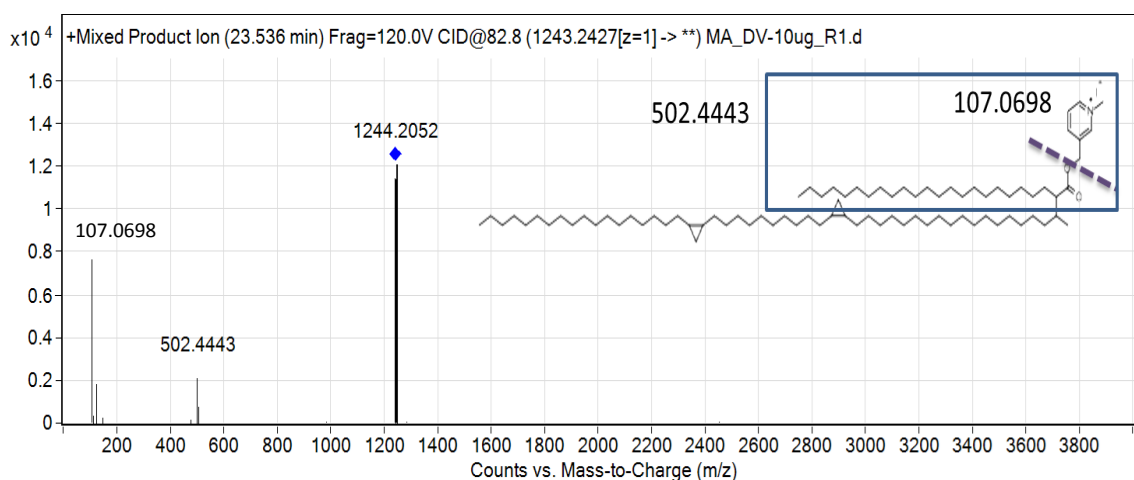


Figure 6. ESI tandem mass spectra showing fragmentation of α -C78 (m/z 1243.2427) Collision energy was applied to α -C78 (m/z 1243.27). Two fragments were identified as 107.0698 corresponding to the quaternary amine mass and 502.443 corresponding to the α -chain of the MA (24 carbon) plus the mass of the quaternary amine.

7.1.4 Cleaning of the sample from derivatizing reagents

The mass spectrometer resolution (ion separation power) was affected after the execution of preliminary derivatization experiments. This appeared to be a problem associated with the derivatizing reagents depositing on the ion transfer

capillary inside the mass spectrometer. Thus to remove excess of derivatizing reagents, a cleaning procedure for the sample after the derivatization reaction was developed and tested.

For cleaning purposes, acetonitrile was used because of its ability to solubilize the derivatizing reagents and because MAs were not expected to be solubilized in this solvent. Sample, control and blank were analyzed in triplicate to evaluate the method as described in Table 1.

Table 1. Cleaning of the sample after derivatization

Sample	Control	Blank
MAs 1µg/ 10 µl in chloroform:acetonitrile (2:1 v/v)	10 µl chloroform:acetonitrile (2:1 v/v)	51 µl chloroform:acetonitrile (2:1 v/v)
20 µl BMP+20 µl CMP+ 1 µl TEA	20 µl BMP+20 µl CMP+ 1 µl TEA	
Incubate 30 min at 50°C	Incubate 30 min at 50°C	Incubate 30 min at 50°C
Wash 1: 100 µl acetonitrile	Wash 1: 100 µl acetonitrile	Wash 1: 100 µl acetonitrile
Wash 2: 100 µl acetonitrile	Wash 2: 100 µl acetonitrile	Wash 2: 100 µl acetonitrile
Wash 3: 100 µl acetonitrile	Wash 3: 100 µl acetonitrile	Wash 3: 100 µl acetonitrile

After the incubation step (30 min at 50°C), samples were dried under nitrogen and suspended in 100 µl of acetonitrile and homogenized. The acetonitrile wash was collected, dried under nitrogen and the resulting residue suspended in 100 µl of water. Two additional washes were performed and processed in the same manner. The UV spectrum (230 to 400 wavelength) was measured for the samples dissolved

in water using a multi-detection microplate reader (BioTek®) and the absorbance for the MAs derivatized sample, blank and control were recorded (Figure 7).

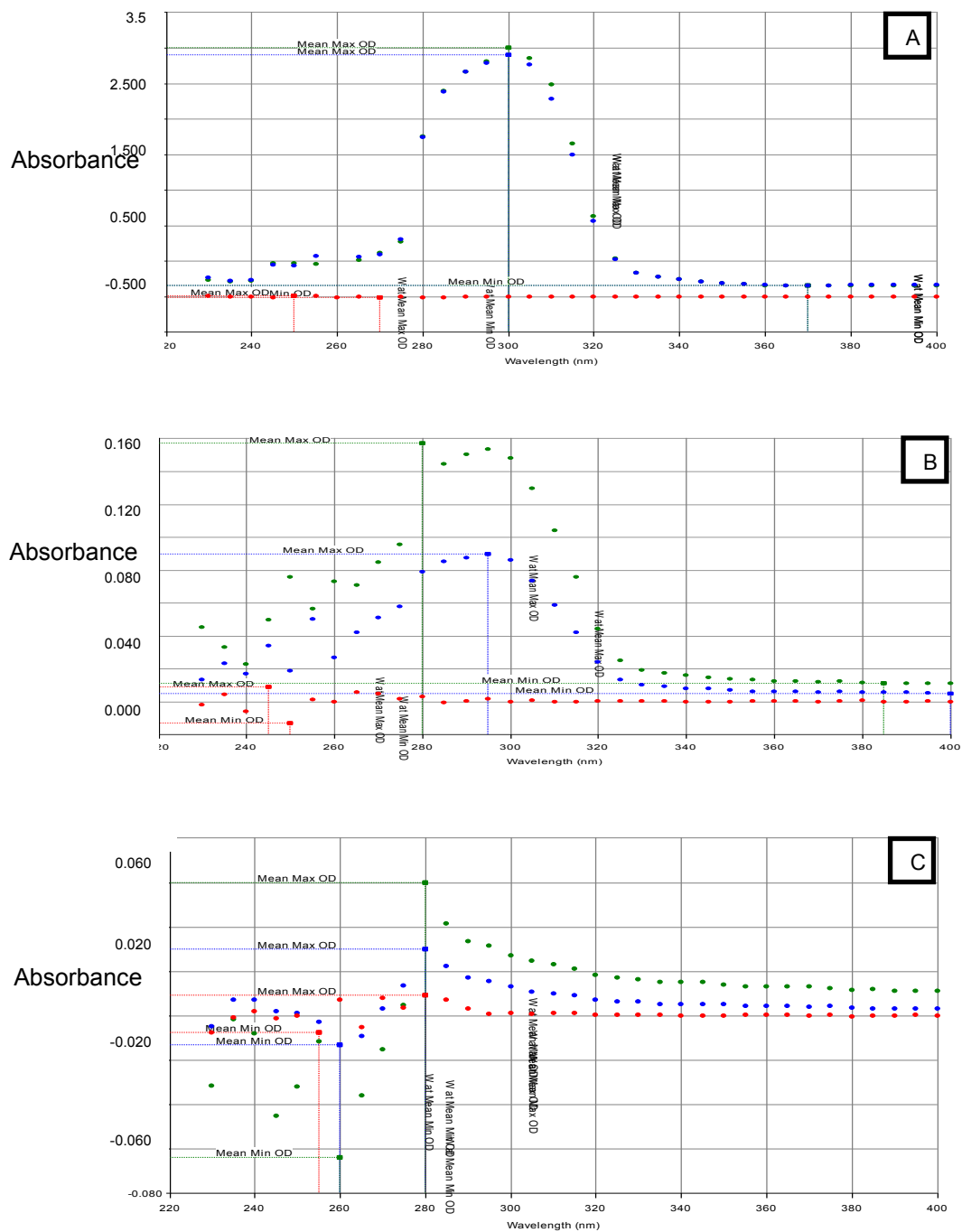


Figure 7. Cleaning process for derivatized samples. Samples were washed with acetonitrile. A=First acetonitrile wash, B= Second acetonitrile wash, C= Third acetonitrile wash. Mean maximum (max) and minimal (min) optical density (OD) are showed for derivatized sample (---), control sample (---) and blank (---).

After the first wash with acetonitrile higher values for the mean maximum (Max) optical density (OD) for the derivatized sample and the control sample were observed compared to the blank (Figure 7 A). This pointed to the removal of derivatizing reagents that was also observed in the second wash (Figure 7 B), but in a lower intensity. Samples did not show major difference with a third acetonitrile wash (Figure 7 C). Based these results it was decided that all derivatized samples would be extracted twice with acetonitrile prior to analysis of LC/MS.

7.2 Comparison of derivatized and non-derivatized mycolic acid standard

The MA standard used was obtained as described in section 6.2. Serial dilutions 1:10 in the range of 100 ng to 1 pg/10 μ l (total weight) of non-derivatized and derivatized MAs standard were analyzed by LC/MS. Chloroform: methanol (2:1 v/v) was used as a solvent to perform the dilutions. After this, the dilutions were dried under nitrogen and suspended in chloroform: acetonitrile (2:1 v/v) to use the same solvent for the derivatized and non-derivatized samples.

To perform the derivatization reaction of MAs standard, 10 μ l of each dilution were derivatized by using 20 μ l of each derivatizing reagent (BMP and CMP) plus 1 μ l of TEA. Samples were incubated at 50°C for 30 min and then they were dried and cleaned twice with 100 μ l of acetonitrile. After this process, samples were suspended in 51 μ l chloroform: acetonitrile (2:1 v/v) and analyzed in the (+) ionization mode.

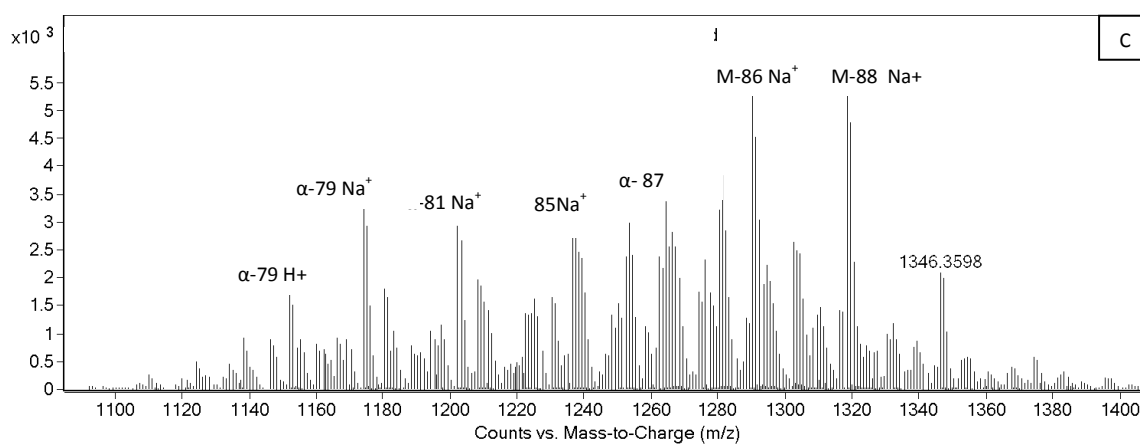
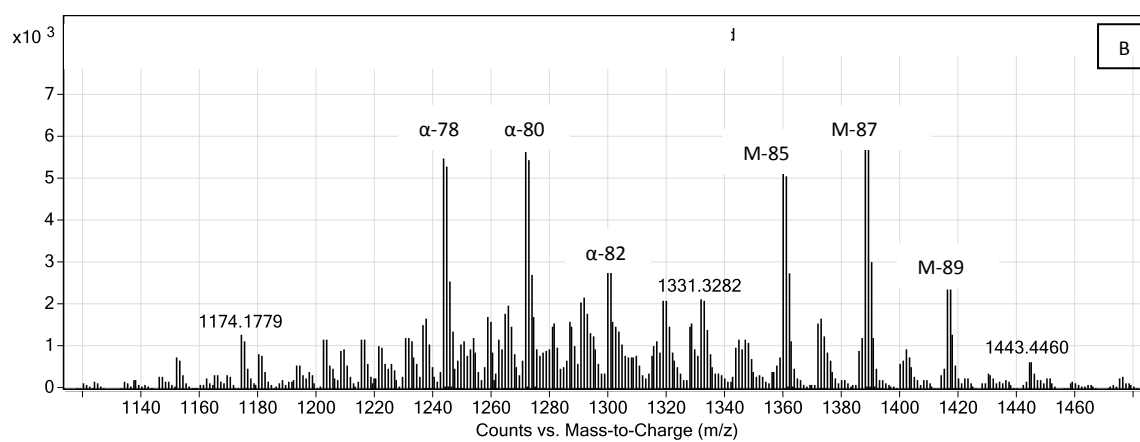
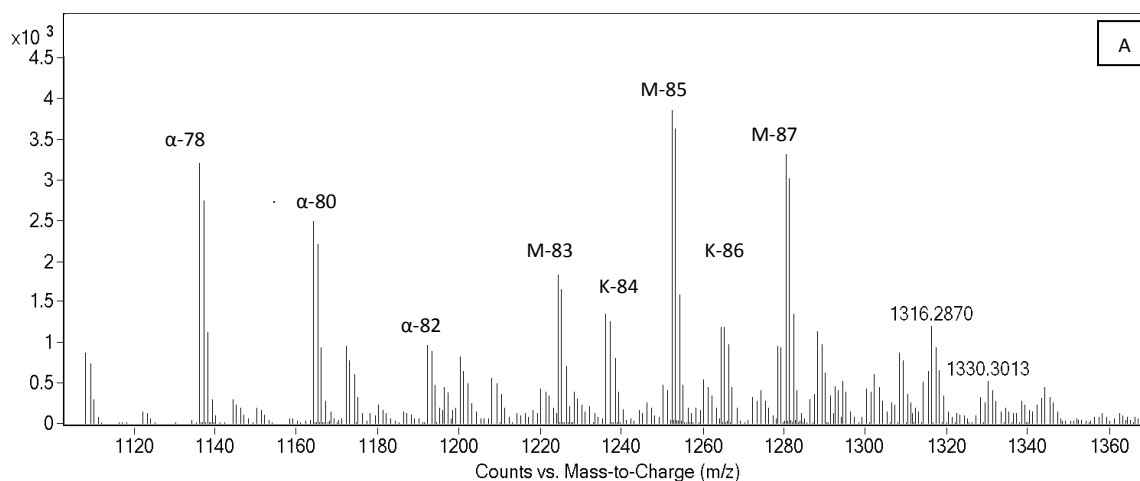
The different dilutions for non-derivatized MAs were analyzed by LC/MS in the (+) and (-) ionization mode. The MFE algorithm from the Agilent MassHunter software along with the use of the Mtb LipidDB (Sartain et al, 2011) allowed for the identification of the different MAs compounds. An extension of the database was

performed to be able to identify protonated MAs in the (+) mode and derivatized MAs.

As a first approach the main MAs were identified. The retention time (Rt), which is the time for a compound to be eluted from the chromatographic column, ranged between 17 and 22 min for the different mycolate classes. This chromatographic range was analyzed to compare the major ions. Non-derivatized MAs standard in (-) mode and derivatized MAs in (+) mode shared a similar profile, where the major ions corresponded to α -C78, α -C80, α -C82, methoxy-C83, methoxy-C85 and methoxy-C87. Within the keto-mycolate class, the ions for keto-C84 and keto-C86 were the most abundant, but the relative intensity was less compared to the ions of the α - and methoxy-MAs (Figures 8 A and 8 B). Shui et al. (2011) analyzed by LC/MS an Mtb Beijing strain culture in the (-) ionization mode and showed that ions correspond to α -C78, methoxy-C85 and keto-C84 were the most abundant. Despite the fact that a different Mtb strain was used in our study (H37Rv) the results of the major ions profile was similar for the (-) mode.

When the same analysis was performed for non-derivatized MAs in (+) mode, the profile was different, α -C79, α -C81, keto-C85, keto-C87, methoxy-C86, and methoxy-C88 were the major ions with a higher relative intensity for the α - and methoxy-class and a lower for the keto-class (Figure 8 C). Regarding the profile of MAs ions in the (+) mode it was important to consider the presence of additional adducts, generally ESI result in protonated $(M+H)^+$ molecules in the (+) ion mode; however, some molecules can be also ionized as $(M+Na)^+$, $(M+K)^+$, or $(M+NH_4)^+$. The elements involved in the adduct formation can originate from glassware or impurities in the chemical solvents, or from their addition to the mobile phase (Mortier et al, 2004). In the case of MAs, $(M+Na)^+$ and $(M+NH_4)^+$ adducts were

observed in the (+) ionization mode (Figure 8 D). The summation of all ion adducts can help to reduce the variation (Mortier et al, 2004) and this approach was used for analysis purposes for non-derivatized MAS in (+) mode in this study.



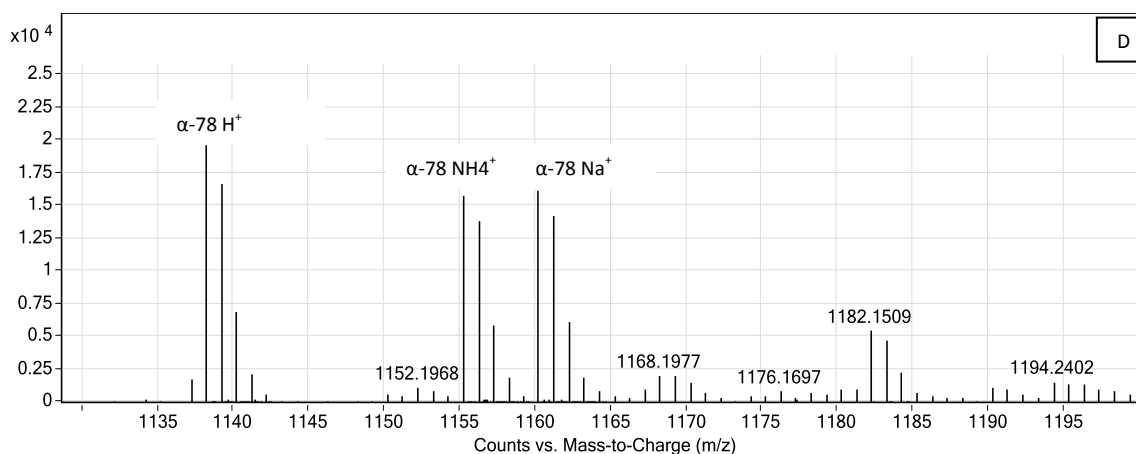


Figure 8. Extracted ion chromatogram for derivatized and non-derivatized MAs (Rt 17-22 min). The profile of the major ions is shown for non-derivatized MAs (-) mode (A), derivatized MAs (+) mode (B), non-derivatized MAs (+) mode (C). An example of adduct formation for α -C78 non-derivatized MA is shown in panel D in the (+) mode with the protonated form and the $(M+Na)^+$ and $(M+NH_4)^+$ adducts. MAs concentration analyzed were 100 ng/10 μ l.

MAs are usually analyzed in (-) mode. Thus, the profile of the most abundant MAs in (-) mode was selected to compare with derivatized and non-derivatized MAs in the (+) mode. The profile was comprised of α -C78, α -C80, α -C82, methoxy-C83, methoxy-C85, methoxy-C87, keto-C84 and keto-C86 (Table 2).

Table 2. Mycolic acid profile used to compare between derivatized and non-derivatized samples¹.

MA	Non-derivatized MAs (-) mode			Non-derivatized MAs (+) mode		
	m/z ²	ion	Rt ³	m/z ²	ion	Rt ³
Alpha-MA (C78)	1136.1663	[M-H]-	18.907	1138.1809	[M+H]+	18.833
Alpha-MA (C80)	1164.1977	[M-H]-	19.381	1166.2125	[M+H]+	19.302
Alpha-MA (C82)	1192.2285	[M-H]-	19.84	1194.2433	[M+H]+	19.7
Keto-MA (C84)	1236.2547	[M-H]-	17.703	1238.2683	[M+H]+	17.636
Keto-MA (C86)	1264.2862	[M-H]-	18.174	1266.3005	[M+H]+	18.103
Methoxy-MA (C83)	1224.2552	[M-H]-	18.7	1226.2702	[M+H]+	18.638
Methoxy-MA (C85)	1252.287	[M-H]-	19.159	1254.2996	[M+H]+	19.086
Methoxy-MA (C87)	1280.3181	[M-H]-	19.599	1282.3342	[M+H]+	19.538

MA	Derivatized MAs (+) mode		
	m/z ²	ion	Rt ³
Alpha-MA (C78)	1243.23	[M+AMMP]+	20.404
Alpha-MA (C80)	1271.26	[M+AMMP]+	20.853
Alpha-MA (C82)	1299.3012	[M+AMMP]+	21.298
Keto-MA (C84)	1343.326	[M+AMMP]+	19.228
Keto-MA (C86)	1371.3579	[M+AMMP]+	19.666
Methoxy-MA (C83)	1331.3269	[M+AMMP]+	20.192
Methoxy-MA (C85)	1359.3584	[M+AMMP]+	20.609
Methoxy-MA (C87)	1387.3901	[M+AMMP]+	21.052

¹ The summation of all adducts were used for quantitative comparisons, but only the protonated or deprotonated ions are shown.

² Mass/charge

³ Retention time

In the case of the MAs standard derivatization, the addition of a quaternary amine to the MA structure increased the mass of all MAs by 106.065126 amu (atomic mass units), the derivatization also resulted in a shift in the Rt for the derivatized compounds explained by the increasing mass (Figure 9).

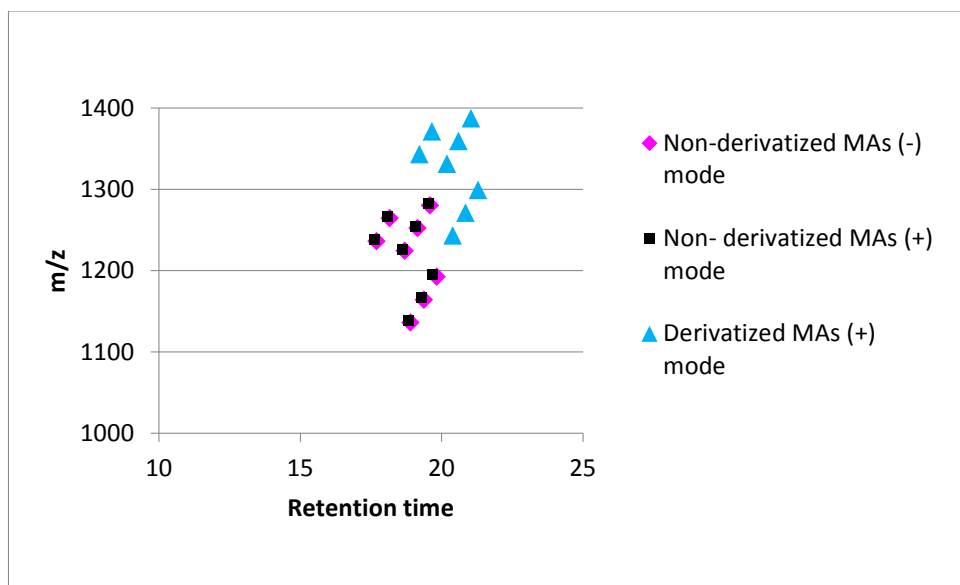


Figure 9. Retention time and m/z of derivatized and non-derivatized MAs. A shift in the m/z and Rt was observed between non-derivatized MAs in (+) and (-) mode and derivatized MAs in (+) mode. MAs profile included α -C78, α -C80, α -C82, keto-C84, keto-C86, methoxy-C83, methoxy-C85, and methoxy-C87.

Non-derivatized MAs in (+) and (-) mode shared a similar chromatographic profile (Figure 10) for keto-C84, keto-C86, methoxy-C83, α -C78, methoxy-C85, α -80, and methoxy C-87. Other non-derivatized MAs such as keto C-85, keto C-87, methoxy C-84, methoxy C-86, methoxy- C88, methoxy- C90 showed a visible signal in the (+) mode, but not in the (-), this fact pointed to a broader signal spectra for non-derivatized MAs in the (+) mode. The derivatized MAs sample showed an enhancement of the signal compared to the non-derivatized samples, and a shift of the Rt to the right.

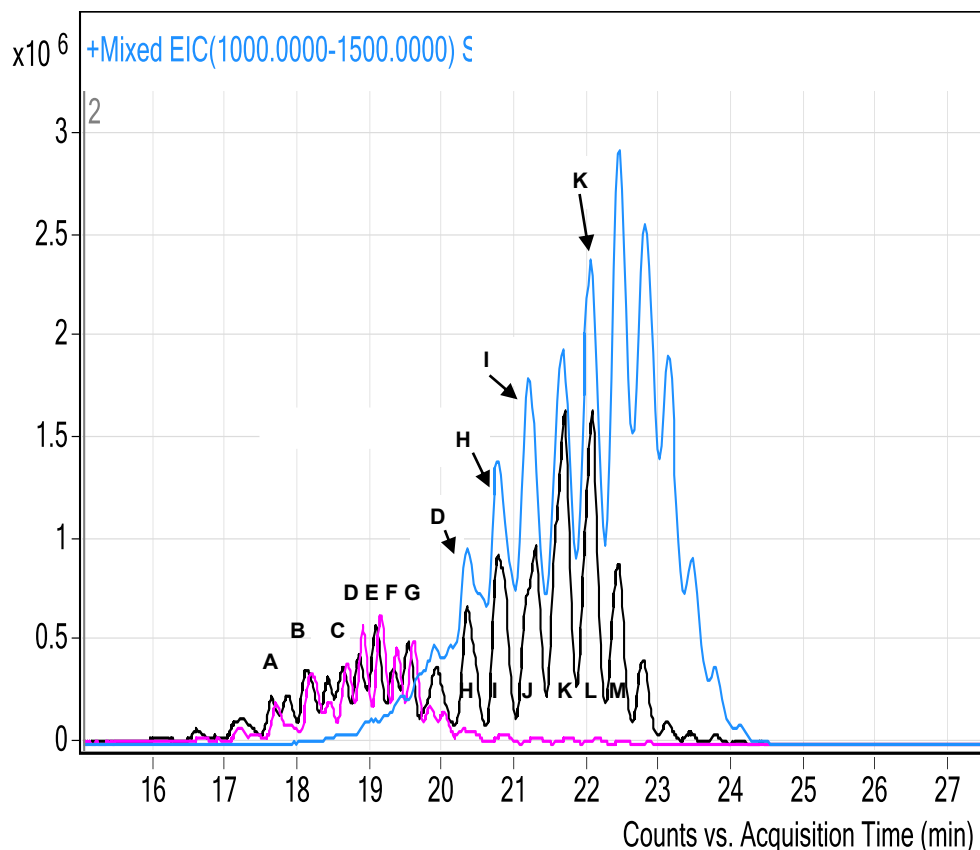


Figure 10. Extracted ion chromatogram (1000-1500 m/z) for derivatized and non-derivatized MAs. 100 ng/10 μ l of MAs were analyzed. Non-derivatized MAs in (-) mode (pink line), non-derivatized MAs in (+) mode (black line) and derivatized MAs in (+) mode (blue line). Capital letters indicate base peak A, (keto-C84); B, (keto-C86); C, (methoxy-C83); D, (α -C78); E, (methoxy-C85); F, (α -C80); G, (methoxy-C87); H, (keto-C85); I, (keto-C87); J, (methoxy-C84); K, (methoxy-C86); L, (methoxy-C88); and M, (methoxy-C90).

The Hypothesis of this study states that the ionization efficiency of MAs could be improved by the addition of a positive charge. To compare the absolute abundance of derivatized and non-derivatized MAs the extracted ion chromatograms

(m/z 1000 to 1500) were analyzed. The intensity of the signal was higher for the derivatized compounds when high concentrations of MAs (100ng/10ul), and lower concentrations of MAs were compared (1 ng/10 ul), the signal was remained higher for derivatized MAs as compared to the underivatized MAs analyzed in the (+) or (-) ion modes (Figure 11).

The median ion volume value between derivatized and non-derivatized MAs was also compared (Figure 12).

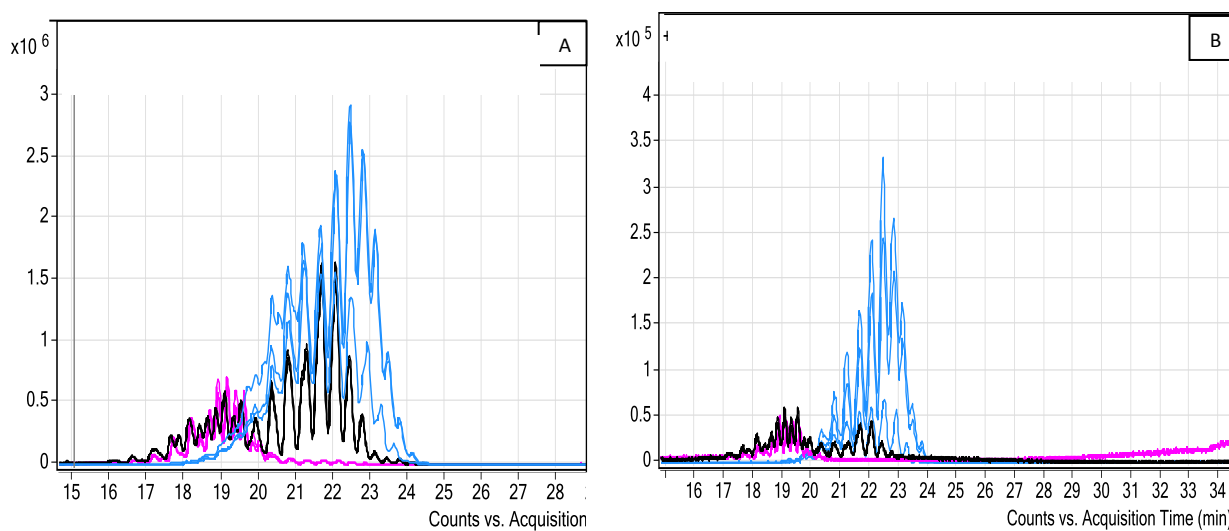


Figure 11. MAs extracted ion chromatogram (1000-1500 m/z). Analysis of 100 ng/10 µl (A) and 1ng/10 µl (B) of MAs were analyzed. Results show samples in triplicate for non-derivatized MAs in (-) mode (pink line), non-derivatized MAs in (+) mode (black line) and derivatized MAs in (+) mode (blue line). An enhancement of the signal was observed for derivatized samples.

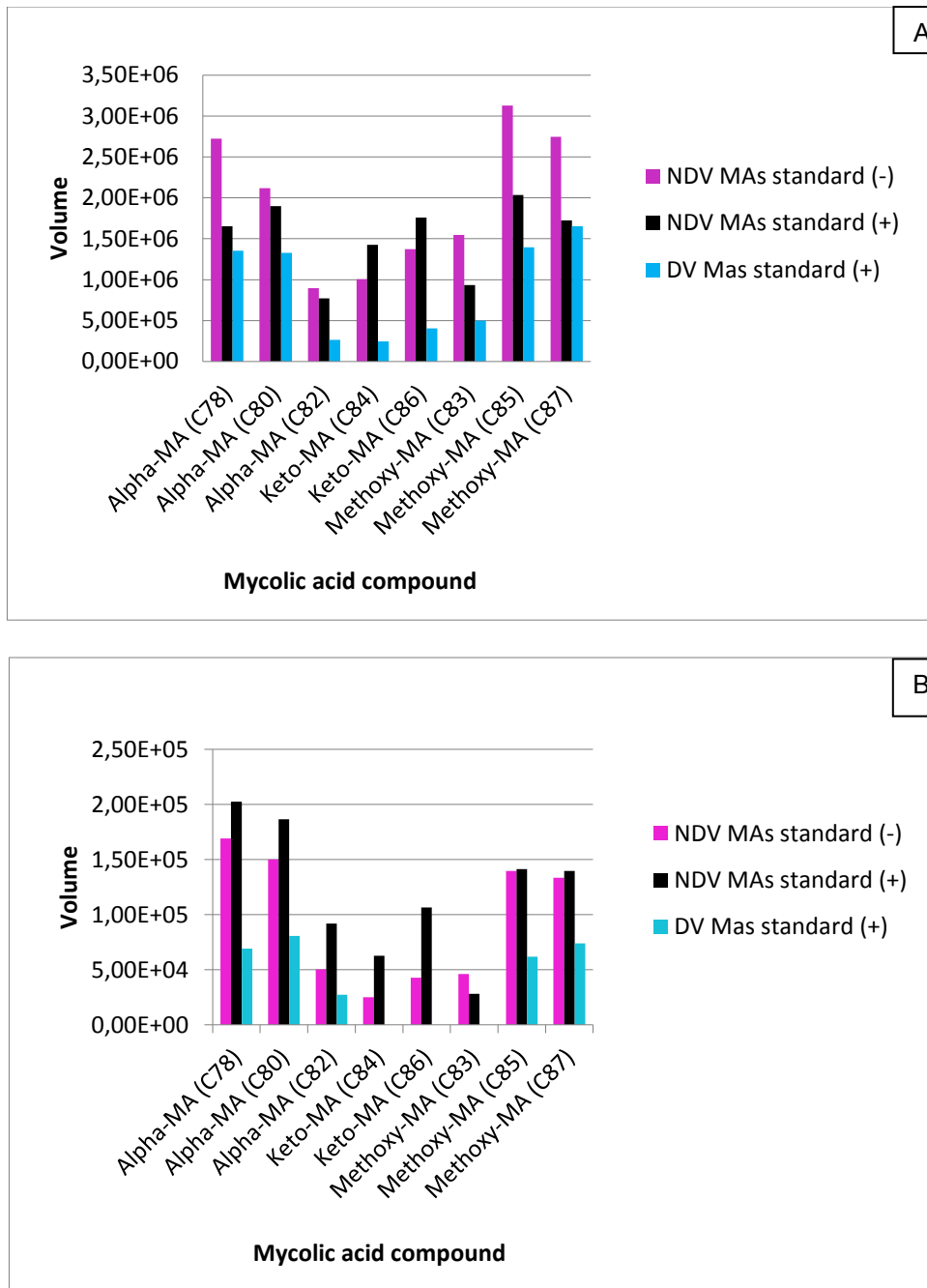


Figure 12. Ion volume comparison between derivatized and non-derivatized MAs at 100 ng/10 µl (A), and 1 ng/10 µl (B). The chart was constructed by using the median ion volume value for the MAs analyzed in triplicate.

For statistical purposes three groups were compared i) non-derivatized MAs (-) mode, ii) non-derivatized MAs (+) mode, and iii) derivatized MAs (+) mode. The Kruskal-Wallis test was applied to two different concentrations of MAs: 100 ng/10µl

and 1 ng/10 μ l (Table 3) to analyze the differences of the median ion volume value between the groups. By using the Kruskal-Wallis test the median ion volume for individual targeted MAs were ranked and differences were observed between the three groups. Thus, based on these rankings the Nemenyi test was applied to identify which of the analyzed groups were significantly different.

Table 3. Analysis of MAs standard by using Kruskal Wallis test¹.

MA 100 ng/10 μ l	(Group i) MAs standard non-derivatized (-) mode	(Group ii) MAs standard non-derivatized (+) mode	(Group iii) MAs standard derivatized (+) mode
Alpha-MA (C78)	2725187 (22)	1652858 (15)	1355323 (10)
Alpha-MA (C80)	2119315 (21)	1899749 (19)	1327511 (9)
Alpha-MA (C82)	896479 (6)	772425 (5)	263167 (2)
Keto-MA (C84)	1007249 (8)	1424689 (13)	244466 (1)
Keto-MA (C86)	1374523 (11)	1758604 (18)	406463 (3)
Methoxy-MA (C83)	1545374 (14)	932925 (7)	499497 (4)
Methoxy-MA (C85)	3127690 (24)	2036600 (20)	1395801 (12)
Methoxy-MA (C87)	2746551 (23)	1724695 (17)	1654712 (16)

MA 1 ng/10 μ l	(Group i) MAs standard non-derivatized (-) mode	(Group ii) MAs standard non-derivatized (+) mode	(Group iii) MAs standard Derivatized (+)mode
Alpha-MA (C78)	169064 (22)	202599 (24)	69054 (12)
Alpha-MA (C80)	150122 (21)	186555 (23)	80552 (14)
Alpha-MA (C82)	50312 (9)	92053 (15)	27355 (5)
Keto-MA (C84)	25107 (4)	62812 (11)	0 (1)
Keto-MA (C86)	42774 (7)	106517 (16)	0 (2)
Methoxy-MA (C83)	46036 (8)	28221 (6)	0 (3)
Methoxy-MA (C85)	139585 (18)	141391 (20)	61805 (10)
Methoxy-MA (C87)	133485 (17)	139620 (19)	73943 (13)

¹The ion volume median value for the different MAs analyzed in triplicate is shown (with ranks of the data in parentheses). The higher the number the greater the rank. MAs concentration analyzed correspond to 100 ng/10 μ l and 1 ng/10 μ l ($\alpha=0.05$).

By using the Nemenyi test for the analysis of the higher concentration of MAs (100 ng/10 μ l), the ion volume value for the group i) was significantly higher

compared to the group iii). There were no significant differences between groups i) and ii) or between groups ii) and iii) (Figure 13 A).

The analysis of the lower MA concentration (1 ng/10 μ l) showed that the ion volume value for the group ii) was significantly higher compared to group iii). There were no significant differences between groups i) and ii) or between groups i) and iii) (Figure 13 B).

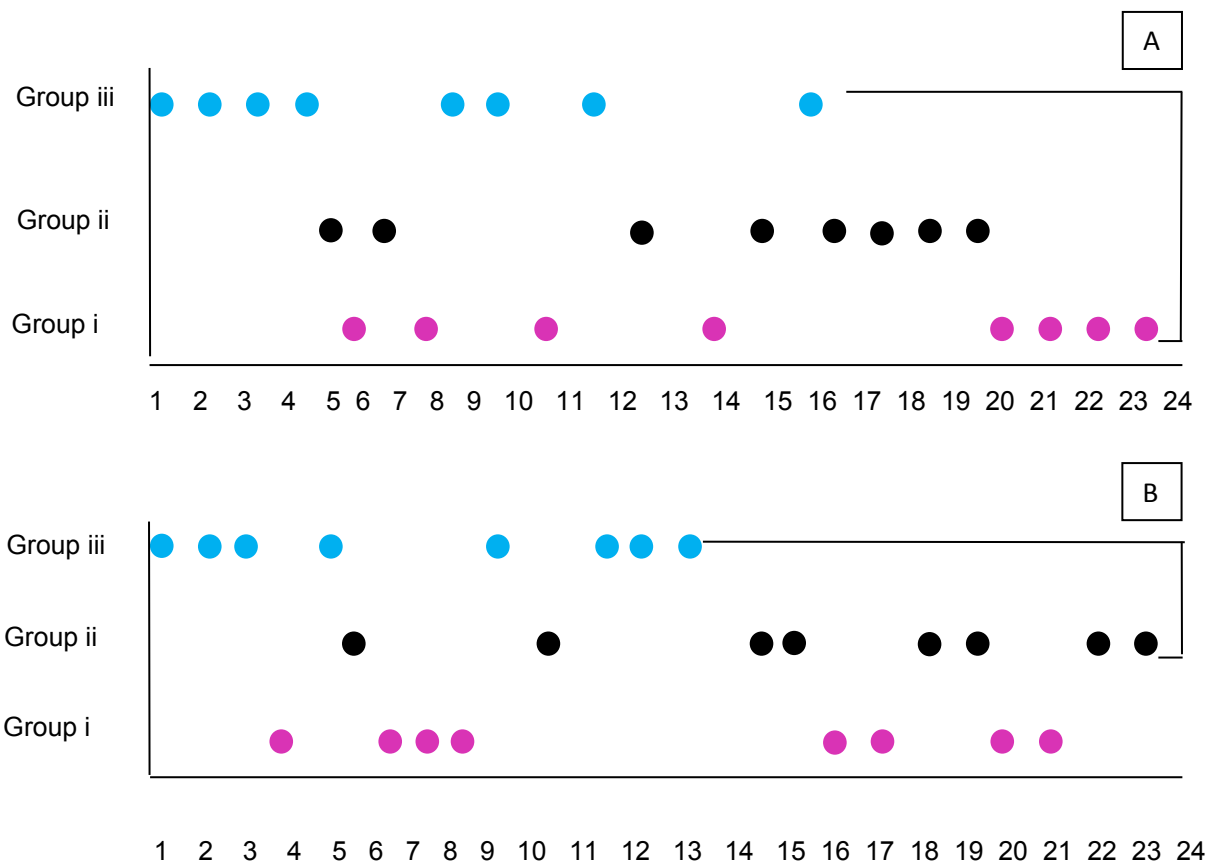


Figure 13. Significant differences in ion volume between groups based on the Nemenyi test. A (100 ng/ 10 µl), B (1 ng/ 10µl). Number 1 and 24 identify the lower and higher ion volume ranking for MAs in group i) non-derivatized MAs (-) mode, group ii) non-derivatized MAs (+) mode, and group iii) derivatized MAs (+) mode. Brackets between groups indicate significant differences in ion volume. The MAs standard concentrations were 100 ng/10µl (A) and 1 ng/10µl (B).

The analysis described above did not provide information about individual MAs, because of this, it was important to analyze the eight MAs separately by applying the same statistical analysis. In this way, each MA was compared in i) non-derivatized (-) mode, ii) non-derivatized (+) mode, and iii) derivatized (+) mode. The ion volume value of triplicates was used for each MA, considering 100 ng/10 µl and 1

ng/10 μ l concentration. Kruskal-Wallis only showed differences for α -C82, keto-C84 and keto C-86 in the lower concentration. When the Nemenyi test was applied for the three MAs, the ion volume was significantly higher for group ii) compared to group iii), and there was not significant differences in ion volume between groups ii) and i) or groups i) and iii) (Figure 14).

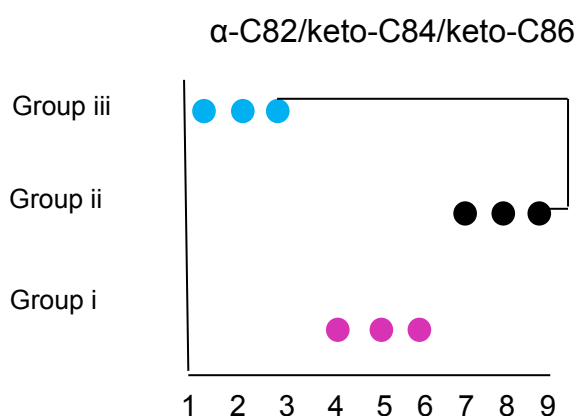


Figure 14. Significant differences in ion volume of individual MAs at 1 ng/10 μ l by using Nemenyi test. Number 1 and 9 identify the lower and higher ion volume ranking for MAs in group i) non-derivatized MAs (-) mode, group ii) non-derivatized MAs (+) mode and group iii) derivatized MAs (+) mode. The three dots grouped by color indicated the ion volume value obtained by triplicates. Brackets between groups indicate significant differences in ion volume.

According chromatogram results derivatized samples showed a higher intensity compared to the non-derivatized. However, when the ion volume for the different MAs were analyzed, non-derivatized MAs showed a significantly higher ion volume. To explain this situation, the profile of derivatized and non-derivatized MAs in (+) mode was compared (Figure 15).

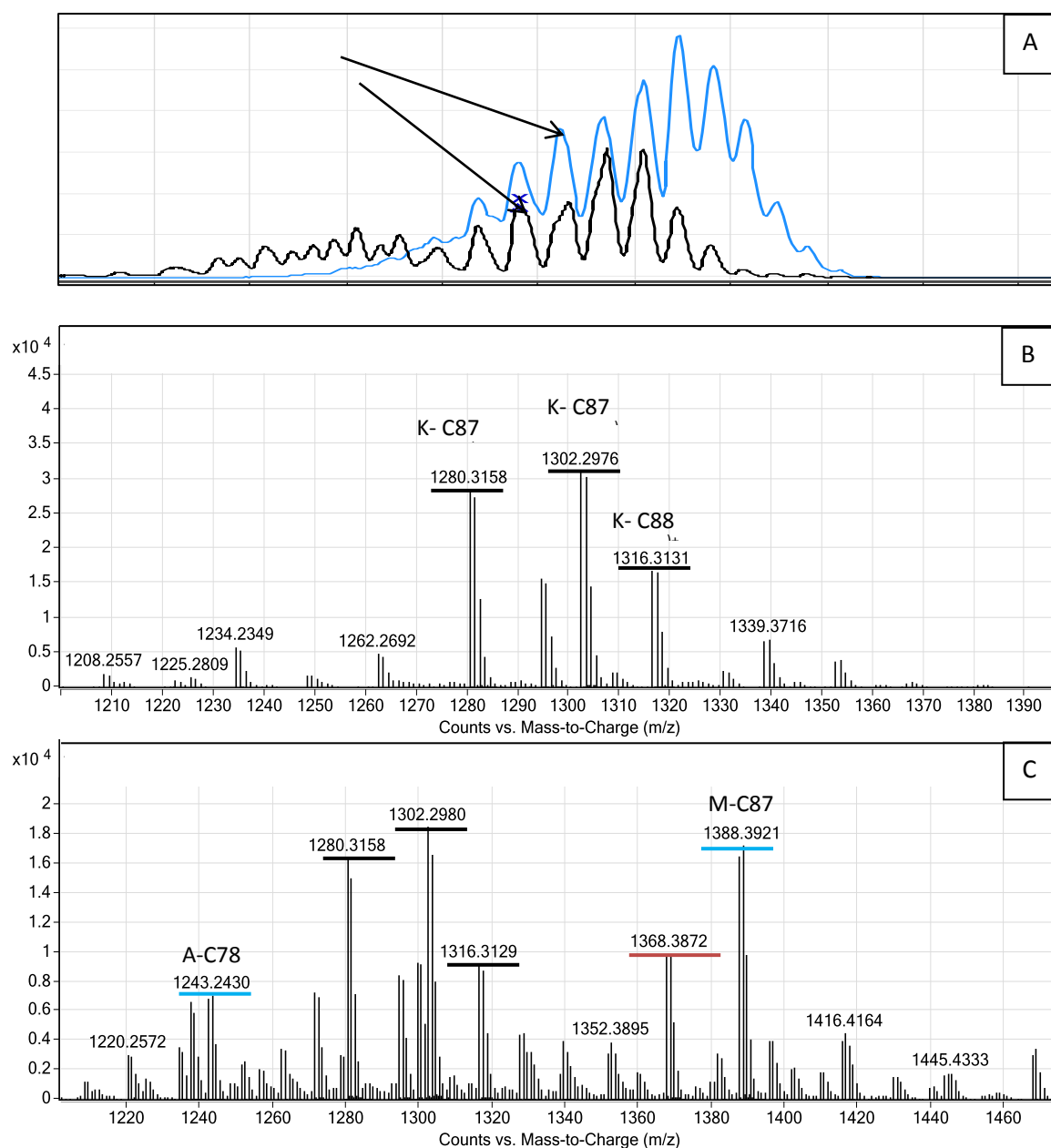


Figure 15. Ion profile comparison between derivatized and non-derivatized MAs in (+) mode. The arrows in box A indicate the peaks of the ion chromatogram (m/z 1000-1500) that were compared between derivatized (blue line) and non-derivatized MAs (black line). The ion profile of non-derivatized MAs in (+) mode (box B) and derivatized MAs (+) mode (box C) highlight in black the ions present in both groups. Derivatized ions are highlighted in blue and non-identified ions in derivatized samples are highlighted in red.

The enhancement of the signal for the derivatized samples could be explained by the presence of derivatized compounds, non-derivatized compounds, and non-identified compounds that contribute to the total ion volume of the peak. Thus it was also important to establish the contribution in the enhancement of the signal of the non-identified compounds compared to the identified compounds. A higher (100 ng/10 μ l) and a lower concentration (1 ng/10 μ l) of MA standard were analyzed (Rt range 20-24 min) (Figure 16).

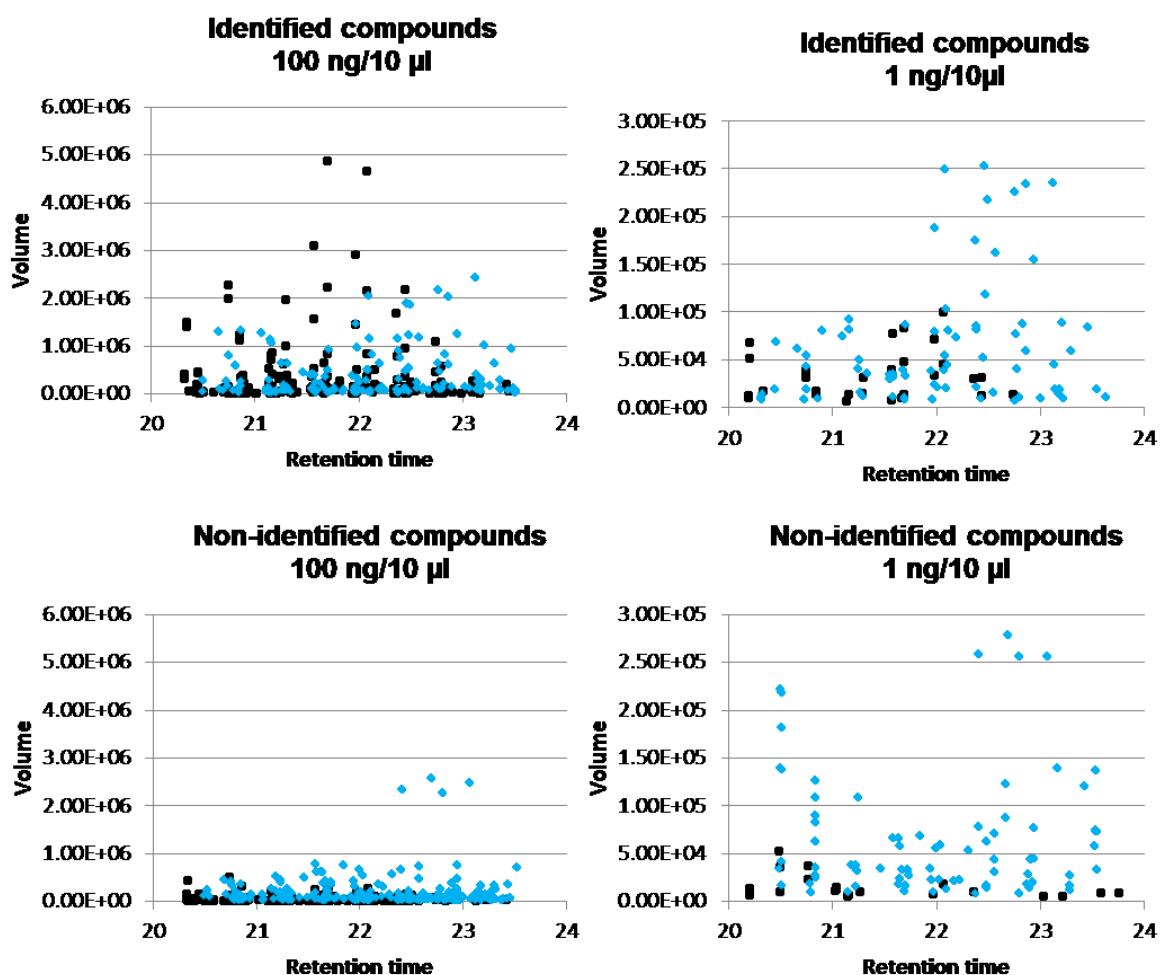
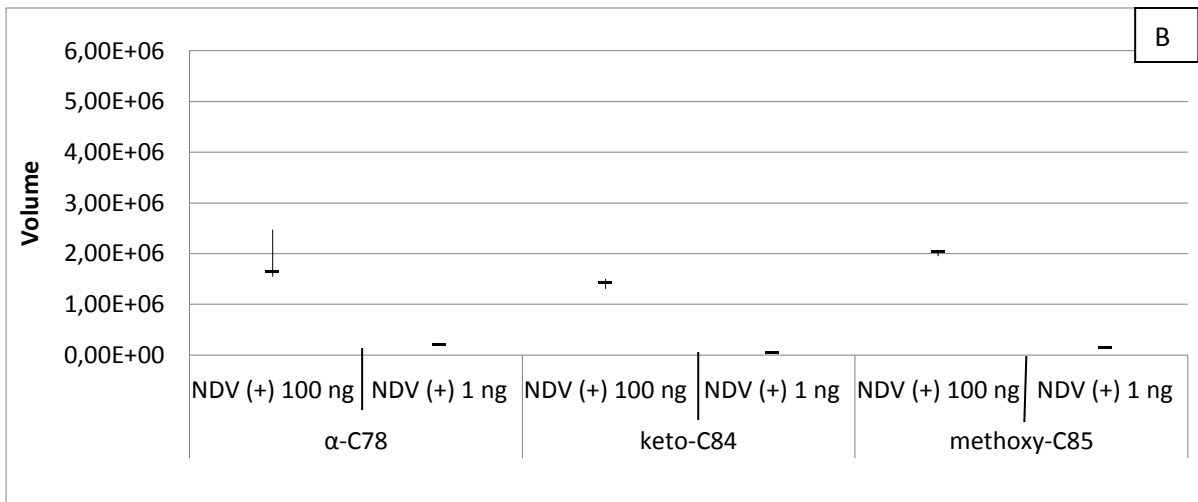
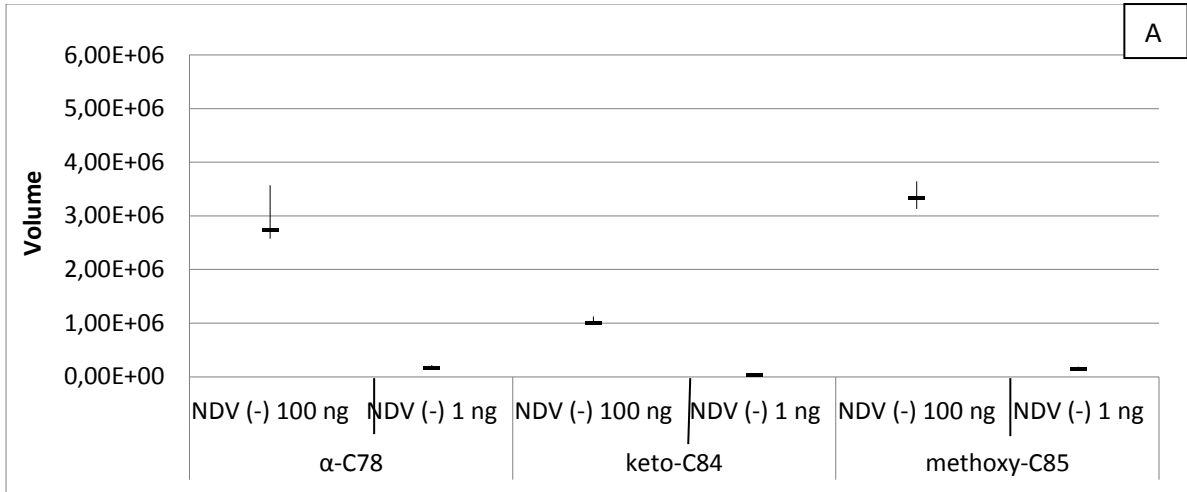


Figure 16. Identified and non-identified compounds in Rt range 20-24 min. Derivatized MA standard (blue dots) and non-derivatized MA standard (black dots) at 100ng/10 μ l and 1ng/10 μ l, and analyzed in the (+) ion mode were compared.

The analysis of the higher concentration of MA standard (100 ng/10 μ l) showed a similar profile for derivatized and non-derivatized identified ions, however, the profile for the non-identified ions showed that derivatized samples had more compounds and some of them were in higher ion volume compared to the non-derivatized MA standard. The analysis of the lower concentration (1 ng/10 μ l) showed that identified and non-identified compounds of the derivatized samples were more abundant and in higher ion volume compared to the non-derivatized MA standard sample. Thus, non-identified compounds in the derivatized samples could be contributing to the enhancement of the signal displayed by the chromatogram.

It was important to test the reproducibility of the results. To achieve this, all the samples were analyzed in triplicate. Higher and a lower concentrations (100 ng/10 μ l and 1 ng/10 μ l for non-derivatized MAs and 100 ng/10 μ l and 10 ng/10 μ l for non-derivatized samples) were compared between derivatized and non-derivatized MA standard. As shown in figure 17 an evaluation of the most abundant MA species of each class, showed greater reproducibility for the non-derivatized samples. Higher concentrations of derivatized MA standard gave the greatest variability between triplicates. In general, higher and lower concentrations showed a similar trend in the variability of the measurements (Figure 17).



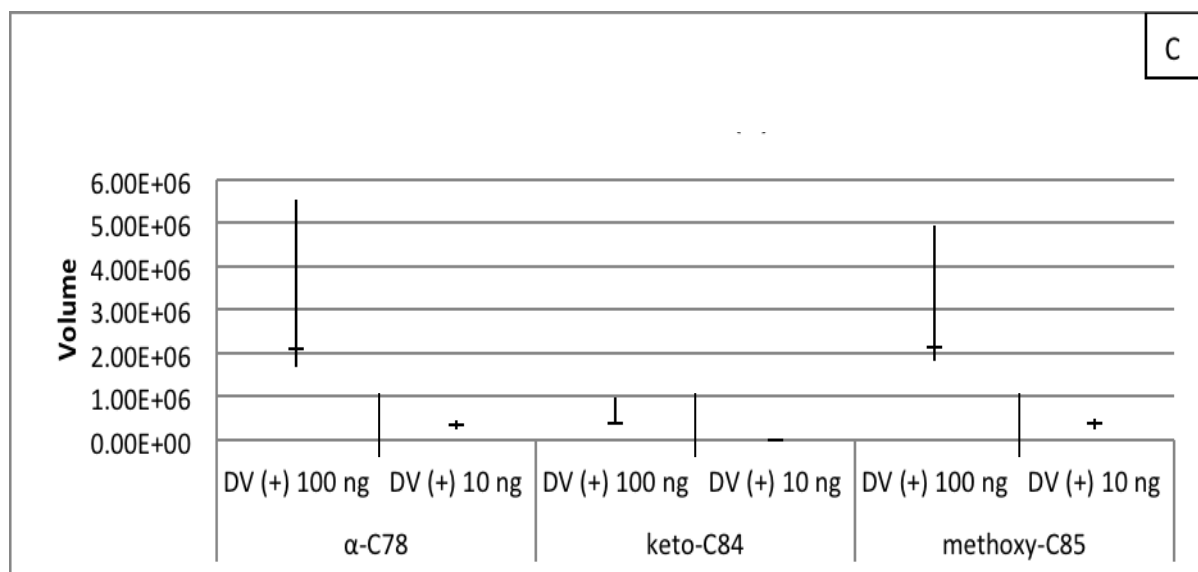
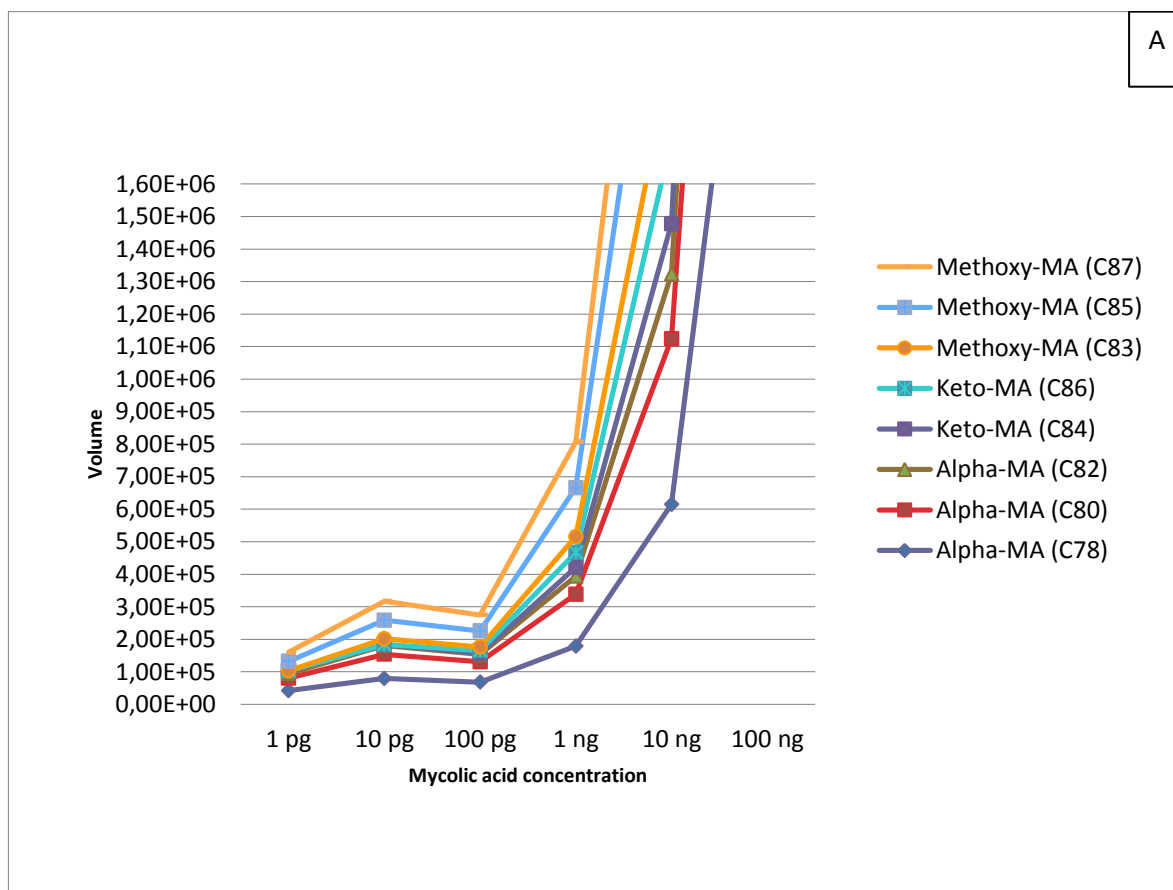


Figure 17. Reproducibility of MAs standards. Triplicates of non-derivatized (NDV) MA standard in the (-) mode (A) and (+) mode (B), and derivatized (DV) MAs in the (+) mode (C) were compared based on ion volume. The vertical lines show the range of variability and the dash marks the median value. α-C78, keto-C84 and methoxy-C85 were analyzed at a 100 ng/10 µl and a 10 ng/10 µl concentrations.

7.2.1 Method detection limit of mycolic acids standard

Method detection limit (MDL) is the minimum concentration of a substance that can be measured and reported to be greater than zero with 99% confidence, and is determined from analysis of a sample in a given matrix containing the analyte (Wisconsin Department of Natural Resources Laboratory Certification Program, Analytical detection limit guidance, 1996). To determine the MDL, different approaches can be used. One method consists in using the matrix (urine, water or other solvent) known to be free of the analyte to be investigated and analyze it repeatedly. The mean value represents the background and the MDL is defined as the statistical mean of these analyses plus 3 to 4 standard deviation units (Needlman

and Romberg, 1990). Another approach, and the one used in this study, utilizes decreasing concentrations of the analyte (MAs) in the appropriate solvent to determine the region of the standard curve where there is a significant change in sensitivity, i.e., a break in the slope of the standard curve (Wisconsin Department of Natural Resources, Laboratory Certification Program Analytical detection limit guidance, 1996). Then the overall MDL was estimated by determining the standard deviation (SD) across seven replicates of the concentration detected as a break in the slope, by multiplying the SD with the Student's *t* value for the appropriate degree of freedom and the 99% confidence limit (3.143 for *n*=7). To make the standard curves comparable between groups, same sets of MAs ions were used, including α -C78, α -C80, α -C82, keto-C84, keto-C86, methoxy-C83, methoxy-C85, and methoxy-C87 (Figure 18).



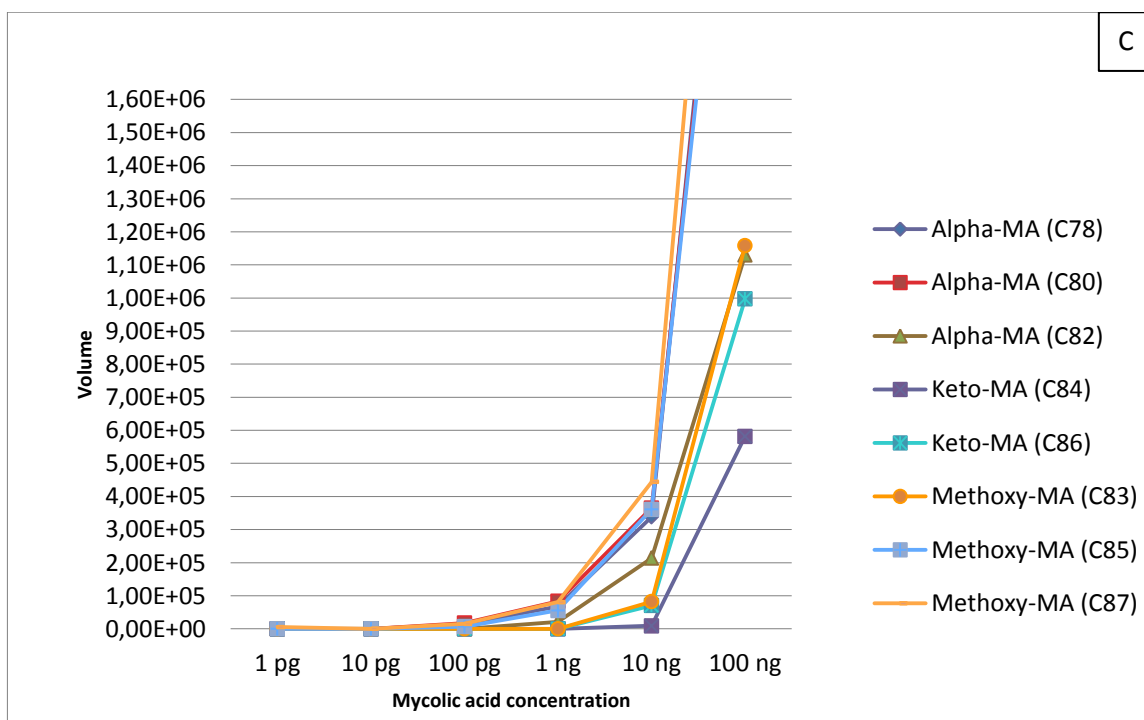
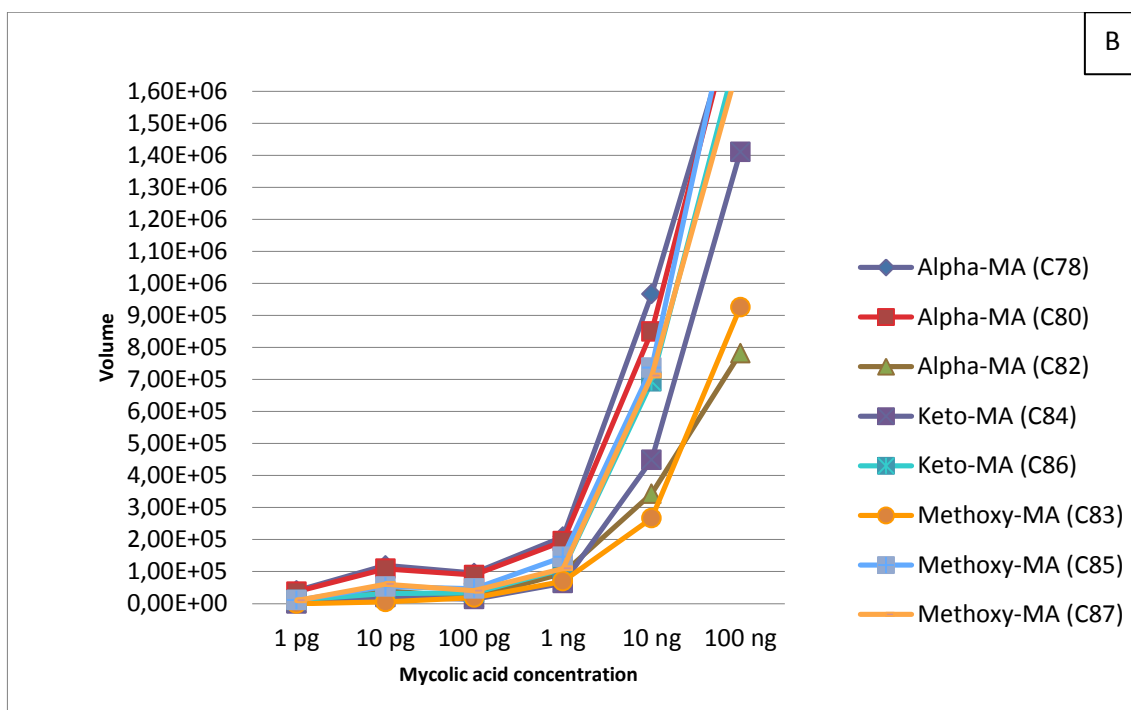


Figure 18. MAs standard curve. Derivatized MAs (-) mode (A), non-derivatized MAs (+) mode (B), and derivatized MAs (+) mode (C). Standard curve was constructed by using the average ion volume of the eight targeted MAs.

The MAs concentration used to determine the MDL was identified as a break in the slope of the standard curve corresponding to 1ng/10 μ l and 10 ng/10 μ l for non-derivatized and derivatized MAs respectively. After that, the MDL was estimated by determining the SD across seven replicates of the concentration detected as a break in the slope.

To determine the background of the method, seven replicates of the blank chloroform: acetonitrile (2:1 v/v) for non-derivatized MAs and seven replicates of a blank of the derivatization reaction for the derivatized MAs were also analyzed by LC/MS. By using the molecular feature algorithm and the Mtb LipidDB, and AMMP databases no compounds that matched the Rt and m/z of the MAs in study were found, for this reason the background of the blank was not included in the MDL analysis. The data used to determine the MDL corresponded to the average ion volume of the seven replicates for each group in study (Table 4).

Table 4. MDL (ng) for non-derivatized and derivatized MAs¹

Mycolic acids	Non-derivatized (-) MDL (ng)	Non-derivatized (+) MDL (ng)	Derivatized (+) MDL (ng)
Alpha-MA (C78)	1	0.82	7.83
Alpha-MA (C80)	0.99	0.94	6.39
Alpha-MA (C82)	1.64	1.69	6.17
Keto-MA (C84)	2.64	0.84	9.01
Keto-MA (C86)	1.39	0.87	7.1
Methoxy-MA (C83)	1.36	1.35	7.61
Methoxy-MA (C85)	1.09	1.01	7.72
Methoxy-MA (C87)	1.04	1	5.89

¹MDL was calculated based on the average ion volume values for the different MAs ($\alpha=0.05$).

The MDL varied around 1 ng/10 ul in the case of non-derivatized MAs and around 10 ng/10 ul for the derivatized MAs standard, equivalent to 0.15 pmol and 1.5 pmol per 10 ul (final volume of injection for LC/MS analysis), respectively. The derivatization process was not able to improve the MAs sensitivity of detection.

7.3 Spiking of mycolic acids in serum and urine

Despite the fact that a significant difference in selected MAs based on the total ion volume of expected ions was not observed when the MAs standard was derivatized compared to the non-derivatized standard, it was decided to test the derivatization protocol for biological fluids. The rationale for this mainly pointed to test the feasibility of derivatization in these fluids. It was also important to establish extraction protocols for MAs and determine the MDL. Although spiking experiments of MAs in these fluids cannot be comparable to the study of clinical samples from individuals with active disease, this approach was intended to have an approximation of the behavior of MAs when they were detected by using LC/MS.

7.3.1 Mycolic acids detection in urine by LC/MS

Non-derivatized MAs spiked in urine analyzed in (+) and (-) ionization mode by LC/MS were compared to MAs spiked in urine that were derivatized and analyzed in (+) mode. Six dilutions of MAs were prepared in chloroform: methanol (2:1 v/v) in the range of 10 µg to 100 pg/10 µl and then dried and suspended in chloroform: acetonitrile (2:1 v/v). Human urine (990 µl) (Gemini- Bioproducts) was spiked with 10 µl of the different MAs concentrations. For the lipid extraction, 3 ml of chloroform: methanol (2:1 v/v) was added to the urine samples. Afterwards they were vortexed and incubated for one hour at room temperature. HPLC grade water (0.5 ml) was

added and samples were centrifuged at 1,800 xg for 10 minutes, removing the upper layer. Following this 0.5 ml of upper Folch solution was added, and samples were vortexed and centrifuged at 1,800 xg for 10 minutes (x2). The chloroform fraction was recovered, dried under nitrogen and suspended in 51 μ l of chloroform: acetonitrile (2:1 v/v) for the LC/MS analysis of non-derivatized MAs. For derivatization, MAs extracted from urine in the same manner were suspended in 10 μ l of chloroform: acetonitrile (2:1 v/v) and derivatized as described for the MA standard.

The ion chromatograms for the derivatized and non-derivatized MAs spiked in urine were compared (Figure 19). The higher (10 μ g/10 μ l) and lower concentration (100 ng/10 μ l) of urine samples spiked with MAs and derivatized, showed an enhancement of the signal compared to non-derivatized samples.

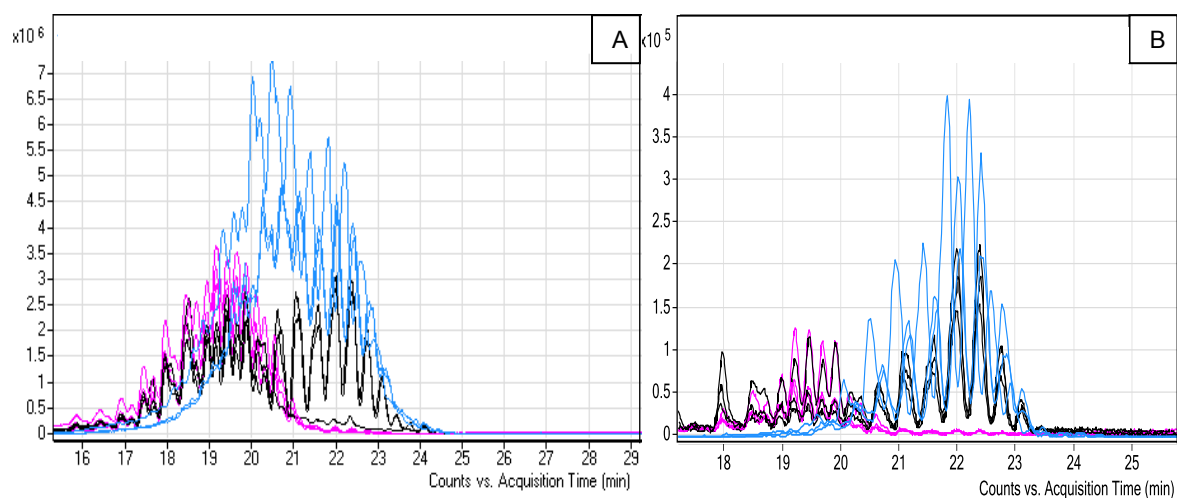


Figure 19. Extracted ion chromatogram (1000-1500 m/z) for derivatized and non-derivatized MAs in urine. Results show samples analysis of 10 μ g/10 μ l (A) and 100ng/10 μ l (B) in triplicate for non-derivatized MAs in (-) mode (pink line), non-derivatized MAs in (+) mode (black line) and derivatized MAs in (+) mode (blue line).

The median value for the ion volume of samples in triplicate was used to construct the graph for derivatized and non-derivatized MAs spiked in urine (Figure 20).

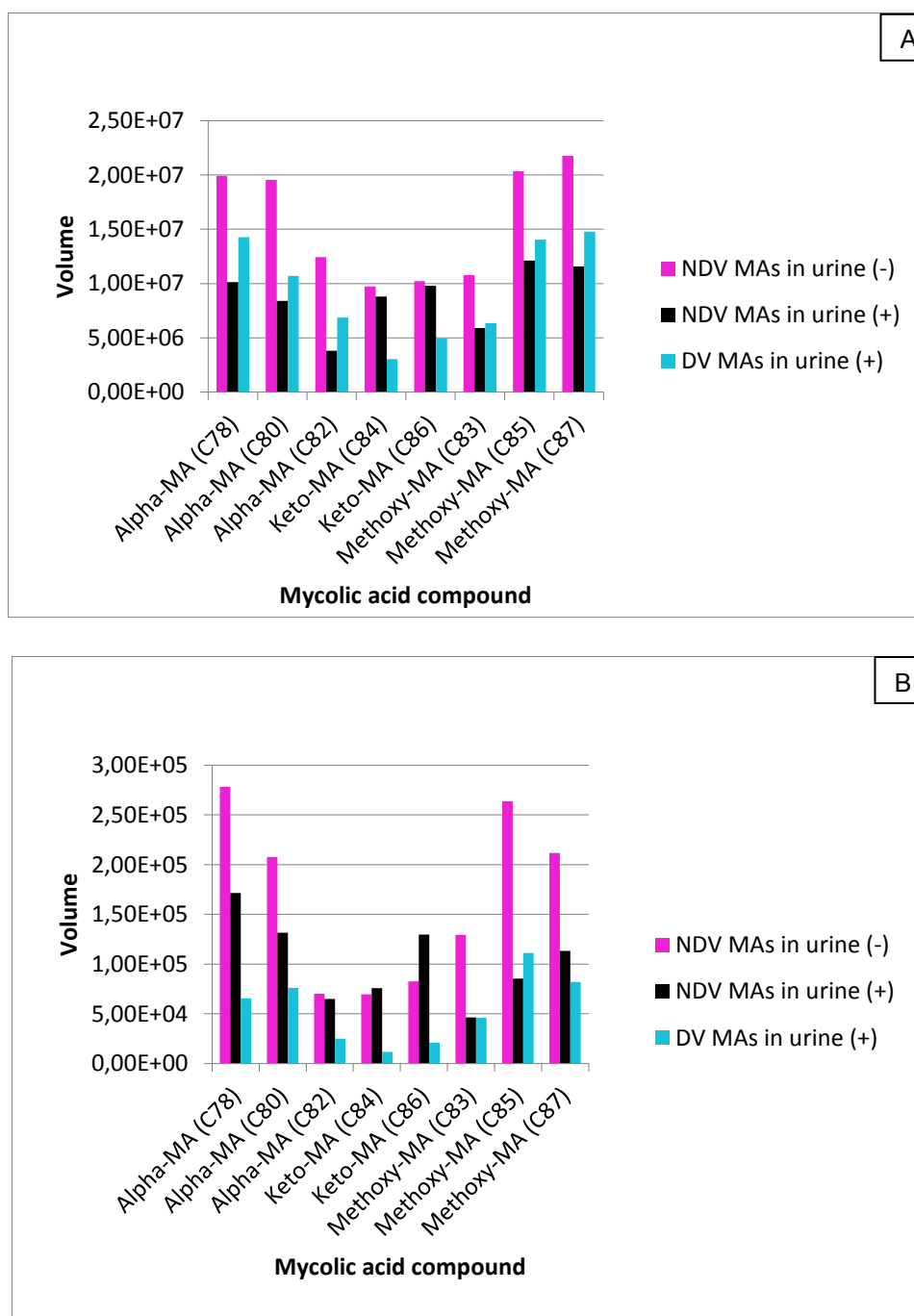


Figure 20. Ion volume comparisons between derivatized and non-derivatized MAs spiked in urine at concentrations of 10 µg/10µl (A), and 100 ng/10µl (B).

The significance of the ion volume results were analyzed using a statistical approach. Kruskal Wallis test (Table 5) revealed that the ion volume values were different between the three groups i) non-derivatized MAs in urine in (-) mode ii) derivatized MAs in urine in (+) mode, and iii) non-derivatized MAs in urine in (+) mode for 10 µg/10 µl and 100 ng/10 µl concentration. By using the Nemenyi test, significant differences between groups were established.

Table 5. Analysis of urine samples spiked with MAs by using Kruskal Wallis test¹.

MA (10 µg/10 µl)	(Group i) Urine spiked with MAs Non-derivatized (-) mode	(Group ii) Urine spiked with MAs Non-derivatized (+)mode	(Group iii) Urine spiked with MAs Derivatized (+) Mode
Alpha-MA (C78)	10123230 (11)	19931842 (22)	14267309 (19)
Alpha-MA (C80)	8401224 (7)	19543336 (21)	10683714 (13)
Alpha-MA (C82)	3805365 (2)	12441092 (17)	6872939 (6)
Keto-MA (C84)	8806390 (8)	9726614 (9)	3029084 (1)
Keto-MA (C86)	9800682 (10)	10199467 (12)	4930313 (3)
Methoxy-MA (C83)	5890396 (4)	10778572 (14)	6357323 (5)
Methoxy-MA (C85)	12127571 (16)	20343990 (23)	14038446 (18)
Methoxy-MA (C87)	11569609 (15)	21756714 (24)	14783297 (20)

MA (100 ng/10 µl)	(Group i) Urine spiked with MAs Non-derivatized (-) mode	(Group ii) Urine spiked with MAs Non-derivatized (+) mode	(Group iii) Urine spiked with MAs Derivatized (+) Mode
Alpha-MA (C78)	278195 (24)	171367 (20)	65599 (7)
Alpha-MA (C80)	207676 (21)	131704 (19)	76158 (11)
Alpha-MA (C82)	70116 (10)	65087 (6)	24967 (3)
Keto-MA (C84)	69738 (8)	75672 (9)	11641 (1)
Keto-MA (C86)	82626 (13)	129572 (18)	21081 (2)
Methoxy-MA (C83)	129360 (17)	46275 (5)	46092 (4)
Methoxy-MA (C85)	263871 (23)	85379 (14)	111265 (15)
Methoxy-MA (C87)	211736 (22)	113345 (16)	81943 (12)

¹The ion volume median value for the different MAs analyzed in triplicate is shown (with ranks of the data in parentheses). The higher the number the greater the rank. MAs concentration analyzed correspond to (10 µg/10 µl) and (100 ng/10 µl) ($\alpha=0.05$).

By using the Nemenyi test for the analysis of the higher concentration of MAs spiked in urine (10 µg/ 10 µl), the ion volume value for the group i) was significantly higher compared to the group ii). There were no significant differences between groups i) and iii) or between groups ii) and iii) (Figure 21 A). The analysis of the lower MA concentration spiked in urine (100 ng/10 µl) showed that the ion volume

value for the group i) was significantly higher compared to group iii). There were no significant differences between groups i) and ii) or between groups ii) and iii) (Figure 21 B).

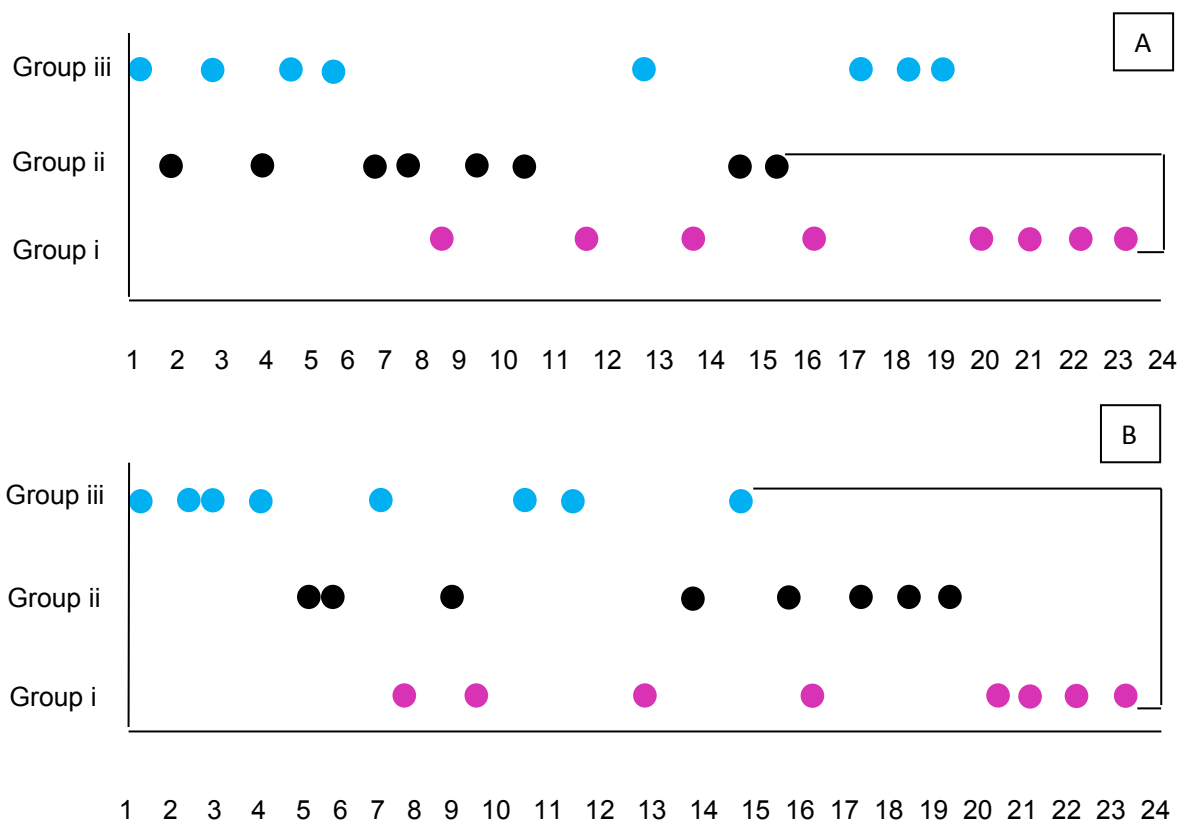


Figure 21. Significant differences in ion volume between MAs spiked urine-groups based on the Nemenyi test. Number 1 and 24 identify the lower and higher ion volume ranking for MAs in group i) non-derivatized MAs (-) mode, group ii) non-derivatized MAs (+) mode, and group iii) derivatized MAs (+) mode. Brackets between groups indicate significant differences in ion volume. The MAs standard concentrations spiked in urine were 10 µg/10 µl (A), and 100 ng/10 µl (B).

The eight target MAs were also analyzed individually applying the same statistical test, and the most abundant species of each class were represented as shown in figure 22. Each MA was compared in i) non-derivatized (-) mode, ii) non-derivatized (+) mode, and iii) derivatized (+) mode. The ion volume value of triplicates was used for each MA, considering 10 $\mu\text{g}/10 \mu\text{l}$ and 100 $\text{ng}/10 \mu\text{l}$ concentration. Kruskal-Wallis only showed differences for $\alpha\text{-C82}$ in the higher concentration. When Nemenyi test was applied for $\alpha\text{-C82}$, the ion volume was significantly higher for group i) compared to group ii), and there were not significant differences in ion volume between groups i) and iii) or groups iii) and ii) (Figure 22).

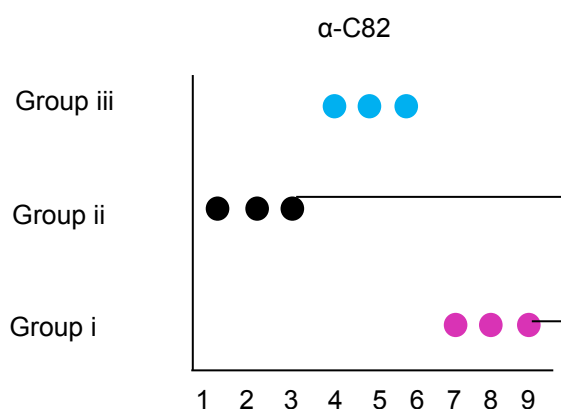
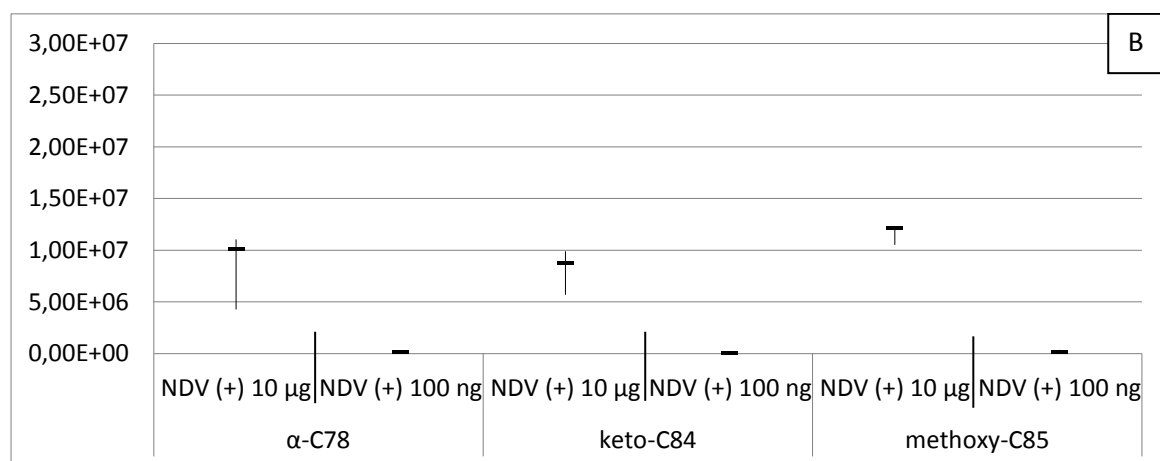
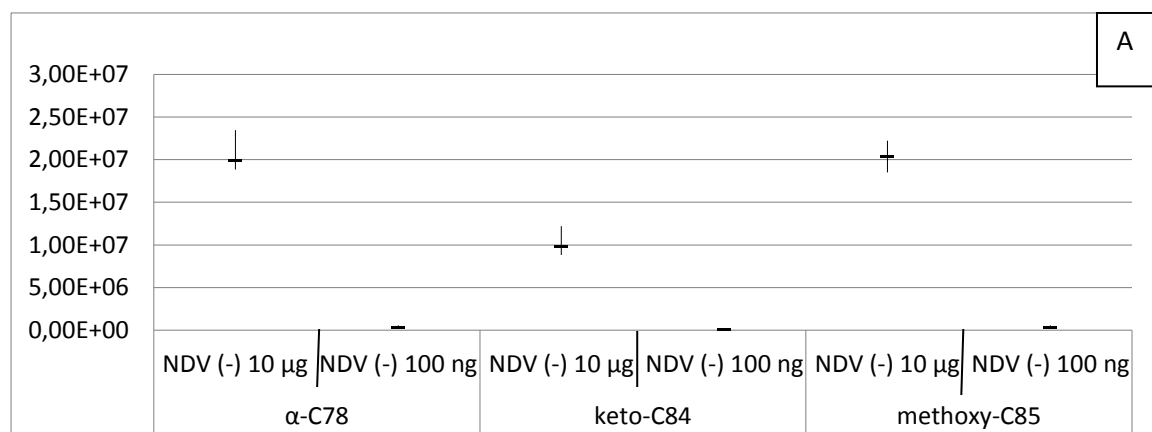


Figure 22. Significant differences in ion volume of the $\alpha\text{-C82}$ MA isolated from urine at 10 $\mu\text{g}/10\mu\text{l}$ by using Nemenyi test. Number 1 and 9 identify the lower and higher ion volume ranking for MAs in group i) non-derivatized MAs (-) mode, group ii) non-derivatized MAs (+) mode, and group iii) derivatized MAs (+) mode. The three dots grouped by color indicated the ion volume value obtained by triplicates. Brackets between groups indicate significant differences in ion volume.

Results were compared to establish the reproducibility between triplicates of derivatized and non-derivatized MAs spiked in urine (Figure 23). In general, the analysis of samples spiked with 10 µg/10 µl and 100 ng/10µl of MAs showed similar levels of variability in the measurements. An exception was the derivatized MAs at the higher concentration where greater variability was observed as compared to the non-derivatized MAs. Also in some cases, such as keto-C84, the analysis of lower concentrations gave an ion volume value of zero for the derivatized samples contributing to the variability.



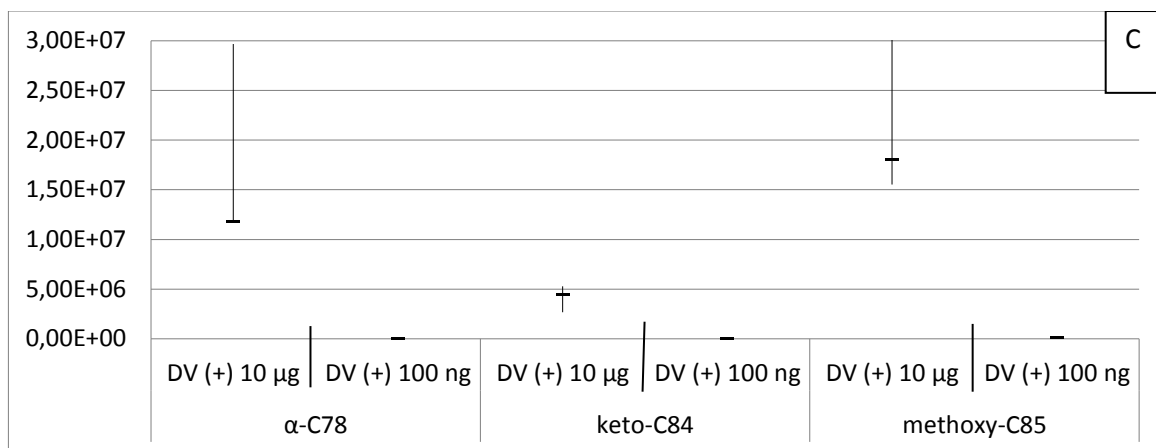


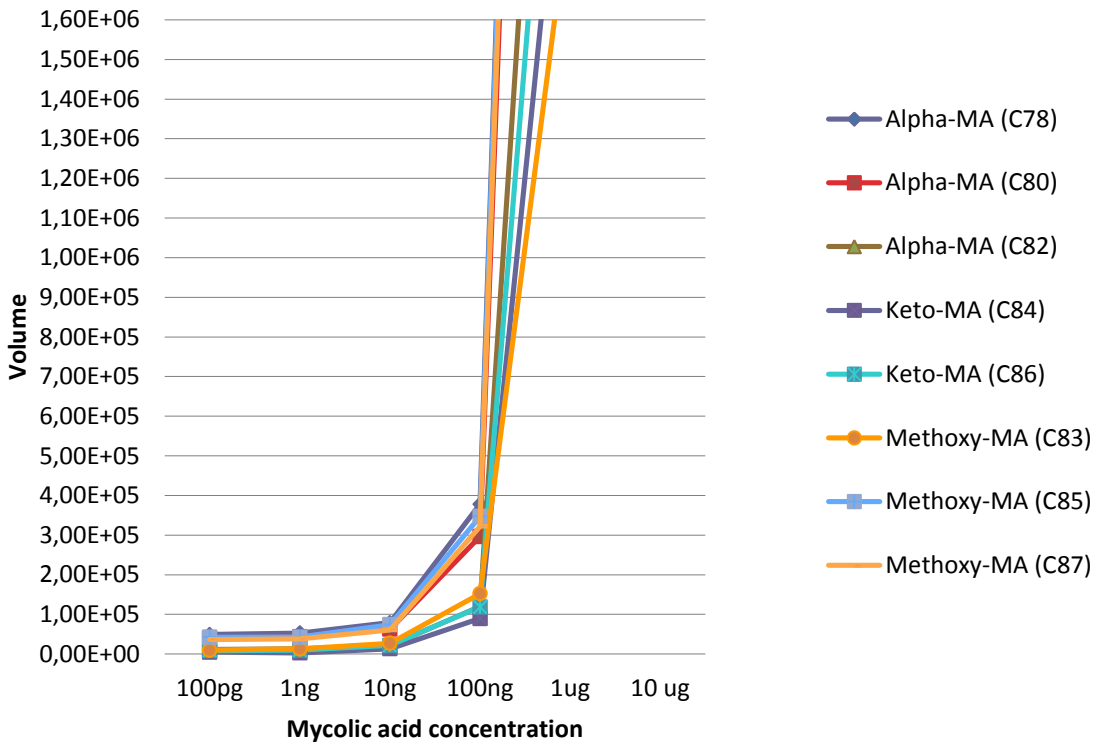
Figure 23. Reproducibility of results in urine samples spiked with MAs.

Triplicates of non-derivatized (NDV) MA standard in the (-) mode (A) and (+) mode (B), and derivatized (DV) MAs in the (+) mode (C) were compared based on ion volume. The vertical lines show the range of variability and the dash marks the median value. α-C78, keto-C84 and methoxy-C85 were analyzed at a 10 µg/10 µl and a 100 ng/10µl concentrations.

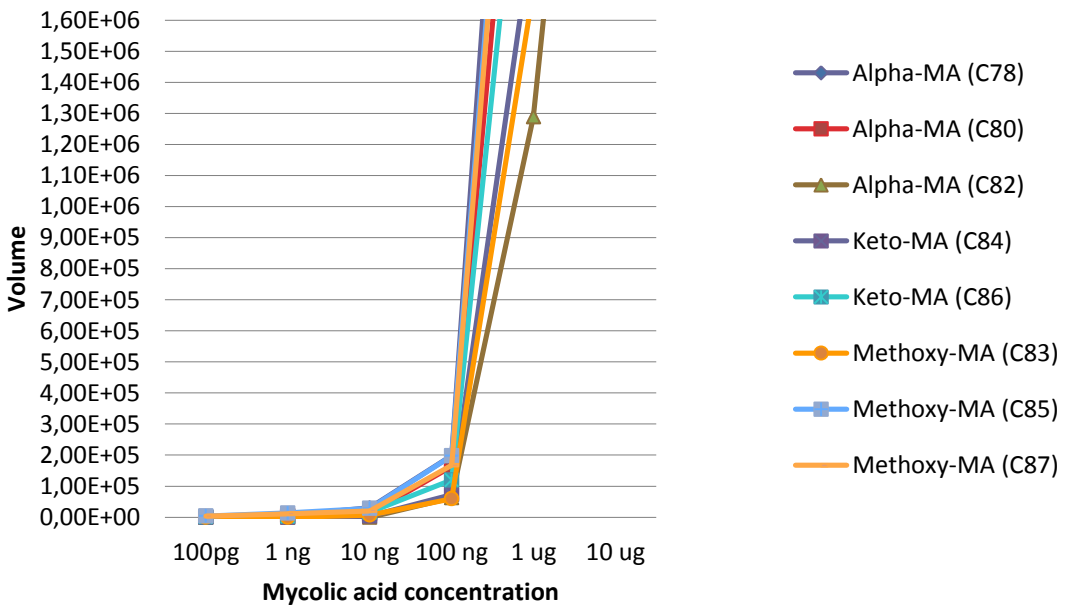
7.3.1.1 Method detection limit of mycolic acids spiked in urine

Standard curves were performed by spiking urine with decreasing dilutions of MAs in the range of 10 µg to 100 pg/10 µl. The ion volume values obtained through the MFE algorithm were plotted against the different MAs concentrations used to spike the urine (Figure 24).

A



B



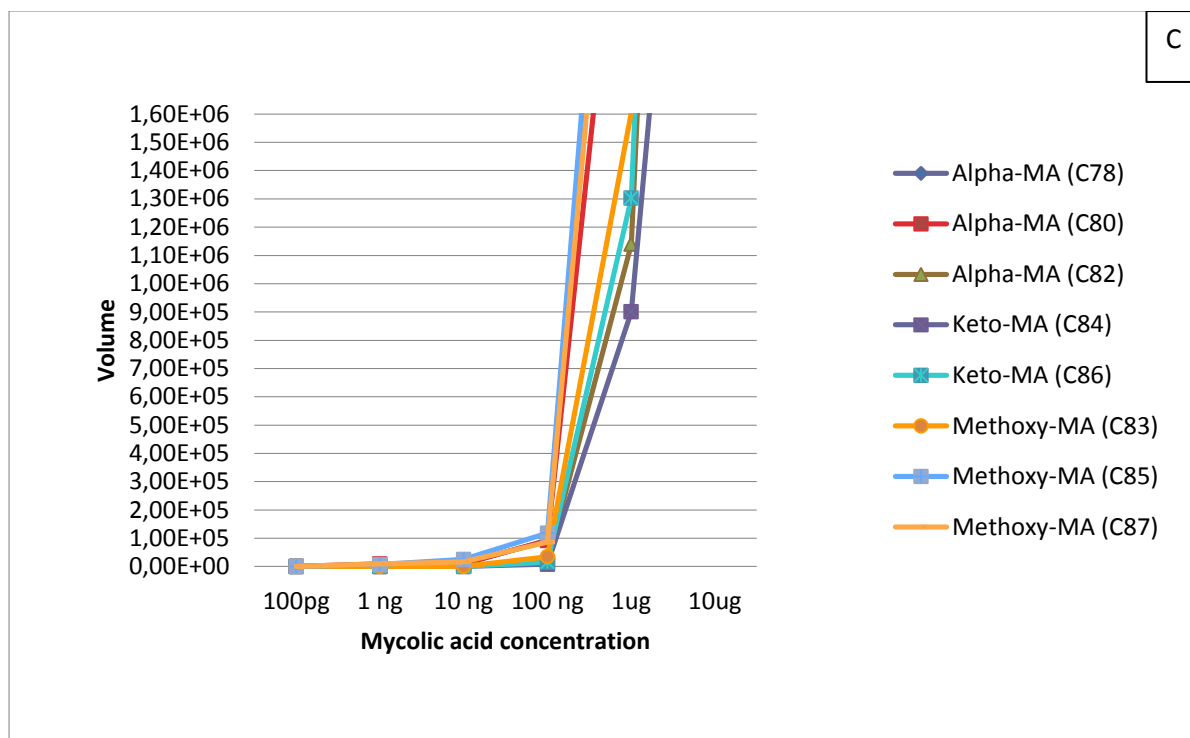


Figure 24. MAs spiked in urine standard curve. Non-derivatized MAs (-) mode (A), non-derivatized MAs (+) mode (B), and derivatized MAs (+) mode (C). Standard curve was constructed by using the average ion volume of the eight-targeted MAs.

Using the same approach applied to the MAs standards, a concentration of 100 ng/10 ul was selected for use in determining the MDL for derivatized and non-derivatized MAs spiked in urine. Seven replicates of the 100 ng/10 ul concentration were analyzed by LC/MS for the three groups (Table 6). Additionally seven replicates of a urine blank (990 ul urine spiked with 10 ul of chloroform: acetonitrile 2:1) in the (-) and (+) ion modes and seven replicates of a derivatized urine blank in the (+) mode were also analyzed. After the MFE analysis with the Agilent MassHunter software no matches were found between the databases and the blanks for those MAs that were in study, therefore the noise was not considered for the MDL of MAs in urine.

Table 6. MDL (ng) for non-derivatized and derivatized MAs spiked in urine¹.

Mycolic acids	Urine Non-derivatized (-) mode MDL (ng)	Urine Non-derivatized (+) mode MDL (ng)	Urine Derivatized (+)mode MDL (ng)
Alpha-MA (C78)	133.66	89.68	152.13
Alpha-MA (C80)	131.93	95.16	82.87
Alpha-MA (C82)	142.45	93.88	76.7
Keto-MA (C84)	144.13	94.6	76.34
Keto-MA (C86)	136.19	81.04	85.62
Methoxy-MA (C83)	128.33	102.27	81.9
Methoxy-MA (C85)	134.2	83.02	73.99
Methoxy-MA (C87)	124.15	86.75	83.72

¹MDL was calculated based on the average volume value for the different MAs. ($\alpha=0.05$).

The MDL was around 15.4 pmol/ 10 μ l (volume injected for LC/MS analysis) for the non-derivatized and derivatized MAs spiked in urine. The sensitivity decreased 10 fold compared to the MAs standard. There was not an improvement in the MDL when the derivatization method was used, but remained the same as compared to non-derivatized MAs.

7.3.2 Mycolic acids detection in serum by LC/MS

To assess the detection of MAs in serum six dilutions of MAs ranging from 100 ng/10 μ l to 1ng/10 μ l in chloroform: methanol (2:1 v/v) was used to spike 90 μ l of human serum (Sigma-Aldrich®). The MAs were extracted from the serum using a C-18 Sep-Pak® Vac RC 100 mg cartridges equilibrated with 5 ml of methanol and eluted with (i) 5ml of methanol, (ii) 5 ml of methanol: n-propanol: hexane (20:4:1 v/v), and (iii) 5 ml of n-propanol: hexane (80:20 v/v). The third fraction containing the MAs was dried under nitrogen and suspended in 51 μ l of chloroform: acetonitrile (2:1 v/v)

for LC/MS analysis in (+) and (-) ionization mode (Bhamidi et al, 2011; Sartain et al, 2011) or derivatization and LC/MS analysis in the (+) ionization mode as described for the MAs standard.

When the chromatograms were compared between derivatized and non-derivatized MAs (Figure 25), the intensity of the signal was higher for the derivatized MAs when the range between 100 ug to 1 ug/10 ul was used to spike the serum. From the 100 ng/10 ul concentration the signal for the derivatized compounds started to disappear (data not shown).

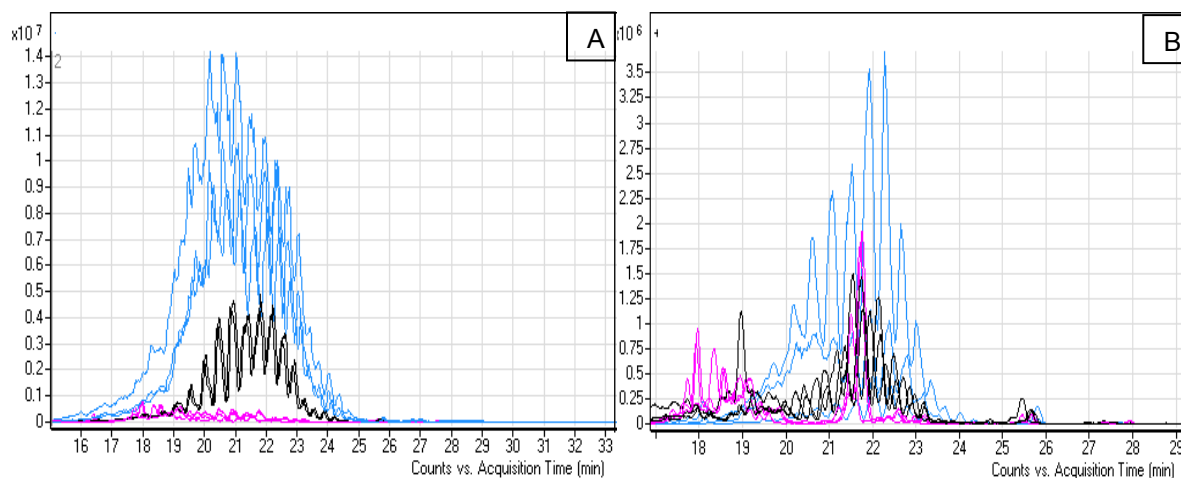


Figure 25. Extracted ion chromatogram (m/z 1000-1500) of derivatized and non-derivatized MAs spiked in serum samples. Different concentrations of MAs at 100 µg/10 µl (A) and 1 µg/10 µl (B) were used to spike human serum. Results (in triplicate) are shown for non-derivatized serum samples spiked with MAs in (-) ionization mode (pink line) and (+) ionization mode (black line) and derivatized serum samples spiked with MAs in (+) mode (blue line).

The median ion volume value of the eight target MAs were compared (Figure 26). The MAs (100 ug/10 ul) ion volumes obtained for the non-derivatized sample analyzed in the (-) or (+) ion mode were approximately 20 to 30 fold lower as compared to the samples subjected to derivatization prior to LC/MS (Figure 26 A). When lower concentrations were analyzed, the volume of the derivatized MAs was 3 to 7 fold higher compared to non-derivatized samples (Figure 26 B).

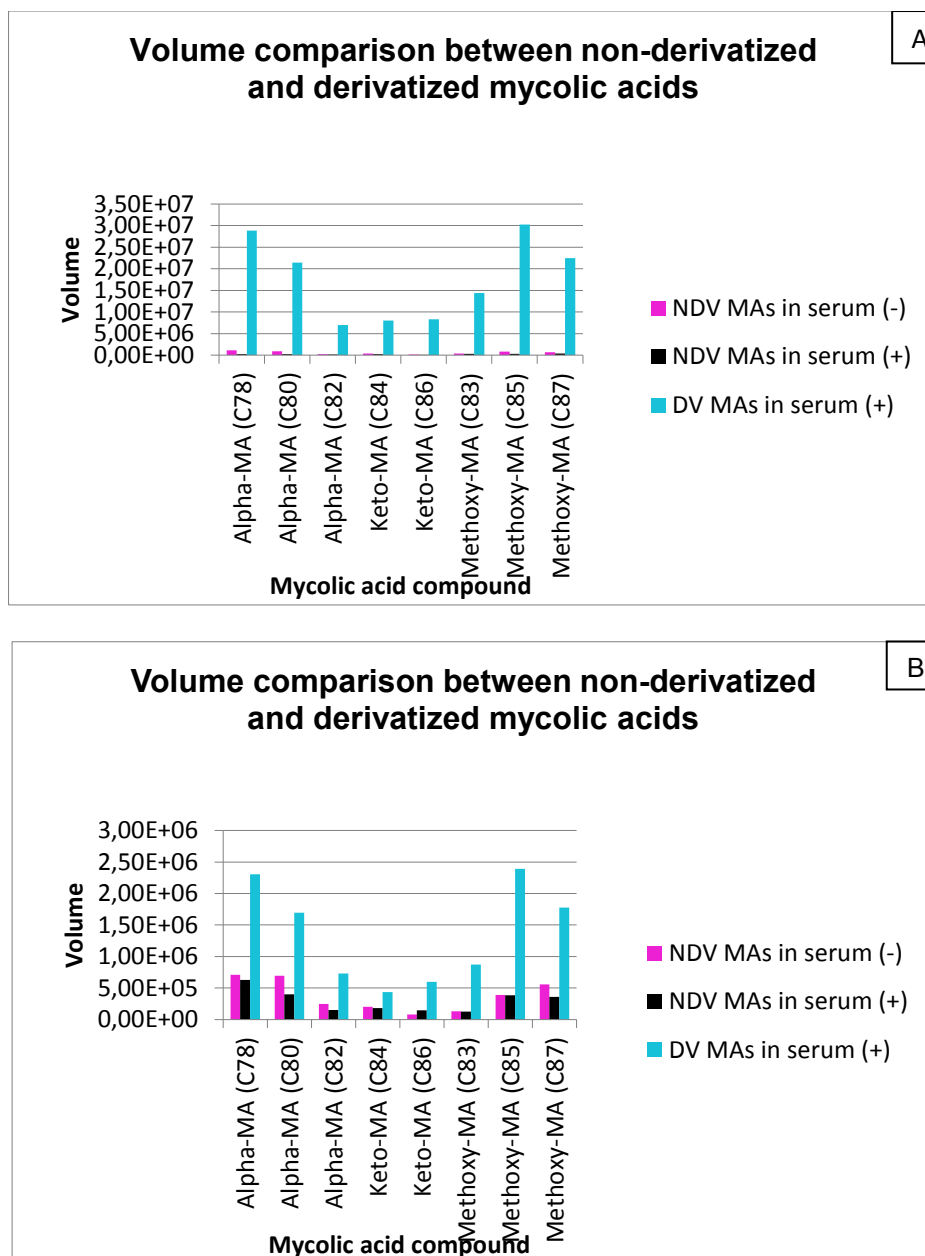


Figure 26. Ion volume comparison between derivatized and non-derivatized MAs spiked in serum. The median values of the triplicate analyses of serum spiked with 100 ug/10ul (A) or 1 ug/10ul (B) were used to construct the graphs.

As with the MA standards and the spiked urine samples the median ion volume values presented in Figure 26 were used to perform a Kruskal Wallis test (Table 7) to rank each MA measurement and these data applied to a Nemenyi test to identify groups that were significantly different in their ion volume values.

Table 7. Analysis of serum samples spiked with MAs by using Kruskal Wallis test¹.

MA (100 µg/10 µl)	(Group i) Serum spiked with MAs Non-derivatized (-) mode	(Group ii) Serum spiked with MAs Non-derivatized (+) mode	(Group iii) Serum spiked with MAs Derivatized (+) mode
Alpha-MA (C78)	1159302 (16)	286290 (6)	28821423 (23)
Alpha-MA (C80)	890002 (15)	253153 (5)	21397593 (21)
Alpha-MA (C82)	248844 (4)	151559 (2)	7017985 (17)
Keto-MA (C84)	380490 (11)	286623 (7)	8046120 (18)
Keto-MA (C86)	211813 (3)	77661 (1)	8314938 (19)
Methoxy-MA (C83)	395646 (12)	320398 (8)	14380284 (20)
Methoxy-MA (C85)	864907 (14)	344723 (9)	30210000 (24)
Methoxy-MA (C87)	678461 (13)	378603 (10)	22456988 (22)

MA (1 µg/10 µl)	(Group i) Serum spiked with MAs Non-derivatized (-) mode	(Group ii) Serum spiked with MAs Non-derivatized (+) mode	(Group iii) Serum spiked with MAs Derivatized (+) mode
Alpha-MA (C78)	710829 (18)	626153 (16)	2304858 (23)
Alpha-MA (C80)	693604 (17)	402061 (12)	1695401 (21)
Alpha-MA (C82)	245397 (8)	151309 (5)	731996 (19)
Keto-MA (C84)	202948 (7)	179919 (6)	436473 (13)
Keto-MA (C86)	77652 (1)	147631 (4)	595882 (15)
Methoxy-MA (C83)	131337 (3)	126267 (2)	870334 (20)
Methoxy-MA (C85)	388556 (11)	382219 (10)	2390037 (24)
Methoxy-MA (C87)	554727 (14)	360073 (9)	1778593 (22)

¹The median ion volume value from derivatized and non-derivatized triplicates of MAs is shown (with ranks of the data in parentheses). The higher the number the greater the rank. MAs concentrations analyzed correspond to 100 ug/10 ul and 1 ug/10 ul ($\alpha=0.05$).

Nemenyi test applied to the data from the higher concentration of MAs spiked in serum (100 µg/ 10 µl), the ion volume value for the group iii) was significantly higher compared to the group i) and ii). There were no significant differences between groups i) and ii) (Figure 27 A). The analysis of the lower MA concentration

spiked in serum (1 $\mu\text{g}/10\ \mu\text{l}$) showed that the ion volume value for the group iii) was significantly higher compared to group i) and ii). There were no significant differences between groups i) and ii) (Figure 27 B).

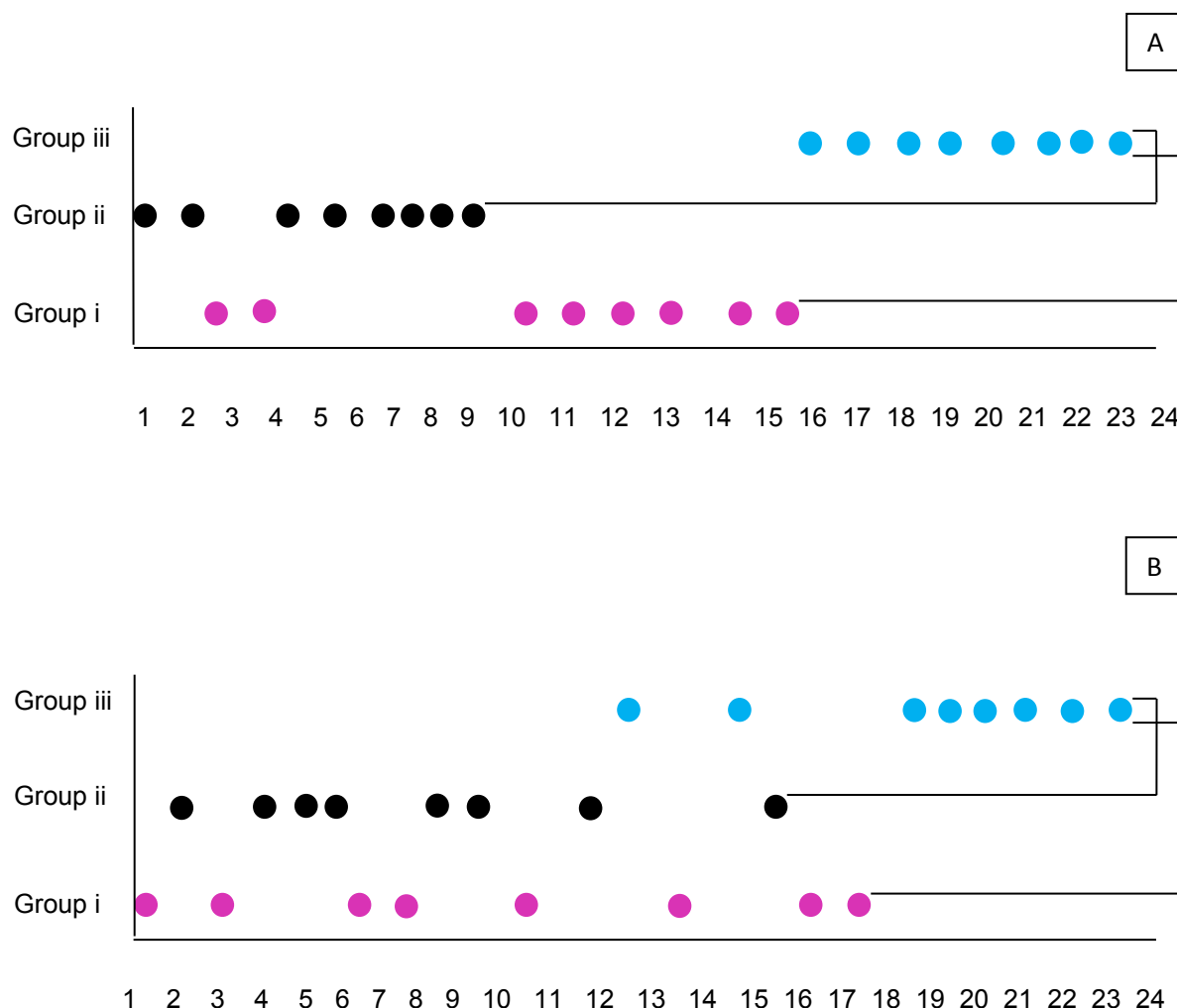


Figure 27. Significant differences in ion volume between MAs spiked in serum-groups based on the Nemenyi test. Number 1 and 24 identify the lower and higher ion volume ranking for MAs in group i) non-derivatized MAs (-) mode, group ii) non-derivatized MAs (+) mode, and group iii) derivatized MAs (+) mode. Brackets between groups indicate significant differences in ion volume. The MA standard concentrations spiked in serum were 100 $\mu\text{g}/10\ \mu\text{l}$ (A), and 1 $\mu\text{g}/10\ \mu\text{l}$ (B).

As with the MA standards and the spiked urine, it was important to compare individually the targeted MAs. The ion volume of the triplicate analysis were applied to the Kruskal-Wallis test for the eight targeted MAs and three groups i) MAs non-derivatized (-) mode, ii) MAs non-derivatized (+) mode, and iii) MAs derivatized (+) mode were compared for each targeted MA. Significant differences between groups were found only in the 100 µg/10 µl concentration for α-C78, methoxy-C85 and methoxy C-87. These three MAs were subjected to Nemenyi test to identify those differences (Figure 28). The analysis showed same results for the three MAs with a significantly higher ion volume for group iii) compared to group ii). There were not significant differences between groups iii) and i) or between groups i) and ii).

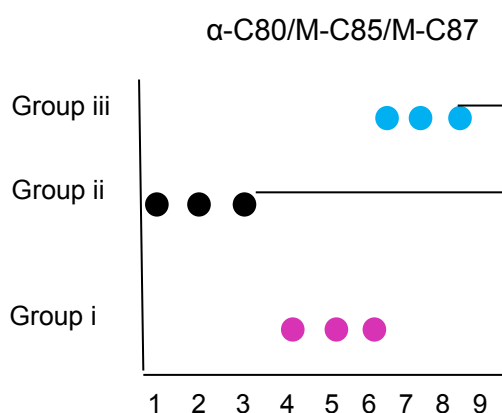
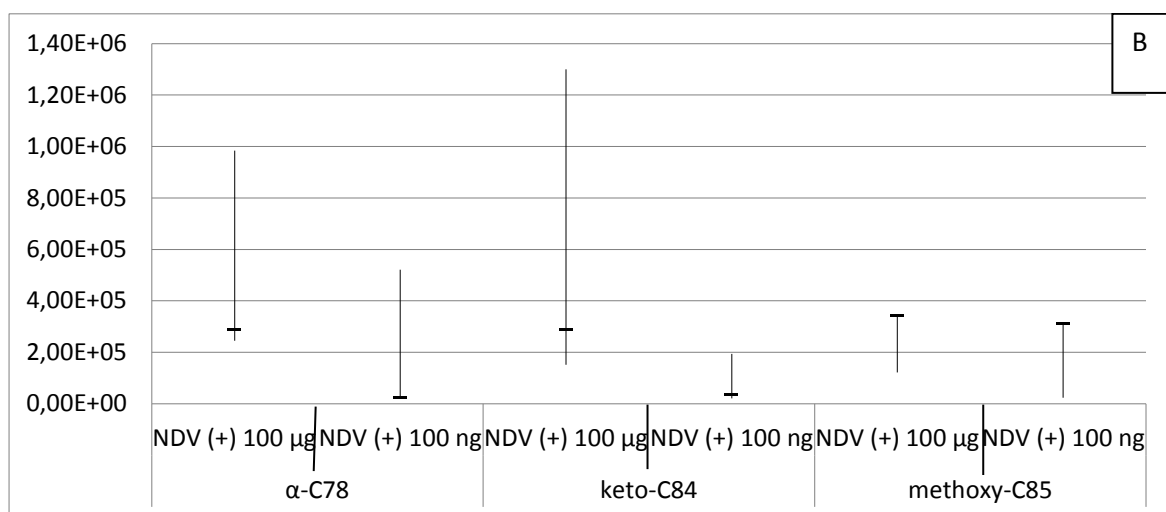
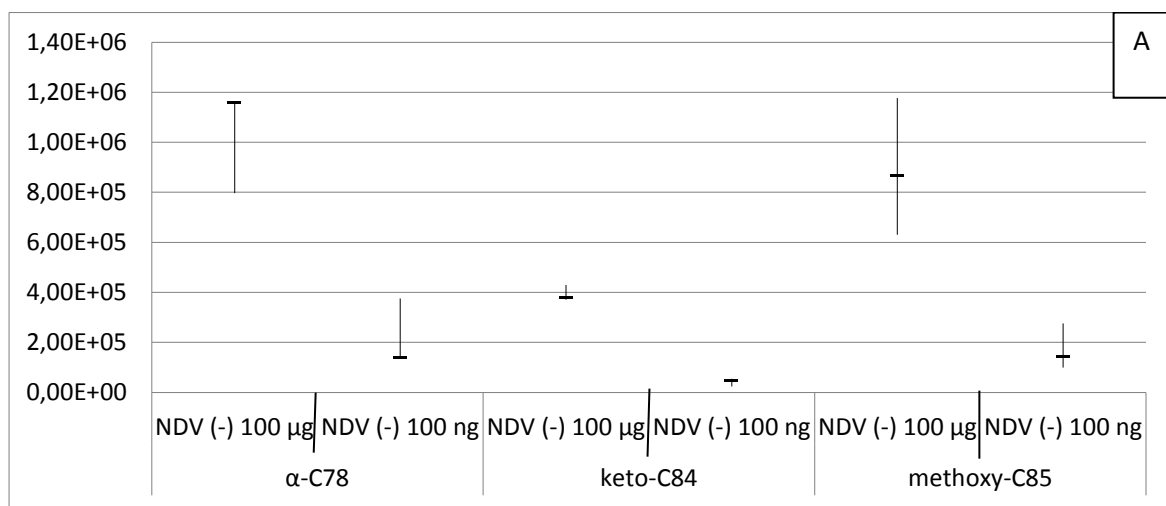


Figure 28. Significant differences in ion volume of individual MAs at 100 µg/10µl by using Nemenyi test. Number 1 and 9 identify the lower and higher ion volume ranking for MAs in group i) non-derivatized Mas (-) mode, group ii) non-derivatized MAs (+) mode, and group iii) derivatized MAs (+) mode. The three dots grouped by color indicated the ion volume value obtained by triplicates. Brackets between groups indicate significant differences in ion volume.

The reproducibility of the results was also tested. 100 µg/10 µl and 100 ng/10µl concentrations were analyzed for non-derivatized MAs and 100 µg/10 µl and 1µg/10 µl for derivatized MAs (Figure 29). The analysis of the different concentrations showed a similar trend in the variability of the measurements. However, the variability between triplicates was higher for the non-derivatized MAs in (+) mode. Lower concentrations were not compared because zero values were common to be found between the triplicates and the presence of three values to establish differences was unavailable.



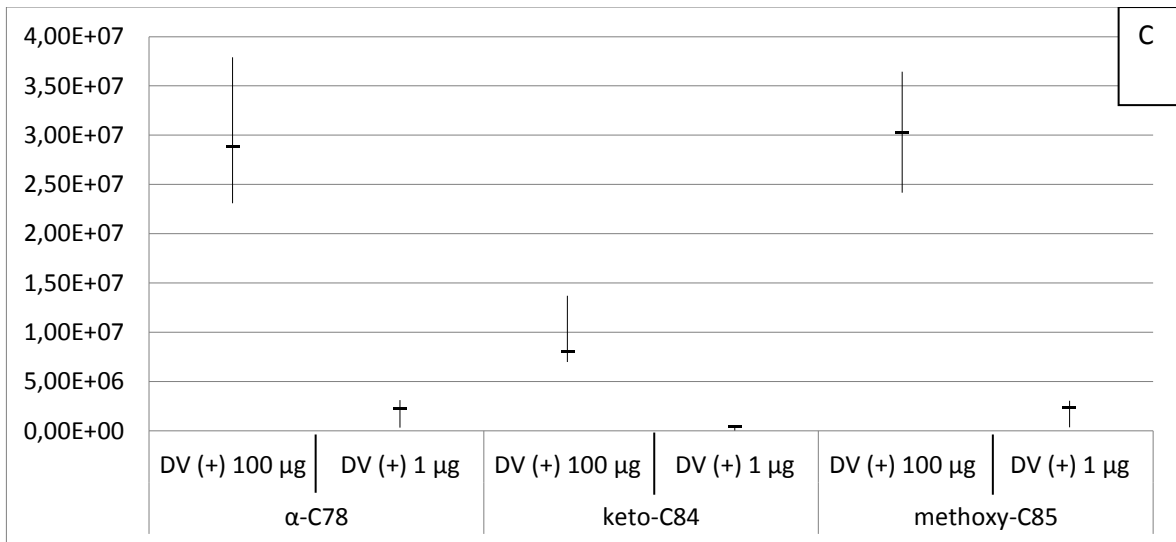
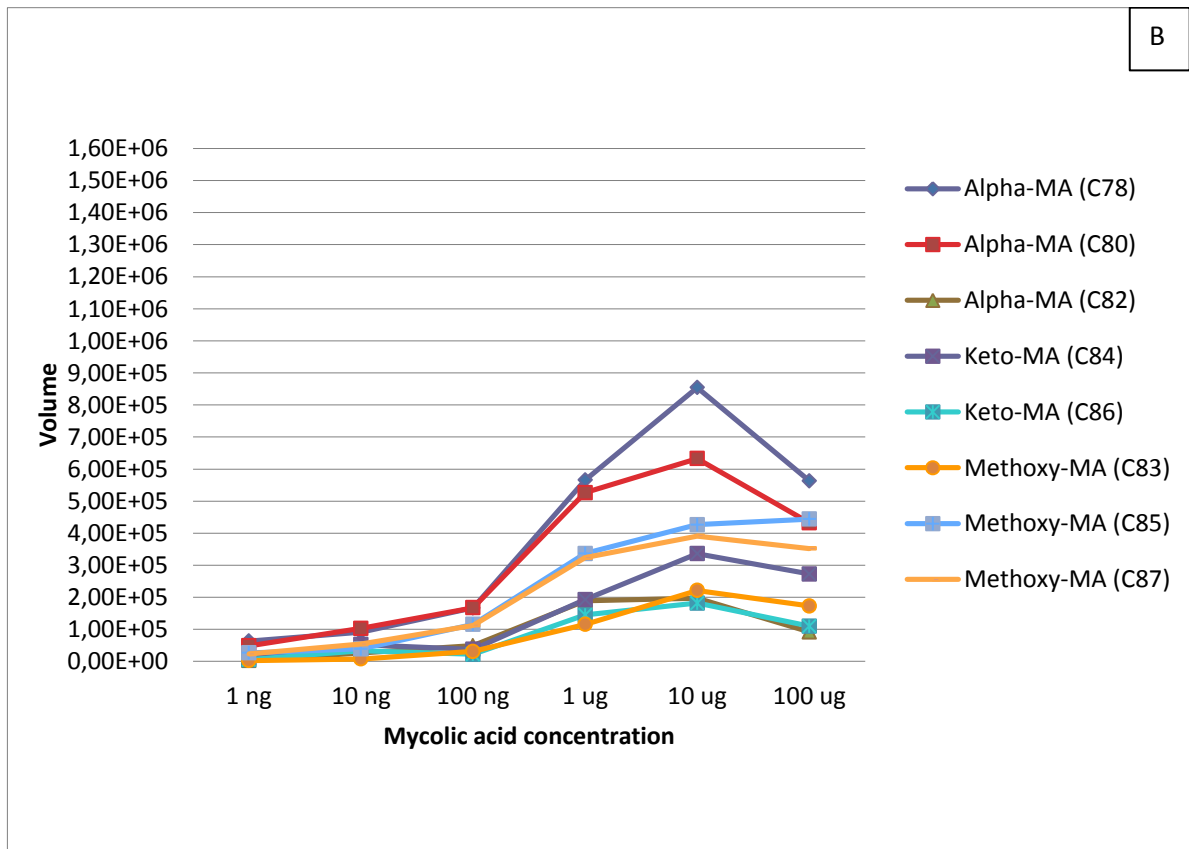
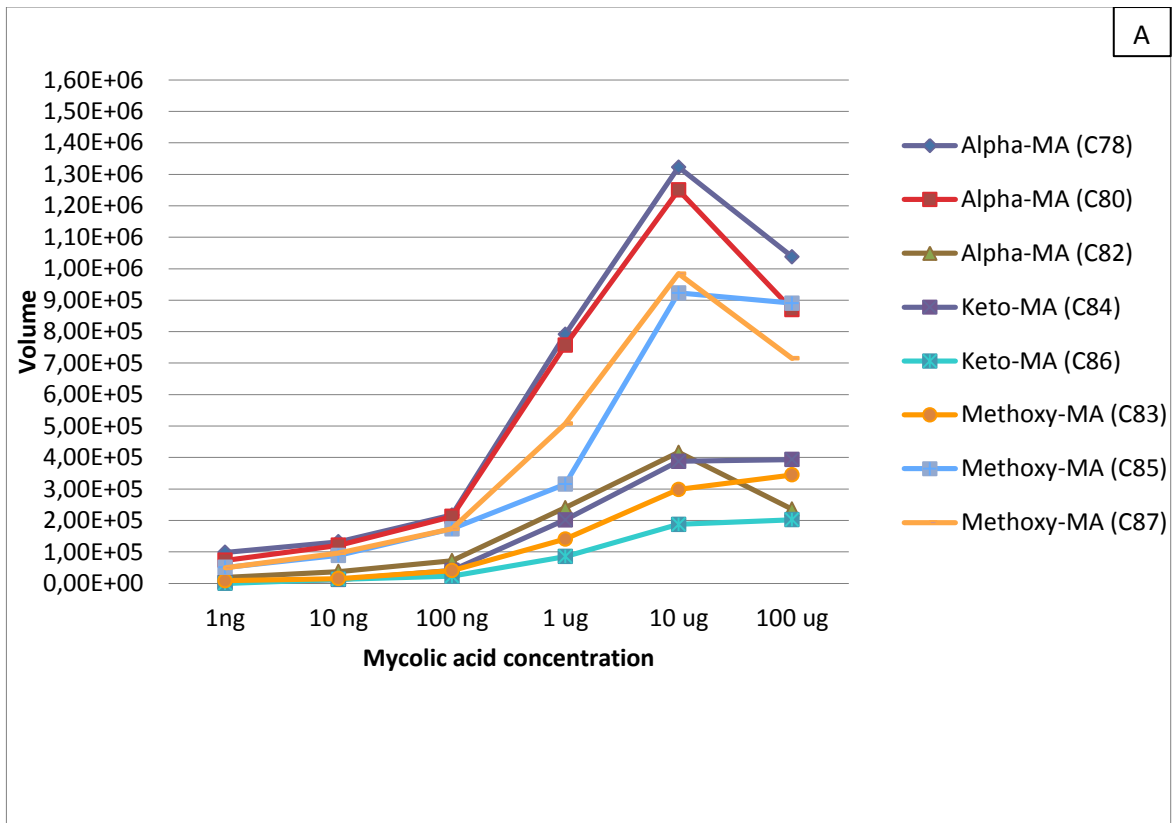


Figure 29. Reproducibility of results in serum samples spiked with MAs standard. Triplicates of non-derivatized (NDV) MA standard in the (-) mode (A) and (+) mode (B) and derivatized (DV) MAs in the (+) mode (C) were compared based on ion volume.

7.3.2.1 Method detection limit of mycolic acids spiked in serum

The standard curves for MAs in serum were constructed by using six MAs concentrations ranging between 1 ng/ 10 ul and 100 ug/ 10 ul. A break in the slope was observed at 100 ng/10 µl for non-derivatized MAs in (+) and (-) and 1 ug/ 10 ul for derivatized MAs in (+) mode (Figure 30).



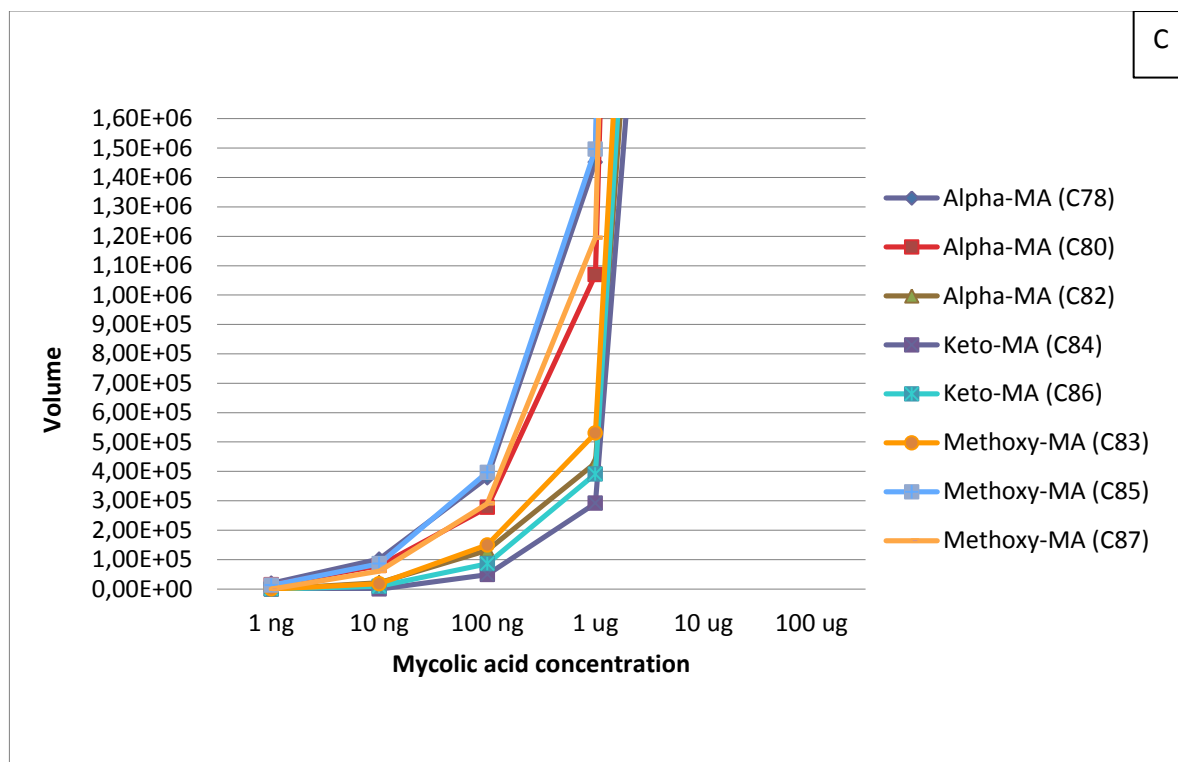


Figure 30. Standard curve of MAs spiked in serum. Non-derivatized MAs (-) mode (A), non-derivatized MAs (+) mode (B), and derivatized MAs (+) mode (C). Standard curve was constructed by using the average ion volume of the eight targeted MAs.

For the MDL seven replicates of the mentioned concentrations were analyzed by LC/MS in the respective ionization mode. To determine the background noise of the method, seven replicates of a serum blank (90 ul o serum spiked with 10 ul of chloroform: acetonitrile (2:1 v/v)) for non-derivatized MAs and seven replicates of a serum blank of the derivatization reaction were also analyzed by LC/MS. By using the MFE algorithm and the Mtb LipidDB and AMMP-MA databases, no matches between the different blanks and the MAs studied were found (including m/z and retention time) excluding the background noise of the MDL analysis (Table 8).

Table 8. MDL (ng) for non-derivatized and derivatized MAs spiked in serum¹.

Mycolic acids	Serum Non-derivatized (-) mode MDL (ng)	Serum Non-derivatized (+) mode MDL (ng)	Serum Derivatized (+) mode MDL (μ g)
Alpha-MA (C78)	99.66	21.89	0.9
Alpha-MA (C80)	101.77	56.24	0.92
Alpha-MA (C82)	119.71	42	0.9
Keto-MA (C84)	164.96	108.99	0.86
Keto-MA (C86)	178.77	23.57	0.95
Methoxy-MA (C83)	108.48	29.18	0.88
Methoxy-MA (C85)	129.94	56.61	0.82
Methoxy-MA (C87)	121.16	30.11	0.67

¹MDL was calculated based on the average ion volume value for the different MAs. ($\alpha=0.05$).

The MDL was around 15.4 pmol/ 10 μ l (final volume of injection for LC/MS analysis) for non-derivatized MAs in (+) and (-) ionization mode and 154 pmol/ 10 μ l for the derivatized MAs in the (+) mode. The derivatization protocol did not improve the limit of detection, following the same trend as before. Regarding the non-derivatized MAs, the MDL sensitivity was 100 fold higher compared to the MAs standard. This was expected due the complex nature of serum.

8. Discussion and conclusions

The limited sensitivity of diagnostic TB tests causes special concern in some world areas and population groups, triggering numerous studies to discover and evaluate biomarkers. The goal of this study was to generate a more sensitive method for the detection of MAs. Available information about the TB cell wall composition linked several of its compounds to virulence and resistant roles; with the MAs exhibiting unique characteristics that support targeting them as a feasible biomarker for TB. The MAs have been analyzed directly from TB cultures to identify and classify mycobacterial species by HPLC (Butler et al., 2001); analyzed from sputum samples by LC/MS (Minnikin et al., 1993; Shui et al., 2011) and were targeted for serological studies (Ryll et al., 2001). However, there are no previous studies that can corroborate the presence of MAs in serum or urine samples from *Mtb* infected patients.

As a first step in determining the feasibility of serum or urine MAs as a biomarker of TB, this study was performed to develop and evaluate for MA detection by LC/MS. Specifically a pre-existing derivatization protocol was modified to make it amenable to the hydrophobic nature of MAs. Other derivatization protocols to improve MA detection have been previously investigated. The formation of MA methyl esters (MAMEs) allows a better separation by TLC (Minnikin et al., 1984). Fluorescent derivatives have been also used for HPLC analysis (Minnikin et al., 1993). The goal of the derivatization protocol used in our study looked for an improvement of the detection sensitivity by increasing the ionization efficiency of MAs by adding a quaternary amine to improve ionization efficiency leading to an increased signal when analyzed by LC/MS. The attachment of a quaternary amine to fatty acids between 24 and 30 atoms carbon residues increases the ionization

efficiency 2,500 fold (Yang et al, 2007).

To assess whether the Yang et al. (2007) methodology could be applied to MAs, these studies first identified a solvent system that was compatible with MAs and the derivatizing reagents, and established a protocol that removed excess derivatizing reagents or by products prior to analysis by LC/MS. This effort resulted in identifying chloroform/acetonitrile (2:1) as an appropriate derivatizing solvent and acetonitrile as an effective method to remove excess derivatizing reagents or by products. Importantly, this basic method development endeavor highlighted the importance of selecting derivatizing reagents that have similar solubility to the targeted fatty acids and that will not interfere with downstream measurements.

To fully evaluate the effectiveness of the derivatization protocol and detection of products by LC/MS the ion volume values of eight targeted MAs were used to compare the derivatized and non-derivatized samples of MA standards, and urine and serum spiked with the MA standards. The statistical analyses of the data included using the median value of triplicate analyses to establish a ranking of the use of (-) and (+) ionization mode LC/MS to measure underivatized MAs versus (+) ionization mode LC/MS to measure derivatized MAs. Additionally, multiple concentrations of MAs were assessed as underivatized samples in the (-) and (+) ionization modes and as derivatized in the (+) ionization mode to establish relative MDL of each process. Further, analyses included detailed inspection of the LC/MS data and evaluation of the variability in data for each process or sample group.

In the case of the MAs standard and urine samples spiked with MAs, the ion volume values for the targeted MAs of the non-derivatized samples were higher compared to the derivatized samples. The Kruskal-Wallis and Nemenyi test (Zar, 1999) for ranking of the groups consistently showed that the non-derivatized

samples analyzed in (+) or (-) ion modes were significantly higher than the derivatized samples. These statistical analyses of targeted MAs, however, did not correlate to the ion chromatograms where the derivatized samples showed a consistently a higher signal of detection. Detailed comparative analyses of the MS data for the MA standard shed some light on to this discrepancy. When different peaks of derivatized and non-derivatized samples were compared in the (+) mode, the ion profiles showed that the total signal of the peak for the derivatized samples was comprised of derivatized MAs, non-derivatized MAs and non-identified compounds. Moreover, the non-identified compounds in the derivatized MAs standard samples showed to be more abundant and in higher ion volume compared to the non-derivatized. These two factors could be explaining the increase of the total signal, leading to an enhancement of the peaks in the chromatogram profile, but a decreased ion volume value for targeted MAs. These observations were also consistent with the variability in reproducibility between sample groups (derivatized versus underivatized) for ion volume measurements for the eight targeted MAs. This increase in variability of data was most evident for derivatized MAs standard and derivatized MAs spiked in urine when the higher concentrations of MAs were evaluated.

The presence of non-derivatized MAs in the derivatized sample and the ion volume variability could be explained by the use of non-polar solvents that can affect in some way the solubilization of the derivatizing reagents. Additionally, a cleaning step applied after the derivatization was necessary to avoid an excess of reagents that could affect the performance of the mass spectrometer. However this process, could also affect the final available amount of derivatized MAs to be analyzed by LC/MS. The incubation period of the derivatization reaction and temperature could

be two factors susceptible to modification to achieve better derivatization efficiency (Duong et al., 2012).

Serum samples spiked with MAs, however, yielded an unexpected result. When higher concentration of MAs were compared (100 µg/10 µl) the total ion volume for the targeted mycolates was increased 20 to 30-fold for the derivatized samples as compared to the non-derivatized samples. The peak intensity in the chromatogram was also higher compared to non-derivatized serum samples. When variability between triplicates analyses was evaluated there was higher variability in the ion volumes for the non-derivatized MAs analyzed in the (+) mode. This points to a phenomenon where the MAs may actually derivatize more efficiently in the presence of serum components. It has been suggested that an interaction between cholesterol and MAs could influence the low sensitivity of serological TB tests when free MAs are used in an ELISA assay (Benadie et al., 2008). Additionally, when MAs were converted into their methyl ester derivatives conformational changes occur in the MAs and this prevents the binding of cholesterol to the MA structure (Benadie et al., 2008). It is speculated that compounds present in the human serum such as cholesterol coelute with the MAs during the enrichment step with C18 cartridges. It is possible that the addition of a quaternary amine through the derivatization could in some way counteract an interaction between MAs and serum components that could be suppressing or inhibiting the ionization of the MAs in the non-derivatized samples. This would lead to appearance of increased detection in the derivatized sample. Alternatively, it can also be hypothesized that the interaction of the MAs with a serum product could increase derivatization efficiency by making the carboxylic acid more accessible for derivatization. It is interesting to note that when lower concentration of MAs spiked in serum were analyzed (1 ng/10 µl, 10 ng/10 µl), the ion volume value

for the derivatized MAs decreased compared to the non-derivatized samples. In this case, we expect that fatty acids compounds present in serum could be competing with MAs in the derivatization process, and diminishing the derivatization efficiency for MAs compounds. It is also possible that the extraction procedures for isolation of the MAs from the serum need to be further optimized.

The MDL of derivatized and non-derivatized MAs by using LC/MS was also calculated. It was important to evaluate the sensitivity of the method and compared it to biological fluids spiked with the MA standard. Shui et al., (2007) used LC/ESI-MS to compare the lipid profiles of mycobacteria grown under different physiological conditions. MAs were analyzed in (-) ionization mode and the limit of detection (signal/ noise 3) was estimated to be 10 pmol. In another study performed by Laval et al., (2001), by using MALDI-TOF in (+) ionization mode, less than 10 pmol of mycolates was sufficient to obtain adequate MA mass spectra. These results are in concordance to the MDL obtained in this study where the MDL for the MA standard was 0.15 pmol. In the case of non-derivatized samples, serum and urine spiked with MAs showed an increased MDL of 100-fold compared to the MA standard. This situation was expected because of the lipid extraction process and the more complex nature of the samples. After the derivatization process, the MA ion volumes were compared to their respective non-derivatized MAs, and resulted in the MDL being increased 10-fold for the derivatized MA standard and MAs in serum. However, the derivatized and non-derivatized MAs in urine were found to have the same MDL. These data indicate that the derivatization process did not improve the MDL.

The MDL was determined by using the concentration that produced a break in the slope of the standard curve of MAs. It is important to consider that the higher MDL obtained for the derivatized MAs was reflected in a more abrupt dropped of the

detection signal between the 10 μg and the 1 μg . There is subjectivity in this approach since with both the derivatized and underivatized samples two different slopes and two break points could be observed for some of the MAs. The use of the most consistent break point for all the targeted MAs typically lead to the selection of a higher concentration of MAs being used to calculate the MDL for the derivatized samples.

The analytical sensitivity can be defined as the smallest amount of a substance in a sample that can be accurately measured by an assay. This has to be differentiated from the diagnostic sensitivity that indicates the percentage of infected individual identified as positive by the technique (Saah et al, 1997). During this study just the analytical sensitivity could be estimated through the MDL, because no clinical samples from infected Mtb patients were include.

The noise was not considered in the MDL because there were not ions with the same mass or Rt that the MAs included in this study. Despite this, other ions detected at the same Rt, but with different mass can be exerting a matrix suppression effect over the MAs in study, affecting the MAs MDL and the analytical sensitivity of the method.

9. Future directions

It is difficult to estimate the applicability of LC/MS for MA detection in serum or urine. The first approach would be having a proof of principle of their presence in clinical samples from infected Mtb patients, and having an adequate standard to quantify the presence of the different MAs. Previous studies have confirmed the presence of MAs in sputum from Mtb infected patients (Minnikin et al., 1993, Shui et al., 2011). Shui et al., (2011) analyzed sputum samples from Mtb infected patients by multiple reaction monitoring (MRM). By using this technique a precursor ion of interest is selected in the first mass analyzer of a tandem mass spectrometer and fragmented in the collision cell, then a characteristic product ion is selected in the second mass analyzer, providing a quantitative analysis. This method was compared to AFB smear and bacterial culture, giving a 100% of accuracy when was compared to smear (+++) and (++) , 97.5% for smears (+) and 25% for smear (-)/culture (+). It could be inferred that by using MRM, the sensitivity of the method can be improved for the detection of MAs in other fluids such as serum and urine. However, it would be important to consider adequately the precursor ions because the MA profile may vary.

Shui et al., (2011) showed the major ions identified in clinical sputum samples were α -MA m/z 1164 (C80), methoxy-m/z 1280 (C87), and keto-m/z (C86) compared to the Mtb Beijing strain culture profile where α -m/z 1136 (C78), methoxy-m/z 1252 (C85), and keto-m/z 1236 (C84) were the most abundant. Bhamidi et al., (unpublished data) analyzed granuloma from Mtb infected guinea pigs by LC/MS showing a MA profile with predominance of even-numbered α -MAs (C78, C80, C82), but also new findings from a few granulomas reported identifying odd-numbered carbon α -MAs in the same or higher abundance than even-numbered α -MAs and the

presence of short chain α -MAs (α') for some granulomas. This uncommon profile with odd α -MAs and α' -MAs was also found in sputum samples from Mtb infected patients. Even though the α -mycolate class appears to be predominant during the analysis of *in vitro* and *in vivo* Mtb, the total profile in biological samples can vary, reflecting unique situations during the disease process.

More studies including clinical samples from Mtb infected patients are necessary to determine MAs pattern profiles. In the case of using LC/MS for the samples analysis, it could be important to analyze them by using (-) and (+) ionization mode, to cover a broader spectrum, identifying the most common compounds. By having the clinical story of the patient, valuable information could be obtained from changes in the MA profile during the course of the disease, and during a treatment regimen.

In the field of biomarkers, LC/MS is a sensitive method to evaluate serial molecules. However, in terms of expertise, management, and cost it is restrictive. If the proof of principle of MAs detection in serum and urine is confirmed, the next steps would be the development of a more portable and less expensive platform for identification. In the field of biomarkers some possibilities have been explored, cardiac biomarkers can be identified by using cleavable tag immunoassays, where the fluorescent tag is cleaved from the detection antibody and analyzed by using a microchip through a chromatographic technique (Caulum et al., 2007). Tagging immunoassay for MAs could be challenging in terms of specificity, because lipids are poor immunogens (Gargir et al., 2002). However, Fujiwara et al., (1999) immunized rabbits with Mtb cord factor (trehalose-6, 6'-dimycolate), showing that their sera reacted especially against methoxy-MAs derivatives; it was also concluded that the IgG antibody recognized the hydrophobic moiety rather than carbohydrate moiety of

the cord factor structure. Considering these results, it is possible to think that MAs can be targeted more specifically.

Fluorescent tagging has also been used for MA detection. Theoretically, fluorescence detection could increase the sensitivity 10 to 1,000 times (Butler et al., 2001). Minnikin et al., (1993), used HPLC to achieve a characteristic profile for the fluorescent anthrylmethyl ester MA derivative. Fluorescent tagging however, can be expected to be unspecific in the presence of other fatty acids, such as in a serum sample. The highly hydrophobic nature of MAs could be exploited to make the detection more specific, for example using fluorescence TAG, and then capturing MAs by using C18 cartridges.

Regarding the study of MAs in serum or urine, there is no precise information about the release or clearance of these molecules. It can be speculated that MAs, as in the case of LAM (Boehme et al., 2005), could be released from TB bacterial cells, reaching the circulatory system and filtered by the kidneys, this idea could be a possible explanation for the hypothesis that MAs can be encountered in serum and urine from infected patients. Ojha et al., (2010) showed the presence of free MAs in *M. smegmatis* biofilms, generated from the enzymatic activity of a specific TDM serine esterase. They also suggested the presence of a TDM specific esterase in *Mtb*. This could be another way to expect free MAs available to be detected.

Bacteremia or renal TB could be possible situations where serum or urine samples may be assimilated to the sputum sample behaviour, due to the proximity to the infectious focus. Urogenital TB is responsible for 30 to 40 % of the extrapulmonary cases and is second to the lymph-node extrapulmonary presentation (Figueiredo et al., 2008). In the case of the bacteremia, it became more common with the emergence of patients with AIDS (Grinsztejn et al., 1997). In a study

performed by Thambu et al., (2004), 43% of HIV-infected infected patients (n=20) had bacteremia detected by culture of blood samples. Another study in Brazil, investigated the prevalence of bacteremia in patients with HIV and with persistent fever by using automated blood. 30% (n=13) of the cases were confirmed as positives (Bacha et al., 2004). Regarding the lower sensitivity of smear microscopy in AIDS patients, and the presence of bacteria in blood, detection in serum appears as an alternative to be explored.

10. References

1. Agranoff, D., Fernandez-Reyes, D., Papadopoulos, M. C., Rojas, S. A., Herbster, M., Loosemore, A., Tarelli, E. (2006). Identification of diagnostic markers for tuberculosis by proteomic fingerprinting of serum. *Lancet*. 368 (9540), 1012-21.
2. Alugupalli, S., Sikka, M. K., Larsson, L., & White, D. C. (1998). Gas chromatography–mass spectrometry methods for the analysis of mycocerosic acids present in *Mycobacterium tuberculosis*. *J Microbiol Methods*. 31(3), 143-150.
3. Andersen, P., Andersen, A. B., & Saren, L. (1995). Recall of Long-lived Immunity to *Mycobacterium tuberculosis* infection in mice. *J Immunol*. 154(7):3359-72.
4. Antunes, A., Nina, J., & David, S. (2002). Serological screening for tuberculosis in the community: an evaluation of the Mycodot procedure in an African population with high HIV-2 prevalence (Republic of Guinea-Bissau). *Res Microbiol*. 153(5), 301-5.
5. Aryan, E., Makvandi, M., Farajzadeh, A., Huygen, K., Bifani, P., Mousavi, S.-L., Fateh, A. (2010). A novel and more sensitive loop-mediated isothermal amplification assay targeting IS6110 for detection of *Mycobacterium tuberculosis* complex. *Microbiol Res*. 165(3), 211-20.
6. Astarie-Dequeker, C., Le Guyader, L., Malaga, W., Seaphanh, F.-K., Chalut, C., Lopez, A., & Guilhot, C. (2009). Phthiocerol dimycocerosates of *M. tuberculosis* participate in macrophage invasion by inducing changes in the organization of plasma membrane lipids. *PLoS pathogens*. 5(2), e1000289.
7. Bacha, H. A., Cimerman, S., de Souza, S. a, Hadad, D. J., & Mendes, C. M. F. (2004). Prevalence of mycobacteremia in patients with AIDS and persistent fever. *BJID*. 8(4), 290–5.
8. Banerjee, R., Schechter, G. F., Flood, J., & Porco, T. C. (2008). Extensively drug-resistant tuberculosis: new strains, new challenges. *Expert Rev Anti Infect Ther*. 6(5), 713-24.
9. Barral, D. C., & Brenner, M. B. (2007). CD1 antigen presentation: how it works. *Nat Rev Immunol*. 7(12), 929–41.
10. Barry, C. E., Lee, R. E., Mdluli, K., Sampson, a E., Schroeder, B. G., Slayden, R. a, & Yuan, Y. (1998). Mycolic acids: structure, biosynthesis and physiological functions. *Prog Lipid Res*. 37(2-3), 143-79.
11. Beckman, E.M., Porcelli, S.A., Morita, C.T., Behar, S.M., Furlong, S.T., and Brenner, M.B. (1994). Recognition of a lipid antigen by CD1-restricted alpha beta+ T cells. *Nature*. 372, 691–694.
12. Benadie, Y., Deysel, M., Siko, D. G. R., Roberts, V. V., Van Wyngaardt, S., Thanyani, S. T., Sekanka, G. (2008). Cholesteroid nature of free mycolic acids from *M. tuberculosis*. *Chem Phys Lipids*. 152(2), 95-103.
13. Berdowska, a, & Zwirska-Korczała, K. (2001). Neopterin measurement in clinical diagnosis. *J Clin Pharm Ther*. 26 (5), 319-29.
14. Berthet, F. X., Rasmussen, P. B., Rosenkrands, I., Andersen, P., & Gicquel, B. (1998). A *Mycobacterium tuberculosis* operon encoding ESAT-6 and a novel low-molecular-mass culture filtrate protein (CFP-10). *Microbiology*. 144 (Pt 11), 3195-203.

15. Besra, G. S., Bolton, R. C., McNeil, M. R., Ridell, M., Simpson, K. E., Glushka, J., van Halbeek, H. (1992). Structural elucidation of a novel family of acyltrehaloses from *Mycobacterium tuberculosis*. *Biochemistry*. 31(40), 9832-7
16. Beukes, M., Lemmer, Y., Deysel, M., Dulayymi, R. A., Grooten, J., Toschi, G., Roberts, V. V. (2010). Chemistry and Physics of Lipids. *Chem Phys Lipids*. 163(8), 800-808.
17. Bhatt, A., Fujiwara, N., Bhatt, K., Gurcha, S. S., Kremer, L., Chen, B., Chan, J. (2007). Deletion of *kasB* in *Mycobacterium tuberculosis* causes loss of acid-fastness and subclinical latent tuberculosis in immunocompetent mice. *Proc Natl Acad Sci USA*. 104(12), 5157–62.
18. Biomarkers Definitions Working Group. (2001). Biomarkers and surrogate endpoints: preferred definitions and conceptual framework. *Clin Pharmacol Ther*. 69, 89–95
19. Blanchard, J. S. (1996). Molecular mechanisms of drug resistance in tuberculosis. *Annu Rev Biochem*. 65:215-39
20. Boehme, C. C., Nicol, M. P., Nabeta, P., Michael, J. S., Gotuzzo, E., Tahirli, R., Gler, M. T. (2011). Feasibility, diagnostic accuracy, and effectiveness of decentralised use of the Xpert MTB/RIF test for diagnosis of tuberculosis and multidrug resistance: a multicentre implementation study. *Lancet*. 377(9776), 1495–505.
21. Boehme, C., Molokova, E., Minja, F., Geis, S., Loscher, T., Maboko, L., Koulchin, V. (2005). Detection of mycobacterial lipoarabinomannan with an antigen-capture ELISA in unprocessed urine of Tanzanian patients with suspected tuberculosis. *Trans R Soc Trop Med Hyg*. 99(12), 893-900.
22. Brennan, P. J., & Nikaido, H. (1995). The envelope of mycobacteria. *Annu Rev Biochem*., 64, 29-63.
23. Britton, W. J., & Lockwood, D. N. J. (2004). Leprosy. *Lancet*. 363(9416), 1209–19.
24. Brosch, S. V. Gordon, M. Marmiesse, P. Brodin, C. Buchrieser, K. Eiglmeier, T. Garnier, C. Gutierrez, G. Hewinson, K. Kremer, L. M. Parsons, A. S. Pym, S. Samper, D. van Soolingen, S. T. Cole. (2002). A new evolutionary scenario for the *Mycobacterium tuberculosis* complex. *PNAS*. March 19; 99(6): 3684–3689
25. Butler, W. R., & Guthertz, L. S. (2001). Mycolic acid analysis by high-performance liquid chromatography for identification of *Mycobacterium* species. *Clin Microbiol Rev*. 14(4):704-726.
26. Camacho, L. R., Constant, P., Raynaud, C., Laneelle, M. a, Triccas, J. a, Gicquel, B., Daffe, M. (2001). Analysis of the phthiocerol dimycocerosate locus of *Mycobacterium tuberculosis*. Evidence that this lipid is involved in the cell wall permeability barrier. *JBC*. 276(23), 19845–54.
27. Cannas, A., Goletti, D., Girardi, E., Chiacchio, T., Calvo, L., Cuzzi, G., Piacentini, M. (2008). *Mycobacterium tuberculosis* DNA detection in soluble fraction of urine from pulmonary tuberculosis patients. *Int J Tuberc Lung Dis*. 12(2), 146-51.
28. Caulum. M, Murphy, B, Ramsay. L, Henry, C. (2007). Detection of Cardiac Biomarkers Using Micellar Electrokinetic Chromatography and a Cleavable Tag Immunoassay. *Anal Chem*. 79 (14), 5249-5256

29. Cech, N. B., & Enke, C. G. (2002). Practical implications of some recent studies in electrospray ionization fundamentals. *Mass Spectrom Rev.* 20(6), 362-87.
30. Cole (2010). *Electrospray and MALDI Mass Spectrometry: Fundamentals, Instrumentation, Practicalities, and Biological Applications.* John Wiley & Sons
31. Constant, P., Perez, E., Malaga, W., Lan elle, M.-A., Saurel, O., Daff , M., & Guilhot, C. (2002). Role of the pks15/1 gene in the biosynthesis of phenolglycolipids in the *Mycobacterium tuberculosis* complex. Evidence that all strains synthesize glycosylated p-hydroxybenzoic methyl esters and that strains devoid of phenolglycolipids harbor a frameshift. *J Biol Chem.* 277(41), 38148-58.
32. Cox, J. S., Chen, B., McNeil, M., & Jacobs, W. R. (1999). Complex lipid determines tissue-specific replication of *Mycobacterium tuberculosis* in mice. *Nature.* 402(6757), 79–83.
33. Crick, D. C., Mahapatra, S., & Brennan, P. J. (2001). Biosynthesis of the arabinogalactan-peptidoglycan complex of *Mycobacterium tuberculosis*. *Glycobiology.* 11(9), 107R-118R.
34. Chan, E. D., Heifets, L., & Iseman, M. D. (2000). Immunologic diagnosis of tuberculosis: a review. *Tuber Lung Dis.* 80(3), 131-40.
35. Chatterjee, D., & Khoo, K. H. (1998). Mycobacterial lipoarabinomannan: an extraordinary lipoheteroglycan with profound physiological effects. *Glycobiology,* 8(2), 113-20.
36. Cole R. A., Lu H. M., Shi Y. Z., Wang J., De-Hua T., Zhou A. T. (1996) Clinical evaluation of a rapid immunochromatographic assay based on the 38 kDa antigen of *Mycobacterium tuberculosis* on patients with pulmonary tuberculosis in China. *Tuber Lung Dis.* 77:363–368
37. Daff , M., & Laneelle, M. A. (1988). Distribution of phthiocerol diester, phenolic mycosides and related compounds in mycobacteria. *J Gen Microbiol.* 134(7), 2049-55.
38. Daff , M., & Etienne, G. (1999). The capsule of *Mycobacterium tuberculosis* and its implications for pathogenicity. *Tuber Lung Dis.* 79(3), 153-69.
39. Daff , M., & Reyrat, J.-M. (2008). *The mycobacterial cell envelope.* Washington: ASM Press.
40. David, S. T., Mukundan, U., Brahmadathan, K. N., & John, T. J. (2004). Detecting mycobacteraemia for diagnosing tuberculosis. *Indian J Med Res.* 119(6), 259–66.
41. Davidson, L. a, Draper, P., & Minnikin, D. E. (1982). Studies on the mycolic acids from the walls of *Mycobacterium microti*. *J Gen Microbiol.* 128(4), 823-8.
42. Demangel, C., Stinear, T. P., & Cole, S. T. (2009). Buruli ulcer: reductive evolution enhances pathogenicity of *Mycobacterium ulcerans*. *Nat Rev Microbiol.* 7(1), 50-60.
43. Demissie, A., Leyten, E. M. S., Abebe, M., Aseffa, A., Abate, G., Fletcher, H., Owiafe, P. (2006). Recognition of stage-specific mycobacterial antigens differentiates between acute and latent infections with *Mycobacterium*. *Clin Vaccine Immunol.* 13(2):179-186
44. Dheda, K., Booth, H., Huggett, J. F., Johnson, M. a, Zumla, A., & Rook, G. a W. (2005). Lung remodeling in pulmonary tuberculosis. *J Infect Dis.* 192(7), 1201-9.
45. Dheda, K., Davids, V., Lenders, L., Roberts, T., Meldau, R., Ling, D., Brunet, L. (2010). Clinical utility of a commercial LAM-ELISA assay for TB diagnosis

- in HIV-infected patients using urine and sputum samples. *PLoS one*. 5(3), e9848.
46. Dubey, V. S., Sirakova, T. D., & Kolattukudy, P. E. (2002). Disruption of *msl3* abolishes the synthesis of mycolipanoic and mycolipenic acids required for polyacyltrehalose synthesis in *Mycobacterium tuberculosis* H37Rv and causes cell aggregation. *Mol Microbiol*. 45(5), 1451-9.
 47. Eggink, M., Wijtmans, M., Kretschmer, A., Kool, J., Lingeman, H., de Esch, I. J. P., Niessen, W. M. (2010). Targeted LC-MS derivatization for aldehydes and carboxylic acids with a new derivatization agent 4-APEBA. *Anal Bioanal Chem*. 397(2), 665-75.
 48. Figueiredo, A. A., & Lucon, A. M. (2008). Urogenital Tuberculosis : Update and Review of 8961 cases from the world literature. *Rev Urol*. 10(3), 207-217.
 49. Fischer, K., Scotet, E., Niemeyer, M., Koebernick, H., Zerrahn, J., Maillet, S., Hurwitz, R. (2004). Mycobacterial phosphatidylinositol mannoside is a natural antigen for CD1d-restricted T cells. *PNAS*. 101(29), 10685-90.
 50. Flynn, J. L., & Chan, J. (2001). Tuberculosis: latency and reactivation. *Infect Immun*. 69(7), 4195-201.
 51. Fu, L. M. (2002). Is *Mycobacterium tuberculosis* a closer relative to Gram-positive or Gram – negative bacterial pathogens? *Tuberculosis (Edinb)*. 82(2-3):85-90
 52. Fujita, Y., Naka, T., McNeil, M. R., & Yano, I. (2005). Intact molecular characterization of cord factor (trehalose 6,6'-dimycolate) from nine species of mycobacteria by MALDI-TOF mass spectrometry. *Microbiology*. 151(Pt 10), 3403-16.
 53. Gagliardi, M. C., Lemassu, A., Teloni, R., Mariotti, S., Sargentini, V., Pardini, M., Daffé, M. (2007). Cell wall-associated alpha-glucan is instrumental for *Mycobacterium tuberculosis* to block CD1 molecule expression and disable the function of dendritic cell derived from infected monocyte. *Cell Microbiol*. 9(8), 2081-92.
 54. Gao, S., Zhang, Z.-P., & Karnes, H. T. (2005). Sensitivity enhancement in liquid chromatography/atmospheric pressure ionization mass spectrometry using derivatization and mobile phase additives. *J Chromatogr B Analyt Technol Biomed Life Sci*. 825(2), 98-110.
 55. Gargir A, Ofek I, Meron-Sudai S, Tanamy MG, Kabouridis PS, Nissim A (2002) Single chain antibodies specific for fatty acids derived from a semi-synthetic phage display library. *Biochim Biophys Acta* 1569:167–173
 56. Gilleron, M., Quesniaux, V. F. J., & Puzo, G. (2003). Acylation state of the phosphatidylinositol hexamannosides from *Mycobacterium bovis* bacillus Calmette Guerin and *Mycobacterium tuberculosis* H37Rv and its implication in Toll-like receptor response. *J Biol Chem*. 278 (32), 29880-9.
 57. Glickman, M. S., Cox, J. S., & Jacobs, W. R. (2000). A novel mycolic acid cyclopropane synthetase is required for cording, persistence, and virulence of *Mycobacterium tuberculosis*. *Molecular cell*. 5(4), 717-27.
 58. Gopinath K, Singh S. (2010). Non-Tuberculous Mycobacteria in TB-Endemic Countries: Are We Neglecting the Danger? *PLoS Negl Trop Dis* 4(4): e615. doi:10.1371/journal.pntd.0000615
 59. Goren, M. B., Brokl, O., & Das, B. C. (1976). Sulfatides of *Mycobacterium tuberculosis*: the structure of the principal sulfatide (SL-I). *Biochemistry*, 15(13), 2728-35.

60. Goto, M., Oka, S., Okuzumi, K., Kimura, S., & Shimada, K. (1991). Evaluation of acridinium-ester-labeled DNA probes for identification of *Mycobacterium tuberculosis* and *Mycobacterium avium*-*Mycobacterium intracellulare* complex in culture. *J Clin Microbiol.* 29(11): 2473–2476.
61. Griffiths, W. J., & Wang, Y. (2009). Mass spectrometry: from proteomics to metabolomics and lipidomics. *Chem Soc Rev.* 38(7), 1882-96.
62. Grinsztejn B, Fandinho FC, Veloso VG, João EC, Lourenço MC, Nogueira SA, Fonseca LS, Werneck-Barroso E. (1997). Mycobacteremia in patients with acquired immunodeficiency syndrome. *Arch Intern Med* 157: 2359-63.
63. Guilhot C, Chalut C, Daffe M. (2008). The mycobacterial cell envelope. Washington: ASM Press.
64. Hall RG, Leff RD, Gumbo T. (2009). Treatment of active pulmonary tuberculosis in adults: current standards and recent advances. *Pharmacotherapy.* 29(12): 1468–1481
65. Harland, C. W., Rabuka, D., Bertozzi, C. R., & Parthasarathy, R. (2008). The *Mycobacterium tuberculosis* virulence factor trehalose dimycolate imparts desiccation resistance to model mycobacterial membranes. *Biophys J.* 94(12), 4718-24.
66. Hershkovitz, I., Donoghue, H. D., Minnikin, D. E., Besra, G. S., Lee, O. Y.-C., Gernaey, A. M., Galili, E. (2008). Detection and molecular characterization of 9,000-year-old *Mycobacterium tuberculosis* from a Neolithic settlement in the Eastern Mediterranean. *PloS one.* 3(10), e3426.
67. Hunter, R. L., Olsen, M. R., Jagannath, C., & Actor, J. K. (2006). Review: multiple roles of cord factor in the pathogenesis of primary, secondary , and cavitory tuberculosis , including a revised description of the pathology of secondary disease. *Ann Clin Lab Sci.* 36(4), 371-386.
68. Hussein, H., and S. Elberg. (1952). Cellular reactions to phtienoic acid and related branched-chain acids. *Amer Rev Tuberc.* 65:655-72
69. Jarlier, V., & Nikaido, H. (1994). Mycobacterial cell wall: structure and role in natural resistance to antibiotics. *FEMS Microbiol Lett.* 123(1-2), 11-8.
70. Jarzembowski, J and Young, M. (2008) Nontuberculous Mycobacterial Infections. *Arch Pathol Lab Med,* 132(8):1333-1341.
71. Jasmer RM, Nahid P, Hopewell PC. (2002). Clinical practice. Latent tuberculosis infection. *N Engl JMed* 347:1860–1866.
72. Johnson, R., Streicher, E. M., Louw, G. E., Warren, R. M., van Helden, P. D., & Victor, T. C. (2006). Drug resistance in *Mycobacterium tuberculosis*. *Curr Issues Mol Biol.* 8: 97–112.
73. Jones, D., & Havlir, D. V. (2002). Nontuberculous mycobacteria in the HIV infected patient. *Clin Chest Med.* 23(3), 665-74.
74. Julián, E., L. Matas, A. Perez, J. Alcaide, M. A. Laneelle, M. Luquin. 2002. Serodiagnosis of tuberculosis: comparison of immunoglobulin A (IgA) response to sulfolipid I with IgG and IgM responses to 2,3-diacyltrehalose 2,3,6-triacyltrehalose and cord factor antigens. *J. Clin. Microbiol.* 40:3782-3788
75. Kaneda, K., Naito, S., Imaizumi, S., Yano, I., Mizuno, S., Tomiyasu, I., Baba, T. (1986). Determination of molecular species composition of C80 or longer-chain alpha-mycolic acids in *Mycobacterium* spp. by gas chromatography-mass spectrometry and mass chromatography. *J Clin Microbiol.* 24(6), 1060-70.

76. Kato, M. (1970). Site II-specific inhibition of mitochondrial oxidative phosphorylation by trehalose-6,6'-dimycolate (cord factor) of *Mycobacterium tuberculosis*. *Arch Biochem Biophys.* 140(2), 379-390.
77. Kato, M., & Goren, M. B. (1974). Synergistic action of cord factor and mycobacterial sulfatides on mitochondria. *Infect Immun.* 10(4), 733-41.
78. Kaufmann, S. H. E., & Parida, S. K. (2008). Tuberculosis in Africa: learning from pathogenesis for biomarker identification. *Cell Host Microbe.* 4(3), 219-28.
79. Khan, S. R., Glenton, P. a, Backov, R., & Talham, D. R. (2002). Presence of lipids in urine, crystals and stones: implications for the formation of kidney stones. *Kidney int.* 62(6), 2062-72.
80. Khoo K-H, Dell A, Morris HR, Brennan PJ, Chatterjee D. (1995) Inositol phosphate capping of the nonreducing termini of lipoarabinomannan from rapidly growing strains of *Mycobacterium*. *J Biol Chem.* 270:12380-12389
81. Kim, S. J. (2005). Drug-susceptibility testing in tuberculosis: methods and reliability of results. *ERJ*, 25(3), 564-9.
82. Kisker, O., Onizuka, S., Becker, C. M., Fannon, M., Flynn, E., D'Amato, R., Zetter, B. (2003). Vitamin D binding protein-macrophage activating factor (DBP-maf) inhibits angiogenesis and tumor growth in mice. *Neoplasia*, 5(1), 32-40.
83. Korf, J. E., Pynaert, G., Tournoy, K., Boonefaes, T., Van Oosterhout, A., Ginneberge, D., Haegeman, A. (2006). Macrophage reprogramming by mycolic acid promotes a tolerogenic response in experimental asthma. *Am. J. Respir. Crit Care Med.* 174(2), 152-60.
84. Lalvani, A., Pathan, A., Durkan, H., Wilkinson, K., Whelan, A., Deeks, J., Reece, W. (2001). Enhanced contact tracing and spatial tracking of *Mycobacterium tuberculosis* infection by enumeration of antigen-specific T cells. *Lancet*, 357(9273), 2017-21.
85. Larsson, L., Odham, G., Westerdahl, G., Olsson, B. (1987). Diagnosis of pulmonary tuberculosis by selected-ion monitoring: improved analysis of tuberculostearate in sputum using negative-ion mass spectrometry. *J Clin Microbiol.* 25(5), 893-6.
86. Laval, F., Lanéelle, M. a, Déon, C., Monsarrat, B., Daffé, M. (2001). Accurate molecular mass determination of mycolic acids by MALDI-TOF mass spectrometry. *Anal Chem.* 73(18), 4537-44.
87. Layre, E., Sweet, L., Hong, S., Madigan, C. a, Desjardins, D., Young, D. C., Cheng, T.-Y. (2011). A Comparative Lipidomics Platform for Chemotaxonomic Analysis of *Mycobacterium tuberculosis*. *Chem Biol.* 18(12), 1537-49.
88. Lederer, E., A. Adam, R. Ciorbaru, J. F. Petit, and J. Wietzerbin. (1975). Cell walls of mycobacteria and related organisms; chemistry and immunostimulant properties. *Mol Cell Biochem*, 7:87-104.
89. Lima, R. I. A. M. F., Bonato, V. L. D., Lima, K. M., Santos, S. A. D. O. S., Santos, R. R. D. O. S., Gonc, E. D. C., Faccioli, L. H. (2001). Role of Trehalose Dimycolate in Recruitment of Cells and Modulation of Production of Cytokines and NO in Tuberculosis. *Infect Immun.* 69(9), 5305-5312.
90. Luh, KT., Yu, CJ., Yang, PC., Lee, LN. (1996). Tuberculosis antigen A60 serodiagnosis in tuberculous infection: application in extrapulmonary and smear-negative pulmonary tuberculosis. *Respirology.* 1, 145-151.
91. Mack, U., Migliori, G. B., Sester, M., Rieder, H. L., Ehlers, S., Goletti, D., Bossink, A. (2009). LTBI: latent tuberculosis infection or lasting immune

- responses to *M. tuberculosis*? A TBNET consensus statement. *Eur Respir J*. 33(5), 956-73.
92. Mahairas, G. G., Sabo, P. J., Hickey, M. J., Singh, D. C., & Stover, C. K. (1996). Molecular analysis of genetic differences between *Mycobacterium bovis* BCG and virulent *M. bovis*. *J Bacteriol*. 178(5), 1274-82.
 93. Marais, B. J., Gie, R. P., Schaaf, H. S., Beyers, N., Donald, P. R., & Starke, J. R. (2006). Childhood pulmonary tuberculosis: old wisdom and new challenges. *Am J Respir Crit Care Med*. 15;173(10):1078-90.
 94. Marei AM, El-Behedy EM, Mohtady HA, Afify AFM. (2003). Evaluation of a rapid bacteriophage-based method for the detection of *Mycobacterium tuberculosis* in clinical samples. *J Med Microbiol*. 52:331–335.
 95. Massire, C., Ivy, C. A., Lovari, R., Kurepina, N., Li, H., Blyn, L. B., Hofstadler, S. (2011). Simultaneous identification of mycobacterial isolates to the species level and determination of tuberculosis drug resistance by PCR followed by electrospray ionization mass spectrometry. *J Clin Microbiol*. 49 (3), 908–17.
 96. McDonough, JA., Sada, ED., Sippola, AA., Ferguson, LE., Daniel, TM. (1992). Microplate and dot immunoassays for the serodiagnosis of tuberculosis. *J Lab Clin Med*, 120 (1992), pp. 318–322
 97. McKinney, J. D., Höner zu Bentrup, K., Muñoz-Elías, E. J., Miczak, a, Chen, B., Chan, W. T., Swenson, D. (2000). Persistence of *Mycobacterium tuberculosis* in macrophages and mice requires the glyoxylate shunt enzyme isocitrate lyase. *Nature*. 406(6797), 735–8.
 98. McNeil, M., Daffe, M., & Brennan, P. J. (1991). Location of the mycolyl ester substituents in the cell walls of mycobacteria. *J Biol Chem*. 266(20), 13217-23.
 99. McNerney, R., & Daley, P. (2011). Towards a point-of-care test for active tuberculosis: obstacles and opportunities. *Nat Rev Microbiol*. 2011; 9(3):204-13
 100. Meier, T., Eulenbruch, H.-P., Wrighton-Smith, P., Enders, G., & Regnath, T. (2005). Sensitivity of a new commercial enzyme-linked immunospot assay (T SPOT-TB) for diagnosis of tuberculosis in clinical practice. *Eur J Clin Microbiol Infect Dis*. 24(8), 529-36.
 101. Menzies, D., Al Jahdali, H., & Al Otaibi, B. (2011). Recent developments in treatment of latent tuberculosis infection. *Indian J Med Res*. 133(3), 257-66.
 102. Minnikin, D. E. (1982). In *The biology of the Mycobacteria*; Ratledge, C., Standford, J. L., Eds.; Academic: London, Vol. 1, pp 95–184.
 103. Minnikin. DE, Minnikin. SM,. O'Donnell. A, Goodfellow. M. (1984). Extraction of mycobacterial mycolic acids and other long-chain compounds by an alkaline methanolysis procedure. *J Microbiol Methods*, 2 (1984), pp. 243–249
 104. Minnikin, D. E., Dobson, G., Goodfellow, M., Magnusson, M., & Ridell, M. (1985). Distribution of some mycobacterial waxes based on the phthiocerol family. *J Gen Microbiol*. 131(6), 1375-81.
 105. Minnikin, D. E. (1991). Chemical principles in the organization of lipid components in the mycobacterial cell envelope. *Res Microbiol*. 142(4), 423-7.
 106. Minnikin D E, Bolton R C, Hartmann S, Besra G S, Jenkins P A, Mallet A I, Wilkins E, Lawson A M, Ridell M. (1993). An integrated procedure for the direct detection of characteristic lipids in tuberculosis patients. *Ann Soc Belg Med Trop*. 73:13–24.

107. Minnikin, D. E., Kremer, L., Dover, L. G., & Besra, G. S. (2002). The methyl-branched fortifications of *Mycobacterium tuberculosis*. *Chemistry & biology*, 9(5), 545-53.
108. Minnikin, D. E., Lee, O. Y.-C., Pitts, M., Baird, M. S., & Besra, G. S. (2010). Essentials in the use of mycolic acid biomarkers for tuberculosis detection: response to "High-throughput mass spectrometric analysis of 1400-year-old mycolic acids as biomarkers for ancient tuberculosis infection" by Mark et al., 2010. *J Archaeol Sci.* 37(10), 2407-2412.
109. Mitchison, D. a. (2000). Role of individual drugs in the chemotherapy of tuberculosis. *Int J Tuberc Lung Dis.* 4(9):796-806.
110. Mompon, B., Federici, C., Toubiana, R., & Lederer, E. (1978). Isolation and structural determination of a "cord-factor" (trehalose 6,6' dimycolate) from *Mycobacterium smegmatis*. *CPLip.* 21(1-2), 97-101.
111. Monot, M., Honoré, N., Garnier, T., Zidane, N., Sherafi, D., Paniz-Mondolfi, A., Matsuoka, M. (2009). Comparative genomic and phylogeographic analysis of *Mycobacterium leprae*. *Nat Genet.* 41(12), 1282-9.
112. Montamat-sicotte, D. J., Millington, K. A., Willcox, C. R., Hingley-wilson, S., Hackforth, S., Innes, J., Kon, O. M. (2011). A mycolic acid – specific CD1-restricted T cell population contributes to acute and memory immune responses in human tuberculosis infection. *J Clin Invest.* 121(6), 2493-2503.
113. Moreno, C., Taverne, J., Mehlert, a, Bate, C. a, Brealey, R. J., Meager, a, Rook, G. (1989). Lipoarabinomannan from *Mycobacterium tuberculosis* induces the production of tumour necrosis factor from human and murine macrophages. *Clin Exp Immunol.* 76, 240-245
- Nahid, P., Pai, M., & Hopewell, P. C. (2006). Advances in the diagnosis and treatment of tuberculosis. *Proc Am Thorac Soc.* 3(1), 103-10.
114. Needleman SB, Romberg RW (1990). Limits of linearity and detection of some drugs of abuse. *J Anal Toxicol.* 14:34-8.
115. Neyrolles, O., & Guilhot, C. (2011). Recent advances in deciphering the contribution of *Mycobacterium tuberculosis* lipids to pathogenesis. *Tuberculosis (Edinb).* 91(3), 187-95.
116. Ng, V., Zanazzi, G., Timpl, R., Talts, J. F., Salzer, J. L., Brennan, P. J., & Rambukkana. (2000). Role of the cell wall phenolic glycolipid-1 in the peripheral nerve predilection of *Mycobacterium leprae*. *Cell.* 103(3), 511-24.
117. Nigou, J., Gilleron, M., Rojas, M., García, L. F., Thurnher, M., & Puzo, G. (2002). Mycobacterial lipoarabinomannans: modulators of dendritic cell function and the apoptotic response. *Microbes Infect.* 4(9), 945-53.
118. Noll, H., Bloch, H., Asselineau, J., & Lederer, E. (1956). The chemical structure of the cord factor of *Mycobacterium tuberculosis*. *Biochim Biophys Acta.* 20, 299-309.
119. Ojha, A. K., Baughn, A. D., Sambandan, D., Hsu, T., Trivelli, X., Guerardel, Y., Alahari, A. (2008). Growth of *Mycobacterium tuberculosis* biofilms containing free mycolic acids and harbouring drug-tolerant bacteria. *Mol Microbiol.* 69(1), 164-74.
120. Ojha, A. K., Trivelli, X., Guerardel, Y., Kremer, L., & Hatfull, G. F. (2010). Enzymatic hydrolysis of trehalose dimycolate releases free mycolic acids during mycobacterial growth in biofilms. *J Biol Chem.* 285(23), 17380-9.
121. Olsen, I. Barletta, R. & Thoen, C. O., 2010. *Mycobacterium*. In: *Pathogenesis of Bacterial Infections in Animals*. In: *Pathogenesis of Bacterial Infections in*

- Animals. Fourth Edition, pp. 113-132 Ed. by C.L. Gyles, J.F. Prescott, J.G. Songer and C.O. Thoen, Wiley/Blackwell Publisher
122. Ortalo-Magné, a, Dupont, M. a, Lemassu, a, Andersen, a B., Gounon, P., & Daffé, M. (1995). Molecular composition of the outermost capsular material of the tubercle bacillus. *Microbiology*.141, 1609-20.
 123. Ortalo-Magné, a, Lemassu, a, Lanéelle, M. a, Bardou, F., Silve, G., Gounon, P., Marchal, G. (1996). Identification of the surface-exposed lipids on the cell envelopes of *Mycobacterium tuberculosis* and other mycobacterial species. *J Bacteriol*. 178(2), 456-61.
 124. Parida, S. K., & Kaufmann, S. H. E. (2010). The quest for biomarkers in tuberculosis. *Drug Discov Today*. 15(3-4), 148-57.
 125. Patel, V. B., Singh, R., Connolly, C., Kasprowicz, V., Zumla, A., Ndungu, T., & Dheda, K. (2010). Comparison of a clinical prediction rule and a LAM antigen-detection assay for the rapid diagnosis of TBM in a high HIV prevalence setting. *PloS one*, 5(12), e15664.
 126. Peyron, P., Vaubourgeix, J., Poquet, Y., Levillain, F., Botanch, C., Bardou, F., Daffé, M. (2008). Foamy macrophages from tuberculous patients' granulomas constitute a nutrient-rich reservoir for *M. tuberculosis* persistence. *PLoS pathogens*, 4(11), e1000204.
 127. Pheiffer, C., Carroll, N. M., Beyers, N., Donald, P., Duncan, K., Uys, P., & Helden, P. V. (2008). Time to detection of *Mycobacterium tuberculosis* in BACTEC systems as a viable alternative to colony counting *Int J Tuberc Lung Dis*. 12(7), 792-798.
 128. Phillips, M., Cataneo, R. N., Condos, R., Ring Erickson, G. a, Greenberg, J., La Bombardi, V., Munawar, M. I. (2007). Volatile biomarkers of pulmonary tuberculosis in the breath. *Tuberculosis (Edinb)*, 87(1), 44-52.
 129. Prodinge, W. M., Brandstätter, A., Pacciarini, M., Kubica, T., Laura, M., Aranaz, A., Nagy, G. (2005). Characterization of *Mycobacterium caprae* isolates from Europe by Mycobacterial interspersed repetitive unit genotyping. *J Clin Microbiol*. 43(10):4984-92
 130. Rafidinarivo, E., Lanéelle, M.-A., Montrozier, H., Valero-Guillén, P., Astola, J., Luquin, M., Promé, J.-C. (2009). Trafficking pathways of mycolic acids: structures, origin, mechanism of formation, and storage form of mycobacteric acids. *J Lipid Res*. 50(3), 477-90.
 131. Rao, V., Fujiwara, N., Porcelli, S. a, & Glickman, M. S. (2005). *Mycobacterium tuberculosis* controls host innate immune activation through cyclopropane modification of a glycolipid effector molecule. *J Exp Med*. 201(4), 535-43.
 132. Rao, V., Gao, F., Chen, B., Jr, W. R. J., & Glickman, M. S. (2006). Trans-cyclopropanation of mycolic acids on trehalose dimycolate suppresses *Mycobacterium tuberculosis*-induced inflammation and virulence. *J Clin Invest*. 116(6).
 133. Rastogi N. (1991). Recent observations concerning structure and function relationships in the mycobacterial cell-envelope: elaboration of a model in terms of mycobacterial pathogenicity, virulence, and drug resistance. *Res. Microbiol*. 142:464-476.
 134. Ratledge, C., & Stanford, J. (1982). *The Biology of the mycobacteria*. London: Academic Press.
 135. Redman, J. E., Shaw, M. J., Mallet, A. I., Santos, A. L., Roberts, C. a, Gernaey, A. M., & Minnikin, D. E. (2009). Mycocerosic acid biomarkers for the

- diagnosis of tuberculosis in the Coimbra Skeletal Collection. *Tuberculosis (Edinb)*, 89(4), 267-77.
136. Reed, M. B., Gagneux, S., Deriemer, K., Small, P. M., & Barry, C. E. (2007). The W-Beijing lineage of *Mycobacterium tuberculosis* overproduces triglycerides and has the DosR dormancy regulon constitutively upregulated. *J. Bacteriol.* 189(7), 2583–9.
 137. Rhoades, E. R., Streeter, C., Turk, J., & Hsu, F.-F. (2011). Characterization of sulfolipids of *Mycobacterium tuberculosis* H37Rv by multiple-stage linear ion-trap high-resolution mass spectrometry with electrospray ionization reveals that the family of sulfolipid II predominates. *Biochemistry*, 50(42), 9135-47.
 138. Rousseau, C., Neyrolles, O., Bordat, Y., Giroux, S., D Sirakova, T., Prevost, M.-C., E Kolattukudy, P. (2003). Deficiency in mycolipenate- and mycosanoate-derived acyltrehaloses enhances early interactions of *Mycobacterium tuberculosis* with host cells. *Cell Microbiol.* 5(6), 405-415.
 139. Russell, D. G. (2007). Who puts the tubercle in tuberculosis? *Nature reviews. Microbiology*, 5(1), 39–47.
 140. Ryll, R., Kumazawa, Y., Yano, I. (2001). Immunological properties of trehalose dimycolate (cord factor) and other mycolic acid-containing glycolipids—a review. *Microbiol Immunol.* 45 (12), 801–811.
 141. Saah, A. J. & Hoover, D. R. (1997). Sensitivity and specificity reconsidered: the meaning of these terms in analytical and diagnostic settings. *Ann. Intern. Med.* 1126, 91–84.
 142. Saita, N., Fujiwara, N., Yano, I., Soejima, K., & Kobayashi, K. (2000). Trehalose 6,6'-dimycolate (cord factor) of *Mycobacterium tuberculosis* induces corneal angiogenesis in rats. *Infect Immun.* 68(10), 5991-7.
 143. Samb, B., Sow, P. S., Kony, S., Diouf, G., Cissokho, S., Bâ, D., Sané, M. (1999). Risk factors for negative sputum acid-fast bacilli smears in pulmonary tuberculosis: results from Dakar, Senegal, a city with low HIV seroprevalence. *Int J Tuberc Lung Dis.*3(4):330-6
 144. Santa, T., Al-dirbashi, O. Y., & Fukushima, T. (2007). Derivatization reagents in liquid chromatography / electrospray ionization tandem mass spectrometry for biomedical analysis. *Drug Discov Ther.* 1(2), 108-118.
 145. Sarfo FS, Phillips RO, Rangers B, Mahrous EA, Lee RE, et al. (2010) Detection of mycolactone A/B in *Mycobacterium ulcerans*-infected human tissue. *PLoS Negl Trop Dis.* 4:1–9.
 146. Sartain, M. J., Dick, D. L., Rithner, C. D., Crick, D. C., & Belisle, J. T. (2011) Lipidomic analyses of *Mycobacterium tuberculosis* based on accurate mass measurements and the novel "Mtb LipidDB". *J Lipid Res.* 2011 May;52(5):861-72.
 147. Saunders, B. M., & Cooper, a M. (2000). Restraining mycobacteria: role of granulomas in mycobacterial infections. *Immunol Cell Biol.* 78(4), 334-41.
 148. Scollard, D. M., Adams, L. B., Gillis, T. P., Krahenbuhl, J. L., Truman, R. W., & Williams, D. L. (2006). The Continuing Challenges of Leprosy. *Clin Microbiol Rev.* 19(2), 338–381.
 149. Schmitz, O. J., Benter, Th. (2007). Atmospheric Pressure Laser Ionization. In *Advances in LC-MS instrumentation.* J Chromatogr. 72, Cappiello, A. Ed.
 150. Seth, M., Lamont, E. a, Janagama, H. K., Widdel, A., Vulchanova, L., Stabel, J. R., Waters, W. R. (2009). Biomarker discovery in subclinical mycobacterial infections of cattle. *PloS one.* 4(5), e5478.

151. Sharma, S. K., & Mohan. (2004). Extrapulmonary tuberculosis. *Indian J Med Res.* 120(4), 316–53.
152. Sharma, S. K., Mohan, A., Sharma, A., & Mitra, D. K. (2005). Miliary tuberculosis: new insights into an old disease. *Lancet Infect Dis.* 5(7), 415-30.
153. Sharp, S. E., Lemes, M., Sierra, S. G., Poniecka, a, & Poppiti, R. J. (2000). Löwenstein-Jensen media. No longer necessary for mycobacterial isolation. *Am J Clin Pathol.* 113(6), 770-3.
154. Shi, W., Zhang, X., Jiang, X., Yuan, H., Lee, J. S., Barry, C. E., Wang, H. (2011). Pyrazinamide inhibits trans-translation in *Mycobacterium tuberculosis*. *Science.* 333(6049), 1630–2.
155. Shingadia, D., & Novelli, V. (2003). Diagnosis and treatment of tuberculosis in children. *Lancet Infect Dis.* 3(10), 624-32.
156. Shui, G., Bendt, A. K., Jappar, I. a, Lim, H. M., Laneelle, M., Hervé, M., Via, L. E. (2011). Mycolic acids as diagnostic markers for tuberculosis case detection in humans and drug efficacy in mice. *EMBO Mol Med.* 2012.4(1):27-37.
157. Shui, G., Bendt, A. K., Pethe, K., Dick, T., & Wenk, M. R. (2007). Sensitive profiling of chemically diverse bioactive lipids. *J Lipid Res.* 48(9), 1976-84.
158. Sinsimer, D., Huet, G., Manca, C., Tsenova, L., Koo, M.-S., Kurepina, N., Kana, B. (2008).The phenolic glycolipid of *Mycobacterium tuberculosis* differentially modulates the early host cytokine response but does not in itself confer hypervirulence. *Infect Immun.* 76(7), 3027-36.
159. Sirakova, T. D., Thirumala, A. K., Dubey, V. S., Sprecher, H. & Kolattukudy, P. E. (2001). The *Mycobacterium tuberculosis* pks2 gene encodes the synthase for the hepta- and octamethyl-branched fatty acids required for sulfolipid synthesis. *J. Biol. Chem.* 276, 16833–16839.
160. Siuzdak, G. (1994). The emergence of mass spectrometry in biochemical research. *Proc Natl Acad Sci U S A.* 91(24), 11290-7.
161. Smith, I. (2003). *Mycobacterium tuberculosis* Pathogenesis and Molecular Determinants of Virulence. *Clin Microbiol Rev.* 2003, 16(3):463-496
162. Smith, K. C. (2001). Tuberculosis in Children. *Curr Probl Pediatr.* 31(1):1-30.
163. Soini, H., & Musser, J. M. (2001). Molecular diagnosis of mycobacteria. *Clin Chem.* 47(5), 809-14.
164. Steingart, K. R., Ng, V., Henry, M., Hopewell, P. C., Ramsay, A., Cunningham, J., Urbanczik, R., et al. (2006). Sputum processing methods to improve the sensitivity of smear microscopy for tuberculosis: a systematic review. *Lancet Infect Dis.* 6(10), 664-74.
165. Stokes, R. W., Norris-jones, R., Brooks, D. E., Beveridge, T. J., Doxsee, D., & Thorson, L. M. (2004). The glycan-rich outer layer of the cell wall of *Mycobacterium tuberculosis* acts as an antiphagocytic capsule limiting the association of the bacterium with macrophages. *Infect Immun.* 72(10), 5676-5686.
166. Sutherland, J. S., Hill, P. C., Adetifa, I. M., de Jong, B. C., Donkor, S., Joosten, S. a, Opmeer, L. (2011). Identification of probable early-onset biomarkers for tuberculosis disease progression. *PloS one.* 6(9), e25230.
167. Syhre, M., Manning, L., Phuanukoonnon, S., Harino, P., & Chambers, S. T. (2009). The scent of *Mycobacterium tuberculosis*--part II breath. *Tuberculosis (Edinb).* 89(4), 263-6.
168. Takayama, K., Wang, C., & Besra, G. S. (2005). Pathway to Synthesis and Processing of Mycolic Acids in *Mycobacterium tuberculosis*. *Clin Microbiol Rev.* 18(1), 81-101.

169. Tapping, R. I., & Tobias, P. S. (2003). Mycobacterial lipoarabinomannan mediates physical interactions between TLR1 and TLR2 to induce signaling. *J Endotoxin Res.* 9(4), 264-8.
170. Teo, J., Jureen, R., Chiang, D., Chan, D., & Lin, R. (2011). Comparison of two nucleic acid amplification assays, the Xpert MTB/RIF assay and the amplified Mycobacterium Tuberculosis direct assay, for detection of Mycobacterium tuberculosis in respiratory and nonrespiratory specimens. *J Clin Microbiol.* 49(10), 3659-62.
171. Thanyani, S. T., Roberts, V., Siko, D. G. R., Vrey, P., & Verschoor, J. a. (2008). A novel application of affinity biosensor technology to detect antibodies to mycolic acid in tuberculosis patients. *J Immunol Methods.* 332(1-2), 61-72.
172. Thoen, C. O., Lobue, P. a, Enarson, D. a, Kaneene, J. B., & de Kantor, I. N. (2009). Tuberculosis: a re-emerging disease in animals and humans. *Veter Ital.* 45(1), 135-81.
173. Tripathi, R. P., Tewari, N., Dwivedi, N., & Tiwari, V. K. (2005). Fighting tuberculosis: an old disease with new challenges. *Med Res Rev.* 25(1), 93-131.
174. Truman, R. W., Shannon, E. J., Hagstad, H. V., Hugh-Jones, M. E., Wolff, a, & Hastings, R. C. (1986). Evaluation of the origin of Mycobacterium leprae infections in the wild armadillo, *Dasypus novemcinctus*. *Am J Trop Mea Hyg.* (3), 588–93.
175. Truman, R., & Fine, P. E. M. (2010). “Environmental” sources of Mycobacterium leprae: issues and evidence. *Leprosy Rev.* 81(2), 89–95.
176. Tufariello, J. M., Chan, J., & Flynn, J. L. (2003). Latent tuberculosis: mechanisms of host and bacillus that contribute to persistent infection. *Lancet Infect Dis.* 3(9):578-90.
177. Tufariello, J. M., Chan, J., & Flynn, J. L. (2003). Latent tuberculosis: mechanisms of host and bacillus that contribute to persistent infection. *Lancet Infect Dis.* 3(9), 578-90.
178. Turgut, T., Akbulut, H., Deveci, F., Kacar, C., & Muz, M. H. (2006). Serum interleukin-2 and neopterin levels as useful markers for treatment of active pulmonary tuberculosis. *Tohoku. J Exp Med.* 209(4), 321-8.
179. Vander Beken, S., Al Dulayymi, J. R., Naessens, T., Koza, G., Maza-Iglesias, M., Rowles, R., Theunissen, C. (2011). Molecular structure of the Mycobacterium tuberculosis virulence factor, mycolic acid, determines the elicited inflammatory pattern. *Eur J Immunol.* 41(2), 450-60.
180. Venisse, a, Berjeaud, J. M., Chaurand, P., Gilleron, M., & Puzo, G. (1993). Structural features of lipoarabinomannan from Mycobacterium bovis BCG. Determination of molecular mass by laser desorption mass spectrometry. *J Biol Chem.* 268(17), 12401-11.
181. Vercellone, A., Nigou, J., Puzo, G. (1998). Relationships between the structure and the roles of lipoarabinomannans and related glycocon- jugates in tuberculosis pathogenesis. *Front Biosci.* 3, 149–163.
182. Vergne, I., Fratti, R. A., Hill, P. J., Chua, J., Belisle, J., & Deretic, V. (2004). Mycobacterium tuberculosis phagosome maturation arrest: mycobacterial phosphatidylinositol analog phosphatidylinositol mannoside stimulates early endosomal fusion. *Mol Biol Cell.* 15(2):751-760.
183. Wagner, D., & Young, L. S. (2004). Nontuberculous mycobacterial infections: A clinical review. *Infection.* 32(5), 257-270.

184. Walsh, G. P., Storrs, E. E., Burchfield, H. P., Cottrell, E. H., Vidrine, M. F., and Binford, C. H. (1975). Leprosy-like disease occurring naturally in armadillos. *J Reticuloendothel Soc.* 18:347-351
185. Wallis, R. S., Johnson, J. L. (2001). Adult tuberculosis in the 21st century: pathogenesis, clinical features, and management. *Curr Opin Pulm Med.* 7(3), 124–32.
186. Wang, X., Zhang, A., Han, Y., Wang, P., Sun, H., Song, G., Dong, T., Yuan, Y., Yuan, X., Zhang, M., Ning, X., Zhang, H., Dong, H., Dong, W. (2012). Urine metabolomics analysis for biomarker discovery and detection of jaundice syndrome in patients with liver disease. *Mol Cell Proteomics.* 10.1074/mcp.M111.016006.
187. Watanabe, M., Aoyagi, Y., Ridell, M., & Minnikin, D. E. (2001). Separation and characterization of individual mycolic acids in representative mycobacteria. *Microbiology.* 147(Pt 7), 1825–37.
188. Weetjens, B. J. C., Mgode, G. F., Machang'u, R. S., Kazwala, R., Mfinanga, G., Lwilla, F., Cox, C. (2009). African pouched rats for the detection of pulmonary tuberculosis in sputum samples. *Int J Tuberc Lung Dis.* 13(6), 737-43.
189. Wenk, M. R. (2005). The emerging field of lipidomics. *Nat Rev Drug Discov.* 4(7), 594-610.
190. Wirth, T., Hildebrand, F., Allix-Béguet, C., Wölbeling, F., Kubica, T., Kremer, K., van Soolingen, D. (2008). Origin, spread and demography of the *Mycobacterium tuberculosis* complex. *PLoS pathogens*, 4(9), e1000160.
191. Wisconsin Department of Natural Resources. (1996). Analytical detection limit guidance & laboratory guide for determining method detection limits. Wisconsin Department of Natural Resources laboratory certification program. PUBL-TS-056-96.
192. Wolk, D. M., Blyn, L. B., Hall, T. a, Sampath, R., Ranken, R., Ivy, C., Melton, R. (2009). Pathogen profiling: rapid molecular characterization of *Staphylococcus aureus* by PCR/electrospray ionization-mass spectrometry and correlation with phenotype. *J Clin Microbiol.* 47(10), 3129–37.
193. World Health Organisation. Geneva. Treatment of tuberculosis: guidelines 2010– 4th ed. WHO/HTM/TB/2009.420.
194. World Health Organization. Geneva. (2007). TB diagnostics and laboratory strengthening-WHO policy.
195. World Health Organization. Global Tuberculosis Control Report (2011). Geneva, Switzerland.
196. World Organisation for Animal Health (OIE), Manual of Diagnostic Tests and Vaccines for Terrestrial Animals. (2009). Paris, France.
197. Yang, W.-C., Adamec, J., & Regnier, F. E. (2007). Enhancement of the LC/MS analysis of fatty acids through derivatization and stable isotope coding. *Anal Chem.* 79(14), 5150-7.
198. Yuan, Y., Lee, R. E., Besra, G. S., Belisle, J. T., & Barry, C. E. (1995). Identification of a gene involved in the biosynthesis of cyclopropanated mycolic acids in *Mycobacterium tuberculosis*. *Proc Natl Acad Sci U S A.* 92(14), 6630-4.
199. Yuan, Y., Zhu, Y., Crane, D. D., & Barry, C. E. (1998). The effect of oxygenated mycolic acid composition on cell wall function and macrophage growth in *Mycobacterium tuberculosis*. *Mol Microbiol.* 29(6), 1449-58.

200. Zar, J. H. (1999). *Biostatistical analysis*. 4th ed. Upper Saddle River, N.J.: Prentice Hall.
201. Zhang, Y., Permar, S., & Sun, Z. (2002). Conditions that may affect the results of susceptibility testing of *Mycobacterium tuberculosis* to pyrazinamide. *J Med Microbiol.* 51(1):42-9.
202. Zhou, M. (2011) Current strategies and future trends, in regulated bioanalytical laboratories: technical and regulatory aspects from global perspectives, John Wiley & Sons, Inc., Hoboken, NJ, USA.
203. Ziv, E., Daley, C. L., & Blower, S. M. (2001). Early therapy for latent tuberculosis infection. *Am J Epidemiol.* 153(4), 381-5.
204. Zuber, B., Chami, M., Houssin, C., Dubochet, J., Griffiths, G., & Daffé, M. (2008). Direct visualization of the outer membrane of mycobacteria and corynebacteria in their native state. *J Bacteriol.* 190(16), 5672-8

LIST OF ABBREVIATIONS

AFB	Acid-fast bacilli
AG	Arabinogalactan Arabinomannan
AIDS	Acquired immune deficiency syndrome
AMMP	3-acyl-oxymethyl-1-methylpyridinium iodide
amu	Atomic mass units
APCI	Atmospheric pressure chemical ionization
AraLAM	Arabinan of Lipoarabinomannan
BMP	2-Bromo-1-methylpyridinium Iodide
CDR	Case detection rate
CMP	3-Carbinol-1-methylpyridinium Iodide
CSF	Cerebrospinal fluid
DAP	Diaminopimelic acid
DAT	Diacyltrehaloses
DBP	D binding protein precursor
DOTS	Directly observed treatment short course
DTH	Delayed-type hypersensitivity
EI	Electron impact
ELISA	Enzyme-linked immunosorbent assay
ELISPOT	Enzyme-linked immunospot
EMB	Ethambutol
ES	Electrospray
ESI	Electrospray ionization
FM	Foamy macrophages
GC	Gas chromatography
GLU	Glucane
HAART	Highly active antiretroviral therapy
HIV	Human immunodeficiency virus
HPLC	High-performance liquid chromatography
IFN- γ	Gamma interferon
IGRAs	Interferon-gamma release assays
IL	Interleukin
INH	Isoniazid
IS	Insertion sequence
katG	Catalase peroxidase enzyme
LAM	Lipoarabinomannan
LC	Latent tuberculosis infection
LM	Lipomannan
LTBI	Liquid chromatography
LAMP	Loop-mediated isothermal amplification
MAMEs	Mycolic acid methyl esters
MHC	Major histocompatibility complex
ManLAM	Mass spectrometry
MS	Mannose lipoarabinomannan
MALDI	Matrix assisted laser desorption/ionization

MDL	Method detection limit
MAC	Mycobacterium avium complex
Max	Maximum
min	Minimal
MFE	Molecular Feature Extraction
MDR	Multidrug-resistance
Mtb	Mycobacterium tuberculosis
MTD	Mycobacterium Tuberculosis Direct
msl	Mycocerosic acid synthase like gene
Magp	Mycolic acid-peptidoglyca arabinogalactan
Mas	Mycolic acids
NK	Natural killer
NTM	Nontuberculous mycobacteria
NAA	Nucleic acid amplification
OD	Optical density
PAT	Pentaacyl trehalose
PG	Peptidoglycan
PGLs	Phtiocerol dimycocerosates
PIMs	Phosphatidil inositol manosside
PE	Phosphatidylethanolamine
PAT	Polyacyltrehaloses
PDIMS	Phenol glycolipids
PILAM	Lipoarabinomannan inositol phosphate
pks	Polyketide synthase
PPD	Purified protein derivative
PZA	Pyrazinamide
RIF	Rifampicin
SDS	Sodium dodecyl sulfate
SD	Standard deviation
SL	Sulfolipid
TLC	Thin layer chromatography
TLR	Toll-like receptor
tr-DNA	Transrenal DNA
TDM	Triacyltrehaloses
TAT	Trehalose 6, 6'- dimycolate
TEA	Triethylamine
TST	Tuberculin skin test
TSA	Tuberculoestearic acid
TB	Tuberculosis
TNF	Tumour necrosis factor
TAT	Turn around time
VOCs	Volatile compounds
WHO	World Health Organization
XDR	Extensively drug-resistant